AD-A136 307 DEVELOPMENT OF X-RAY LASER MEDIA MEASUREMENT OF GAIN AND DEVELOPMENT OF C..(U) ROCHESTER UNIV N Y LAB FOR LASER ENERGETICS J FORSYTH FEB 83 1/3

UNCLASSIFIED AFOSR-TR-83-1136-VOL-3 AFOSR-81-0059 F/G 20/8 NL

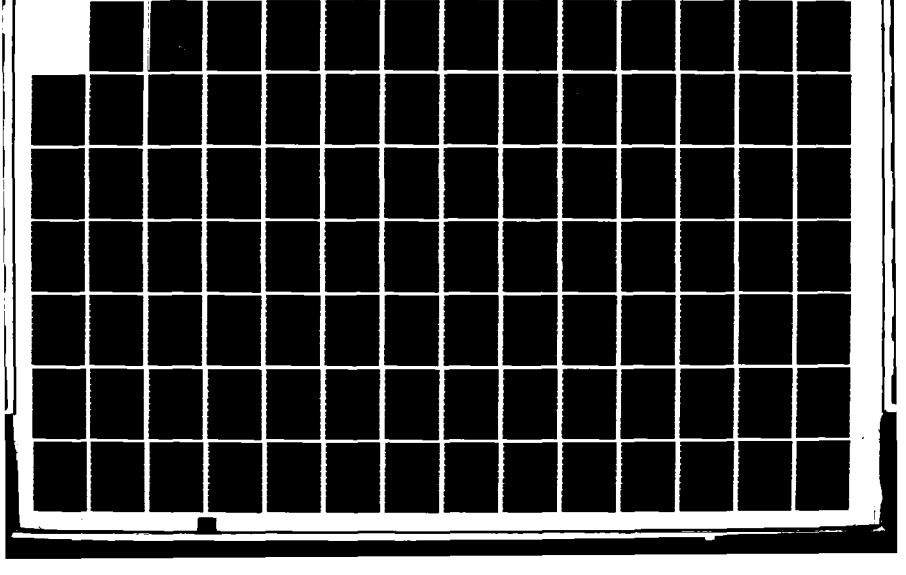

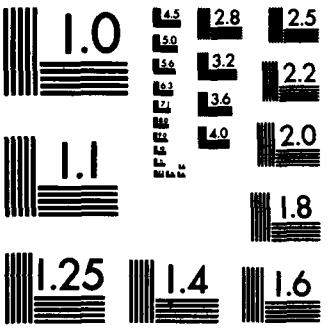

MICROCOPY RESOLUTION TEST CHART
NATIONAL BUREAU OF STANDARDS-1963-A

AFOSR-TR- 83-1136

February 1983
Volume 3

Annual Scientific Report
1 January 1982 - 31 December 1982

Grant AFOSR-81-0059

Development of X-Ray Laser Media: Measurement of Gain and Development of Cavity Resonators for Wavelengths Near 130 Angstroms

Laboratory for Laser Energetics
University of Rochester
250 East River Road
Rochester, New York 14623

3.0 Reflecting Properties of X-Ray Multilayer

Chapter IV and Appendices

Chapter IV Conclusion

Section 1 - Summary of This Work

Part A) Introduction

In this document the authors summarize our investigation of the reflecting properties of x-ray multilayers. The breadth of this investigation indicates the utility of the difference equation formalism in the analysis of such structures. The formalism is particularly useful in analyzing multilayers whose structure is not a simple periodic bilayer. The complexity in structure can be either intentional, as in multilayers made by in-situ reflectance monitoring, or it can be a consequence of a degradation mechanism, such as random thickness errors or interlayer diffusion.

Both the analysis of thickness errors and the analysis of interlayer diffusion are conceptually simple, effectively one-dimensional problems that are straightforward to pose. Each problem has recieved attention from previous authors (Shellan, et al. 1978; Underwood and Barbee, 1982), and in each case we have been able to significantly extend previous work with an analysis that uses the difference equation formalism.

In the authors' analysis of in-situ reflectance monitoring, they provide a quantitative understanding of an experimentally successful process that has not previously been treated theoretically.

As x-ray multilayers come into wider use, there will undoubtedly be an increasing need for a more precise understanding of their reflecting properties. Thus, it is expected that in the future more detailed modeling will be undertaken of less easily specified structures than those above. The authors believe that their formalism will continue to prove useful in the modeling of these more complex structures.

One such structure that may be of interest is that of a multilayer degraded by interfacial roughness. To date there has been one direct experimental indication that roughness produces a detectable effect on multilayer performance (Spiller et al., 1980, see sec. III-1). We have used the difference equation formalism to make a preliminary investigation of the effect of roughness on multilayer reflectivity.

Thus far our treatment is not general, in that we only treat certain limiting case kinds of roughness that may or may not resemble the roughness actually present in multilayers. Further, the formalism that we use to treat roughness makes new assumptions about the multilayer structure in addition to those made in Chapter II; these new assumptions are due to Eastman (1978), and in effect reduce the three-dimensional rough structure to a structure that is quasi-one-dimensional. The applicability of these new assumptions to x-ray multilayers is considerably less certain than are those made in sec. II-1.

For these two reasons, and for the sake of brevity, we have chosen not to include this preliminary treatment of roughness in the analysis presented in Chapter II. The results of Chapters II and III are summarized in part B of this section (sec. IV-1).

We summarize our initial investigation of roughness in part A of section IV-2; section IV-2 as a whole deals with suggestions for future work. In the same section we discuss, in a general way, the basis for measurements with which a future experimental program might characterize the kinds of defects present in multilayers. The roughness analysis indicates that roughness of different kinds (along with other kinds of structural defects) may produce qualitatively different signatures in the reflecting properties of multilayers. Part B of section II concludes with some suggestions for other future investigations based on the results of the present work.

Part B) Summary of Chapters II and III

Our analysis is based on a characteristic matrix solution we derive for the unit cell of an x-ray multilayer (eq. II-1-14). Our formalism resembles the Ewald-von Laue dynamical theory of x-ray diffraction in that it begins with a physical representation of the multilayer in terms of a spatially varying complex dielectric constant. Unlike the dynamical diffraction theory, we do not require that the dielectric constant be periodic; however we do require that it vary only in one dimension. Like the dynamical theory, our formalism exploits the fundamental optical property of materials at x-ray wavelengths, in assuming that the dielectric constant departs only slightly from unity. However, the explicit characteristic matrix form of our solutions is one that is commonly used in predicting the performance of optical multilayer coatings (Born and Wolf, 1975).

Since our present interest is in the reflecting properties of multilayers, we convert eq. II-1-14 into a difference equation that propagates the amplitude reflectivity ρ_K from the Kth cell to the K+1st cell in mth order; this equation (reproduced from eq. II-1-20) is

$$\rho_{K+1} = e^{-2it_K}\rho_K + (-1)^m e^{-it_K}(ir_K - \rho_K) + (-1)^m e^{-3it_K}(ir_K + \rho_K)\rho_K^2 \qquad (IV-1-1)$$

The parameters t, r, and p are essentially amplitude transmittances and reflectances for the cell (they are defined explicitly in eq. II-1-15).

Fig. II-1-3 shows how this result resembles the Airy recursion formula that is often used in optical thin-film calculations; however eq. IV-1-1 exploits the small departure of the dielectric constant from unity in that multiple reflections are represented only in a single non-linear term in ρ_u . Our difference equation has the advantage of being written explicitly in terms of the discrete properties of the separate unit cells.

The case of reflection from ideal periodic x-ray multilayers has been treated by Vinogradov and Zeldovich (1977), and by Lee (1981). The solution for the periodic case (given in eq. II-2-11) is essentially the Darwin-Prins solution for the reflectivity of an ideal crystal (James, 1965). We have extended previous work on the periodic case only in minor ways.

In sec. II-2-B we present a detailed analysis of the criterion by which one chooses the period length that maximizes the absorption-limited multilayer reflectivity (eq. II-2-30). We show that this condition is essentially a Bragg condition (equivalent in the centrosymmetric case to a result derived by Miller, 1935, for crystalline reflection); however this Bragg condition contains a correction for absorption as well as the usual dispersion correction. We show that this condition can be simply expressed as a requirement that the real part of the parameter known as the equivalent phase thickness be π for a resonance. (The concept of equivalent parameters is discussed in Knittl, 1976, see also sec. II-1). We show that the absorption-dependent term is a consequence of phase changes that occur during multiple reflections within a structure having a complex index of refraction.

We also derive a condition for maximizing the reflectivity in secondary degrees of freedom other than the period length (eqs. II-2-41 and 42); this is a generalization of a result for bilayer structures that has been derived by Vinogradov and Zeldovich (1977). We show that these secondary optimization conditions obtain only when the period length of the structure is already optimized.

We used these computationally simple optimization conditions as the basis for a computer program that searched for new multilayer materials combinations (see table II-2-1). The nominal reflectivities attainable with these new materials are usually significantly higher than those attainable with the more common materials choice of tungsten and carbon (the reflectivities of the new materials combinations are plotted in red in fig. II-2-4, the maximum reflectivities attainable with tungsten and carbon are plotted in fig. II-2-5).

Nickel is found by the search program to be a good high index material for the region around $\lambda = 50\text{Å}$. (Nickel is not included at 50A in table II-2-1 because table II-2-1 lists only the best combination for each wavelength; however nickel was first choice of the search program at 50A when the program was modified to maximize integrated reflectivity).

In a preliminary effort to test this prediction of our search program, Spiller (1982a) has made an evaluation of the effective roughness in individual nickel layers using a technique described in Broers and Spiller (1980a, 1980b). He has found that nickel layers appear to have approximately the same low level of roughness as do carbon layers. However, with that partial exception, the results of table II-2-1 have yet

to be tested experimentally.

In sec. II-3 we discuss the approximate scaling of the reflecting properties of tungsten-carbon multilayers with wavelength, 2d-spacing, and angle of incidence. We show that the optimum ratio in thickness between high and low index layers does not depend strongly on wavelength. (It is also independent of 2d-spacing, angle of incidence, and polarization.)

We show that the number of layer pairs N required to approach absorption-limited reflectivity (as distinguished from J, the number of layer pairs actually present in a particular multilayer), is approximately

$$N \cong \frac{2.5 \times 10^5}{\left(2d_{(\text{Å})}\right)^2} \qquad (\text{IV-1-2})$$

For a given 2d-spacing N is thus approximately independent of wavelength and angle of incidence. Eq. IV-1-2 also implies that the spectral resolution $\delta\lambda/\lambda$ scales quadratically with 2d-spacing.

In eq. II-3-23 we show that the acceptance angle in radians of a tungsten-carbon multilayer scales approximately as

$$\delta\theta_{FWHM} \cong 5.1 \times 10^{-6} \frac{\lambda^2_{(\text{Å})}}{\sin 2\theta_B} \qquad (\text{IV-1-3})$$

and thus has a symmetric character in the grazing and normal incidence regimes. (In these two regimes the acceptance angle is also larger than

at intermediate angles of incidence.)

In sec. II-4 we discuss the utility of defect-free designs that are non-periodic. Through a combination of mathematical demonstration and numerical simulation, we find strong indications that the use of aperiodic designs will not yield increased reflectivities in the x-ray regime.

In sec. II-4 we show that non-periodic multilayers which are optimized in the layer-by-layer fashion discussed by Carniglia and Apfel (1980) will not be able to attain quite as high a reflectivity as will the optimum periodic structure. (For example, in a 67.6Å tungsten-carbon multilayer, $\Delta R/R \cong 0.15$). Multilayers made with the in-situ reflectance monitoring technique devised by Spiller et al. (1980) will also suffer this slight loss in reflectivity relative to the theoretical limit, unless the deposition conditions are adjusted slightly in compensation.

In sec. II-5 we use our formalism to analyze the problem of random thickness errors in the layers of an x-ray multilayer. We treat the most straightforward case in which the errors in the different layers are random and uncorrelated. (We refer to this case as "accumulating" thickness errors).

We have been able to significantly extend previous work on the problem (Shellan, 1978). Except in assuming a small coupling constant, Shellan's perturbation treatment does not apply to the x-ray regime where absorption, and operation away from the dielectric Bragg condition, must usually be considered. Further, our analysis is not based on a perturbation treatment, so we are able to consider errors that are large

enough in comparison with the layer thicknesses to cause a substantial degradation in reflectivity.

Our treatment is based on a decomposition of the amplitude reflectivity into what are essentially coherent and incoherent parts; $\rho \equiv \langle\rho\rangle + \tilde{\rho}$. By neglecting cubic and higher powers in $\tilde{\rho}$ we obtain a solution for the coherent reflectivity $\langle\rho\rangle$ that is rigorously accurate in the limits of both large and small thickness errors, and that tends also to be quite accurate in the intermediate regime.

This solution is presented in eq. II-5-42; an approximate steady-state version that has a qualitatively correct scaling is here reproduced from eq. II-5-27

$$|\langle\rho\rangle|^2 \cong \frac{|r+i\rho|^2/4}{\left(\langle\varphi\rangle - \mu'\right)^2 + \left(\langle\Delta\varphi^2\rangle + \mu''\right)^2} \qquad (IV-1-4)$$

Here μ'' is essentially the absorption per cell (defined in eq. II-1-15), and $\langle\Delta\varphi^2\rangle$ is the variance in the unit cell thickness caused by the random errors ($\langle\Delta\varphi^2\rangle$ is in phase units as defined in eq. II-5-3).

The μ'' in the denominator of eq. IV-1-4 represents the limitation imposed by absorption on the number of layers that can participate in the coherent reflection process. Through the $\langle\Delta\varphi^2\rangle$ term, the thickness errors thus impose a parallel limitation on the number of participating layers; this second limitation results from the random-walk accumulation

of dephasing.

Our solution for the incoherent reflected component is given in eq. II-5-45; sec. II-5 also contains a discussion in physical terms of the generation of this component. In eq. II-5-49 we derive a tolerance on the RMS random thickness error per cell σ allowed in x-ray multilayers

$$\sigma_{(\mathring{A})} \lesssim 3 \times 10^{-4} \cdot \left(2d_{(\mathring{A})}\right)^2 \qquad (II-1-5)$$

Spiller et al. (1980) have developed an in-situ reflectance monitoring technique (ISRM) that eliminates the random-walk accumulation of dephasing; this group has verified experimentally that ISRM substantially increases the number of layers that can successfully be fabricated in an x-ray multilayer.

In order to provide a quantitative explanation of this effect, we attempt in sec. II-6 to model the complex ISRM process. We refer to the residual kind of thickness error that can occur in such multilayers as "non-accumulating" thickness errors.

In eq. II-6-15 (together with eqs. II-6-6,7 and 8), we present a difference equation that propagates the expectation value of the amplitude reflectivity from cell to cell in the presence of non-accumulating errors. (This equation is deterministic in the sense that it contains only the variance of the random errors).

This equation is only applicable under special conditions; specifically, errors in the high-index layers (which are truncated at well-defined points on a strong ISRM signal) are considered to be negligible, and the ISRM beam is treated as linearly polarized. (In addition the equation assumes the same Gaussian statistics for all layers, but in this respect the analysis is readily generalized.)

In sec. II-6 we also present a phenomenological treatment of non-accumulating errors that can include both the effects of errors in the high index layers, and of an unpolarized probe beam.

In the steady-state limit that the number of layers is large, the reflectivity under our phenomenological model satisfies a Darwin-Prins solution. In the special case where the errors in the L and H layers are equal, this solution is

$$R = \left| \frac{r_0 e^{-2\langle \xi^2 \rangle}}{\sqrt{t_0^2 - r_0^2 e^{-4\langle \xi^2 \rangle}} - t_0} \right|^2 \qquad (IV-1-6)$$

Here $\langle \xi^2 \rangle$ is the variance in the phase error for each interface. According to eq. IV-1-6 the reflectivity in each cell is degraded by a Debye-Waller factor; such a factor also represents the degradation in x-ray reflectivity that results from the random displacement of the atoms in a diffracting crystal (James, 1965, chapter V).

Debye-Waller factors can also arise when multilayer reflectivity is degraded by interlayer diffusion. If the multilayer suffers diffusion of a kind where its ideal, sharp-interface structure is convolved with a smoothening function, then the reflectivity of the cell (r_e in eq. IV-1-6) will be multiplied by the transform of the smoothening function (the transform will be a Debye-Waller factor if the smoothening function is Gaussian).

Thus, interlayer diffusion as well as non-accumulating errors can be modeled with expressions like eq. IV-1-6.

This implies that the unit cells in the randomly disturbed structure interact together in the same way as do a corresponding set of cells having an "averaged" structure. This can be shown to be true because the incoherent reflectivity $\tilde{\rho}$ of the random structure is quite small with non-accumulating errors.

We should acknowledge at this point the previous treatment of interlayer diffusion made by Underwood and Barbee (1982).

They treat the problem of reflection from a diffused multilayer by modeling each graded interface as a stack of very thin homogeneous layers ("laminae"). They then propagate the amplitude reflectivity through each of the microlayers numerically using the standard (non x-ray) Airy recursion formula. Such a treatment will be broadly consistent with the treatment we have made, so long as the interfacial gradient is chosen in such a way that the total mass per unit cell is independent of the extent of diffusion (i.e. t_e is constant).

One limitation of the analysis presented in chapter II is that the multilayer structures considered are all one-dimensional; i.e. the structures vary only in the direction normal to the substrate. This limitation is fundamental to the characteristic matrix formalism (Born and Wolf, 1975, p.51).

At the present early stage in the development of x-ray multilayers, this limitation has not proven unduly restrictive, since in chapter II we have been able to significantly extend previous analyses of a number of basic effects that are only beginning to be investigated experimentally. However, in the future the one-dimensionality of the formalism may prove more restrictive.

Eastman (1978) has shown that one can apply what are essentially algorithms for the analysis of one-dimensional thin-film structures to the analysis of multilayers containing interfacial roughness (a three-dimensional structure) in the special case where the roughness has a very gradual variation within the layers. We have used similar physical assumptions to make a preliminary investigation of roughness in x-ray multilayers; this investigation is discussed in sec. IV-2 below.

Another limitation in our analysis is that it requires that the interaction of each unit cell with the radiation field is weak. Our formalism therefore becomes invalid as the grazing incidence regime is approached; the fractional error e introduced with our formalism is of order

$$e \sim \frac{|\Delta|}{\xi^2} \qquad (IV-1-7)$$

where ξ is the angle of incidence to the surface in radians.

Finally, we note that our analysis of non-accumulating thickness errors is somewhat more tentative than the other topics treated. This may be a useful area for future research, but the complexity of the ISRM process suggests that a more detailed analysis is likely to be most successful if made in conjunction with a parallel experimental investigation.

In Chapter III we discuss applications for x-ray multilayers. We find that in general, the reflectivity of multilayers will be strongly limited by absorption throughout the soft x-ray region. Our calculations indicate that the absorption-limited reflectivity can be at most 0.8, and that reflectivities will usually be considerably lower unless new materials combinations prove feasible.

The weak interaction of the layer materials with the radiation will cause x-ray multilayers to have a narrow spectral bandwidth. However, at longer wavelengths ($\lambda \sim 100\text{Å}$), and at normal incidence, a multilayer focussing element can have a fairly large aperture (typically f/3).

The multilayer acceptance angle decreases as the 2d-spacing or angle of incidence to the surface is reduced (so long as the latter is greater than 45°). If the wavelength is less than about 40Å, structural defects are likely to prohibit operation at normal incidence. The largest possible acceptance angle is then obtained near grazing incidence. At such angles, geometrical aberrations impose strong additional limitations on the performance of focussing elements.

We should note that despite these limitations, multilayers are likely to prove quite attractive in comparison with alternative optical technologies for the soft x-ray regime, in certain applications.

Chapter III discusses the specific application of multilayers to the problem of constructing an optical cavity for future x-ray lasers. The most promising cavity configuration appears to be one based on multilayers whose structure is optimized for maximum reflectivity at normal incidence; in such a cavity each single loss upon reflection is compensated for by a

pass through the amplifier. The tolerance on systematic error in d-spacing that must be satisfied to achieve resonance at normal incidence is (reproduced from eq. III-2-1)

$$\delta d_{(\text{Å})} \cong 1.3 \times 10^{-6} \left(2d_{(\text{Å})}\right)^3 \qquad (\text{III-1-8})$$

Damage may be an important consideration in an x-ray laser cavity. As an example we consider preliminary experiments carried out at the Laboratory for Laser Energetics (LLE) of the University of Rochester (Bhagavatula and Yaakobi, 1978, Conturie, 1982); we estimate that if these experiments can be scaled up to produce a true x-ray laser, the permissible thermal loading on the mirrors will limit nanosecond x-ray laser pulses to energies of order $8 \cdot 10^{-5}$ Joules.

Since, in the scheme considered, the beam aperture will probably be considerably smaller than the mirror substrates, it may be possible to use the mirrors in a quasi-one-shot mode, in which only a small portion of the substrates are exposed in each shot.

The most attractive alternative to a cavity configuration based on normal incidence multilayers may be the ring cavity devised by Bremer and Kaihola (1980), in which a large number of specular reflections are used to return the beam to the amplifier (fig. III-2-2b). We have written a computer program to search for optimum materials for the ring cavity; the results listed in table III-2-1 indicate that efficiencies as high as 0.4

may be possible.

In sec. III-3 we consider the possible use of x-ray multilayers in a Kirkpatrick-Baez short-wavelength ($\lambda \cong 2\text{Å}$) x-ray microscope (Kirkpatrick and Baez, 1948). At present such systems use single layer coatings illuminated at very glancing angles. Multilayer coatings might be useful as a means of operating such a system at an increased angle of incidence to the surface (this would reduce the geometrical aberrations of the focussing elements); however our analysis of the LLE system indicates that one will have to accept a trade-off between collection aperture (limited by spherical aberration) and field of view, since the larger angles of incidence that will reduce spherical aberration will also reduce the acceptance angle of the coatings.

We have designed multilayer coatings to convert the Kirkpatrick-Baez system in use at LLE to operation at 1.66Å. The principal difficulty in fabricating such a coating is likely to be the need for an absolute thickness accuracy of about 1Å per layer (the layer thicknesses are about 40Å), with the exact thickness required being strongly dependent on the optical constants of the layers. The tolerance is determined primarily by the need to accurately align the narrow zone of high reflectance with the optical axis.

Section IV-2 - Suggestions for Future Work

Part A) Interfacial Roughness

As x-ray multilayers come into wider use, there is likely to be an increasing interest in using experimental measurements of performance to characterize multilayer structures in detail (see part B below). The methodology and analysis presented in chapter II provide both tools for such future modeling, and an indication of the range of effects that will have to be accounted for.

With the possible exception of our neglect of interfacial roughness, we have attempted in Chapter II to form more or less as comprehensive a theoretical treatment of x-ray multilayers as is reasonable at the present early stage of experimental investigation.

Multilayers containing interfacial roughness will have a three-dimensional structure, to which the one-dimensional formalism of Chapter II can only be applied in special cases. Further, in the absence of contrary experimental evidence, it is impossible to rule out any of an enormous range of possible magnitudes and statistical correlations for the roughness; these parameters might vary from interface to interface, and the statistical correlations might extend between the interfaces as well as within them.

In this section we present a brief summary of a preliminary investigation we have made of certain limiting case roughness models (see fig. IV-2-1); these models may be representative of the categories of roughness that could be encountered in practice, so that our analysis may

CATEGORIES OF ROUGHNESS - REPRESENTATIVE MODELS

UR LLE

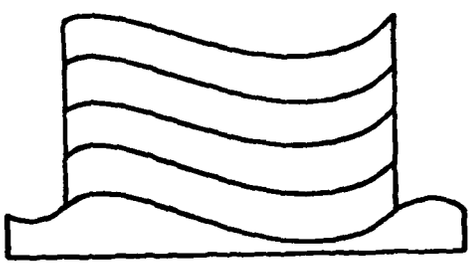

"Identical Films" — All layers reproduce a common roughness profile present in the substrate. This is typical of roughness in optical multilayers.

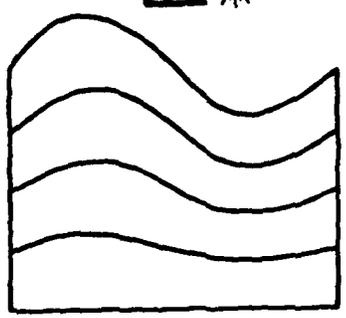

"Columnar Films" - Growth rate of films varies randomly across substrate. Multilayer is periodic within each columnar region. Roughness increases linearly with thickness.

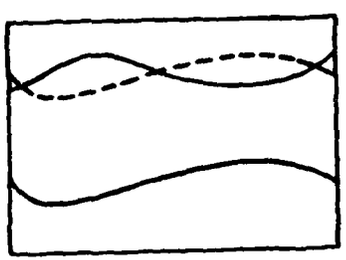

"Roughening Films" — Thicknesses of films vary randomly and in an uncorrelated way. Granularity in each film adds to a baseline of roughness established by preceeding layers. Roughness accumulates in a random-walk fashion.

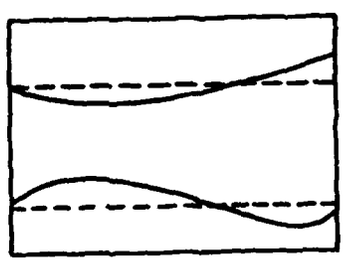

"Smoothening Films" — Roughness in different interfaces is uncorrelated. Films have a leveling property during formation. Cell boundaries can be those of ideal structure. Mean roughness heights are equal in all interfaces.

Figure IV-2-1

X365

serve as a basis for future work.

Eastman (1978) has developed numerical matrix methods to treat the effect of interfacial roughness in optical multilayers. We have used similar physical assumptions to treat certain kinds of roughness in periodic x-ray multilayers analytically. These physical assumptions are discussed more fully in Appendix 14. In effect, our model assumes that the near-field reflected amplitude above any point on the multilayer's surface can be calculated (in principle) by inserting local values for the layer properties into a one-dimensional formalism. Such a scalar model of the roughness requires that the transverse autocorrelation length of the roughness be large compared to the layer thicknesses. Carniglia (1981) provides a review of Eastman's formalism and physical assumptions, and extends Eastman's formalism to the treatment of what he calls "additive roughness" (which we call "roughening films"; see below), and bulk scattering.

Elson (1979) discusses the limitations of scalar scattering theory in comparison with more rigorous theories (in the context of single-surface reflection). In general, we expect the scalar theory to be best at predicting total specular and diffuse reflectivities, and at predicting the angular distribution of the diffusely reflected beam at angles close to the specular beam; it cannot predict polarization effects.

We also note that the use of a one-dimensional scalar formalism to treat the field within the multilayer is shown in Appendix 14 to be valid only when the separation between the specular and diffuse beams is within the acceptance angle of the multilayer. Since the acceptance angle is likely to be of the order of the field of view in imaging applications,

the scalar model is applicable to the problem of resolution degradation via scattering.

One disadvantage (in the x-ray context) of existing vector analyses of multilayer roughness is that they are first-order perturbation theories (Elson, 1977; Bousquet et al., 1981; Elson et al., 1980), and so cannot treat roughness large enough to substantially degrade the reflectivity. In addition, first-order perturbation theories take the scattered beam to be driven by the undegraded one-dimensional electromagnetic field. They therefore do *not* calculate the change in transmission or absorption of this one-dimensional field, and so cannot be used to calculate the degradation in specular reflectivity.

Eastman's (1978) matrix method is based on what is in essence a sophisticated Taylor expansion (carried out in a one-dimensional formalism), of the reflectivity in terms of successive powers of the interfacial displacements that correspond to the rough features. Eastman derives systematic numerical procedures with which to evaluate the terms in such an expansion. At second order one can obtain the lowest order term for the degradation in specular reflectivity.

In the x-ray case, our analytic expressions for the reflectivity of rough periodic multilayers do not result from any kind of expansion of the reflectivity in terms of the roughness heights, and so we can readily treat the effect of large roughness.

One kind of multilayer roughness that has been treated with the scalar theory is that which Eastman (1978) calls "identical films", in which all layers are considered to reproduce a common roughness profile

(generally that of the substrate, see fig. IV-2-1). The autocorrelation length of the roughness in the longitudinal direction is therefore very large. Haelbich, Segmuller, and Spiller (197[illegible], and Barbee (1982), have modeled the observed degradation in x-ray multilayer reflectivity with the same expression as results from the identical film model (eq. III-1-1).

The analysis of the identical films case is the same in both the x-ray and optical regimes. Essentially, the near-field reflected wavefront is found to undergo the same kind of phase deformations as does a wavefront reflected from a single rough surface.

We have modeled two kinds of non-identical roughness in which the longitudinal autocorrelation length is very small, so that the roughness contributions from the different layers are either completely uncorrelated, or correlated across only a small number of layer pairs. We refer to the two as "roughening films" and "smoothening films". Roughening films and smoothening films have been analyzed by Carniglia (1981), who refers to them as "additive" and "uncorrelated" roughness, respectively. We have also modeled rough films of a kind we call "columnar films" which, like identical films, have a very large longitudinal autocorrelation length. The four roughness models are illustrated schematically in fig. IV-2-1.

In the case of roughening films, we assume that the errors in the local layer thicknesses above each point on the surface cause a cumulative dephasing, so that the absolute roughness of the top layer increases in a random walk fashion as more layers are added. One may consider the formation of these films to be such that the granularity introduced by

each layer is added independently to a baseline of roughness established by preceeding layers.

Under the assumptions of the scalar model, the near-field amplitude under roughening films is given by our solution for one-dimensional accumulating random thickness errors, derived in sec. II-5. The far field coherent amplitude reflectance is obtained by evaluating:

$$\langle \rho(\Delta\theta, \varphi) \rangle =$$

$$\frac{\cos\theta_B}{\lambda r_B} \int_{-\infty}^{\infty}\int dx\,dy \left[\left\langle \rho_J(x,y)\, e^{2i \sum_{k=1}^{J-1} \Delta\varphi_k(x,y)} \right\rangle \cdot e^{-ikx\,\Delta\theta\cos\theta_0}\, e^{-iky\varphi} \right] \qquad (IV\text{-}2\text{-}1)$$

We have defined $\langle \rho(\Delta\theta, \varphi) \rangle$ in such a way that its magnitude squared is the far-field power per unit area divided by the incident power per unit area. In letting the limits on the integrals go to infinity, we neglect diffraction from the edges of the multilayer.

In eq. IV-2-1, x and y are coordinates along the surface, r_β is the distance from x,y to the observation point, and $\rho_J(x,y)$ is the near-field amplitude as measured at the upper surface of the multilayer (fig. IV-2-2). This upper surface is rough, so the factor $\exp\left(2i \sum_{k=1}^{J-1} \Delta\varphi_k(x,y)\right)$ must be used to propagate $\rho_J(x,y)$ to a mean plane,

COORDINATE SYSTEM FOR SCATTERED RADIATION
(not standard polar coordinates)

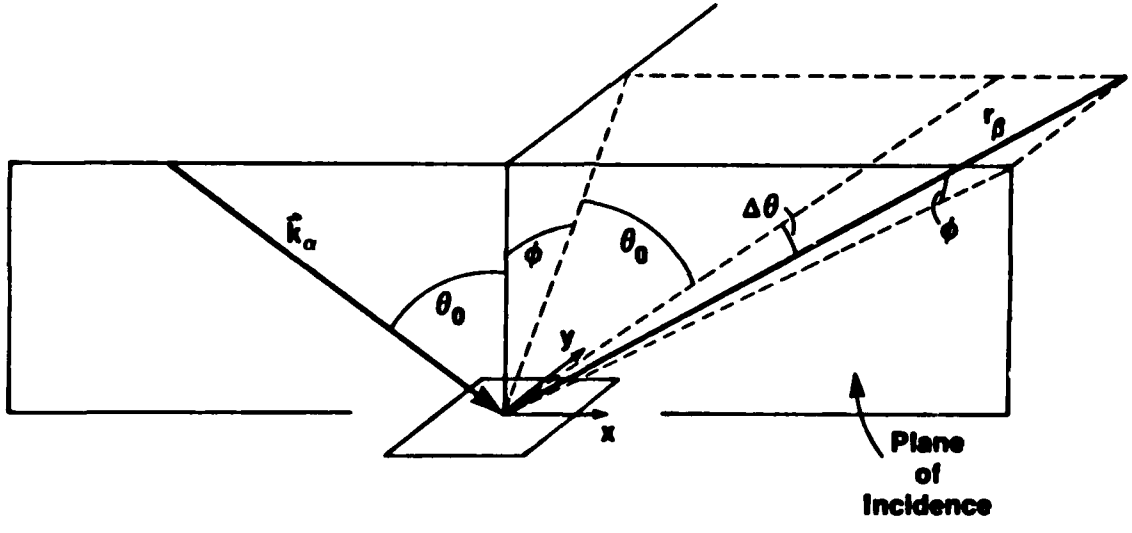

The scattering angles $\Delta\theta$ and ϕ are assumed to be small.

X361

Figure IV-2-2

where the far-field amplitude can properly be evaluated via the Fourier transform. This equation is derived in more detail in Appendicies 14 and 15. Similar results are derived by Eastman (1978) and Carniglia (1981).

We assume that the statistical properties of the roughness do not vary across the surface. Thus, assuming as we have that the expectation value can be interchanged with the transform, the transform's argument is independent of x and y, and $\langle \rho(\Delta\theta, \varphi) \rangle$ will be a delta-function of the angle of reflection. (As noted, we neglect diffraction from the mirror boundaries.)

$|\langle \rho_y e^{2i\sum_{n=1}^{J-1}\Delta\varphi_n} \rangle|^2$ can therefore be identified as the specular reflectivity. The assumptions of the scalar scattering theory thus permit reduction of the problem to one dimension, where our difference equation formalism can be exploited. Our expression for $\langle \rho_y e^{2i\sum_{n=1}^{J-1}\Delta\varphi_n} \rangle$ in the soft x-ray regime is derived in Appendix 15, and is

$$\langle \rho_y(x,y)\, e^{2i\sum_{n=1}^{J-1}\Delta\varphi_n(x,y)} \rangle$$

$$= \langle\rho\rangle e^{-2(J-1)\langle\Delta\varphi^2\rangle} + 2\langle\Delta\varphi^2\rangle\langle\rho\rangle \frac{e^{2i(J-2)\tilde{\delta}} - e^{-2(J-1)\langle\Delta\varphi^2\rangle}}{i\tilde{\delta} + \langle\Delta\varphi^2\rangle}$$

$$- \langle\rho\rangle e^{2i(J-1)\tilde{\delta}} \frac{i\tau + \rho}{i\langle t\rangle + \langle\Delta\varphi^2\rangle} \langle\rho\rangle \qquad (\text{IV-2-2})$$

where $\langle\rho\rangle$ (the near-field coherent reflectivity) is given by

eq. II-5-35, and $\tilde{\delta}$ is given by eq. II-5-15. This expression asumes that absorption has reached its steady-state value.

A diffuse beam is also present. The total intensity of the diffuse and specular beams is determined by the total absorption, which is the same as in the case of one-dimensional random thickness errors (sec. II-5).

The diffuse beam can be regarded as radiation that has been diffracted from the rough structure impressed on the near-field reflected wavefront. This rough structure is represented by variations in the near-field phase and amplitude, which are caused by rough features in the underlying multilayer. The transverse scale-length of these features determines the angular spread of the diffuse beam.

If, under roughening films, the transverse variations in layer phase thickness obey a Gaussian bivariate distribution with autocorrelation $C_T(v)$, where

$$C_T(v) \equiv \langle \Delta\varphi_R(x,y)\, \Delta\varphi_R(x',y') \rangle \Big/ \langle \Delta\varphi^2 \rangle \qquad (IV-2-3)$$

with

$$v \equiv \sqrt{(x-x')^2 + (y-y')^2} \qquad (IV-2-4)$$

then we find (Appendicies 14 and 15) that the diffuse beam is given by

$$\frac{1}{W_0}\frac{dW_{Diffuse}}{d\Omega} = \frac{2\pi\cos\theta_0}{\lambda^2}\int_0^\infty dv \cdot v \cdot \langle \tilde{\rho}_J(x,y)\,\tilde{\rho}_J^*(x',y')\rangle \cdot J_0\left(\frac{2\pi}{\lambda}\sqrt{\cos^2\theta_0\,\Delta\theta^2+\varphi^2}\;v\right) \qquad (IV-2-5)$$

where W_0 is the incident power, $dW_{Diffuse}$ is the power scattered into the solid angle $d\Omega = d(\Delta\theta)\,d\varphi$, and where, for roughening films, we have defined

$$\tilde{\rho}_J(x,y) \equiv \rho_J(x,y)\,e^{2i\sum_{k=1}^{J-1}\Delta\varphi_k(x,y)} - \langle \rho_J(x,y)\,e^{2i\sum_{k=1}^{J-1}\Delta\varphi_k(x,y)}\rangle \qquad (IV-2-6)$$

We find (Appendix 15)

$$\langle \tilde{\rho}_J(x,y)\,\tilde{\rho}_J(x',y')\rangle = -2\mathrm{Re}\left\{2a''e^{-2k(\mu''+\langle\Delta\varphi^2\rangle)}\left[F\cdot H\cdot e^{2kC_T(v)\langle\Delta\varphi^2\rangle} - G\cdot M - N\cdot e^{-ik\langle t\rangle}(F-G)\right] - a|\langle\rho\rangle|^2\left[He^{2kC_T(v)\langle\Delta\varphi^2\rangle} - M\right]\right\} \qquad (IV-2-7)$$

where

$$a \equiv (K-1)(ir+p)\langle\rho\rangle^{*}$$

$$F \equiv \frac{1}{1-\dfrac{2\langle\Delta\varphi^{2}\rangle(1-C_{T}(v))}{i\langle t\rangle+\langle\Delta\varphi^{2}\rangle}}$$

$$G \equiv \frac{1}{1-\dfrac{2\langle\Delta\varphi^{2}\rangle}{i\langle t\rangle+\langle\Delta\varphi^{2}\rangle}}$$

$$H \equiv \operatorname{sinch}\left(2(K-1)(\mu''-\langle\Delta\varphi^{2}\rangle(1-C_{T}(v))\right)$$

$$M \equiv \operatorname{sinch}\left(2(K-1)(\mu''-\langle\Delta\varphi^{2}\rangle)\right)$$

$$N \equiv \operatorname{sinch}\left((K-1)(\mu''-i\langle t'\rangle-\langle\Delta\varphi^{2}\rangle)\right)$$

$$\operatorname{sinch}(x) \equiv \sinh(x)/x \qquad \text{(IV-2-8)}$$

We have also developed an analytic model for the kind of roughness we call "smoothening films" (fig. IV-2-1). Such films may be considered to have a leveling nature during some stage of formation, but to nonetheless possess an intrinsic roughness after formation is complete. We consider the resulting rough interfaces to vary randomly with zero mean about the defect-free interfacial planes.

We therefore assume that an error in the local thickness that a layer has at some position on the reflector will (on average) be compensated for in the thickness of the next layer deposited.

Smoothening films are thus analogous to non-accumulating random thickness errors under the phenomenological model of sec. II-6-C. The mathematical analysis of smoothening films is carried out in Appendix 14. We show there that the specular reflectivity in the presence of smoothening films is given by

$$\langle \rho_s \rangle = \langle \rho_{ss} \rangle \left(1 - e^{2i\tilde{\delta}(K-1)}\right) \Big/ \left(1 - \langle \rho_{ss} \rangle^2 e^{2i\tilde{\delta}(K-1)}\right) \qquad (IV-2-9)$$

where

$$\langle \rho_{ss} \rangle = \left(r_0 e^{-2\langle \xi^2 \rangle}\right) \Big/ \left(\sqrt{t_0^2 - r_0^2 e^{-4\langle \xi^2 \rangle}} - t_0\right) \qquad (IV-2-10)$$

and

$$\tilde{S} \equiv -t_0 - r_0 e^{-2\langle \xi^2 \rangle} \langle \rho_{ss} \rangle \qquad \text{(IV-2-11)}$$

Eq. IV-2-9 assumes Gaussian statistics for the roughness. $\langle \xi^2 \rangle$ is the variance in the phase error per interface.

In the case of smoothening films we have made a preliminary investigation of the effect of finite longitudinal autocorrelations on the magnitude of the diffusely scattered radiation; in other words, we allow the rough features in the interfaces to be correlated across a small number of layers. The reflectivity of the group of layers within one longitudinal autocorrelation length must be small compared to one (implicitly defining an upper limit for the autocorrelation length), and, at a minimum, the roughness must be strongly correlated across the two interfaces of at least one of the two layers in each layer pair.

We find that the fraction of the total power scattered into the diffuse beam is

$$\frac{W_{Diffuse}}{W_0} = \frac{|r_0|^2 e^{-4\langle \xi^2 \rangle}}{4\tilde{S}''} \left[\left(1 + |\langle \rho \rangle|^4\right) A - 2B\,\mathrm{Re}\left(\langle \rho \rangle^2\right) \right]$$

(IV-2-12)

where

$$A = \left(e^{4\langle\xi^2\rangle} - 1\right) + 2\sum_{s=1}^{\infty}\left(e^{4\langle\xi^2\rangle C_L(s)} - 1\right)$$

$$B = \left(1 - e^{-4\langle\xi^2\rangle}\right) + 2\sum_{s=1}^{\infty}\left(1 - e^{-4\langle\xi^2\rangle C_L(s)}\right) \qquad (IV-2-13)$$

Here $C_L(s)$ is the longitudinal autocorrelation function defined by

$$\langle \xi_K \xi_{K'} \rangle = C_L(s)\langle\xi^2\rangle$$

$$s \equiv |K - K'| \qquad (IV-2-14)$$

(Gaussian statistics are again assumed). If $C_L(s)$ has a width s_{Typ}, the number of cells within one longitudinal autocorrelation length will be of order $2s_{Typ} + 1$ (s is non-negative). According to eq. IV-2-12, the diffusely scattered intensity will scale approximately linearly with this quantity.

In the case of longitudinally uncorrelated roughness, the angular distribution in the diffuse beam is given by eq. IV-2-5 with the kernal (for smoothening films)

$$\langle \tilde{\rho}(x,y)\,\tilde{\rho}^*(x',y') \rangle \equiv \langle \tilde{\rho}(x,y)\,\tilde{\rho}^*(x',y') \rangle$$

(continued on next page)

$$= \left[|r_0|^2 e^{-2\langle \xi^2 \rangle (2 - C_T(v))} \sinh\left(2\langle \xi^2 \rangle C_T(v)\right) \right.$$

$$\left. \times \left(1 - 2\mathrm{Re}\,|\langle \rho \rangle^2|\, e^{-4\langle \xi^2 \rangle C_T(v)} + |\langle \rho \rangle|^4\right)\right] \Big/ 2\tilde{s}^4$$

(IV-2-15, continued)

Here C_T is the transverse autocorrelation function defined in eq. IV-2-3.

The roughness height necessary to cause a given drop in specular reflectivity is much larger with smoothening films than with roughening films, because the thickness errors do not accumulate (see fig. IV-2-3). (In the case of roughening films, the horizontal axis in the figure represents the RMS roughness increment added by each unit cell.)

The leveling property of smoothening films causes the intensities of the diffuse and specular beams to become equal only at a level of roughness where the total reflectivity has been decreased quite substantially (via an increase in absorption). In contrast, with roughening films, the two become equal at a roughness level where the total reflectivity is only moderately decreased. With identical films, the total reflectivity is unaffected by the magnitude of the roughness.

With films of both the roughening and smoothening types, the total absorption reaches a steady-state level as more and more layers are added. However, in the case of roughening films the proportion of the reflected radiation in the specular beam steadily decreases, since the upper surfaces get steadily rougher.

EFFECT OF ROUGHNESS - REFLECTION INTO SPECULAR BEAM

UR LLE

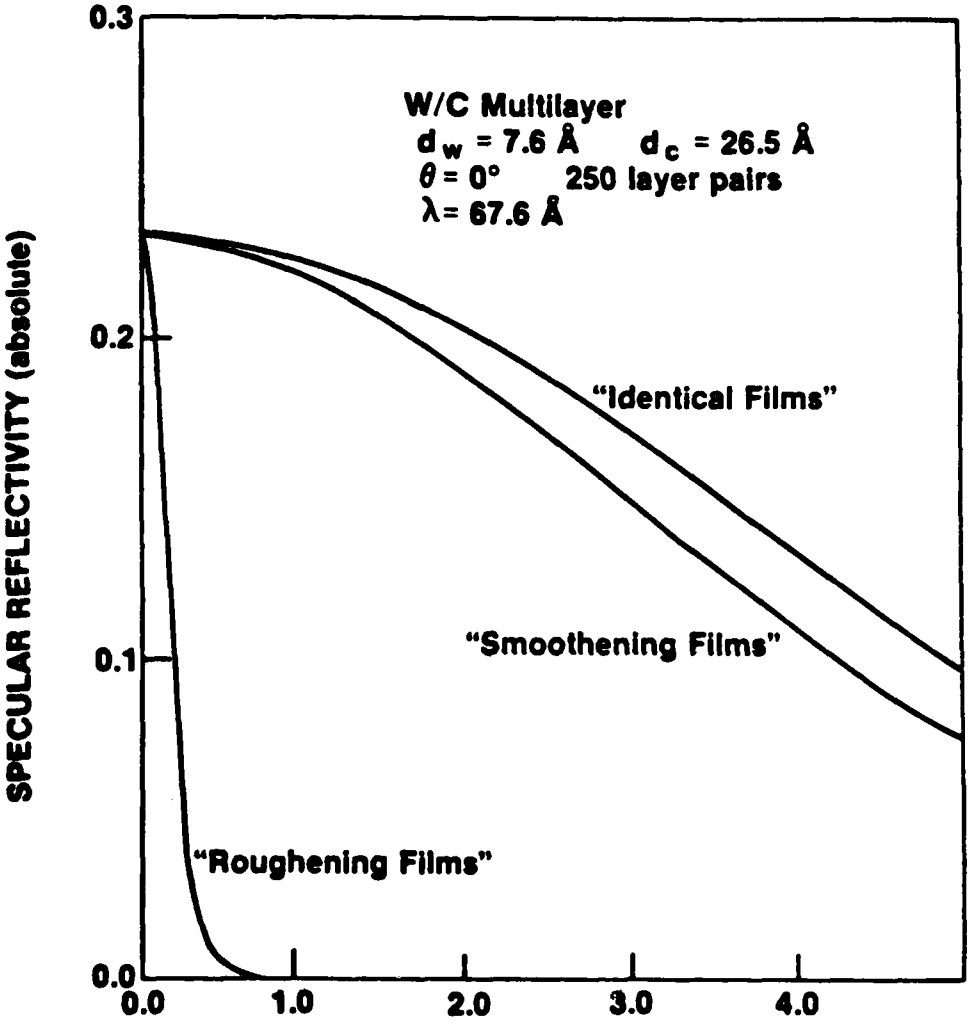

(For roughening films, abscissa is roughness increment per cell)

X282

Figure IV-2-3

The acceptance angle of multilayers with smoothening films is not greatly influenced by the RMS magnitude of the roughness. In the case of roughening films, the acceptance angle is increased in somewhat the same way as would be caused by an increase in the layer bulk absorption constants.

We note that the effect of smoothening films is very similar to that of interlayer diffusion. As in the case of non-accumulating thickness errors, this is a consequence of the relatively small intensity of the diffuse or incoherent beam. The intensity of the diffuse beam will usually be small compared to that of the specular beam under smoothening films, even though the specular reflectivity may be considerably less than it would be in the absence of roughness. The main effect of the roughness in the smoothening films case is to cause an increase in absorption, not an increase in scattering. This is because the diffusely scattered components from the different interfaces add incoherently, and incoherent scattering is a weak process in the x-ray regime.

We have also made a preliminary analysis of a kind of roughness we call "columnar films" (fig. IV-2-1). Here the growth rate of the films is assumed to vary randomly across the substrate surface, so that the roughness of the upper interface increases linearly as more layers are added. Such a linear increase has been observed in thin single films of Au and AuPd (not multilayers) by Broers and Spiller (1980a, 1980b).

In the case of columnar films we have only calculated the specular reflectivity, which we show in Appendix 15 to be given by (assuming Gaussian statistics)

$$\langle \rho_J \rangle = \rho_{0,J} \frac{i\langle t\rangle e^{-2i\langle t\rangle(J-1)}}{\left(1 - e^{-2i\langle t\rangle(J-1)}\right)} \frac{e^{-\langle t\rangle^2/2\pi^2\langle \Delta K^2\rangle}}{\sqrt{2\pi\langle \Delta K^2\rangle}}$$

$$\times \left[\Phi\left(\frac{i\langle t\rangle}{\sqrt{2\pi^2\langle \Delta K^2\rangle}}\right) - \Phi\left(\frac{i\langle t\rangle}{\sqrt{2\pi^2\langle \Delta K^2\rangle}} - 2\pi^2\langle \Delta K^2\rangle\right)\right]$$

(IV-2-16)

where $\rho_{0,J}$ is the defect-free solution of eq. II-2-13, $\langle \Delta K^2 \rangle$ is the variance in growth rate (i.e. $\langle \Delta d^2 \rangle / \langle d \rangle^2$), and Φ is the error function in the complex plane

$$\Phi(w) \equiv \frac{2}{\sqrt{\pi}} \int_0^w dx\, e^{-z^2} \qquad \text{(IV-2-17)}$$

where the path is arbitrary. Eq. IV-2-16 is based on the approximate results in eqs. II-3-1 and 2, and so is less accurate than the results for smoothening films and roughening films. Eq. IV-2-16 is plotted for our usual example (tungsten-carbon multilayer at 67.6Å) in fig. IV-2-4.

In terms of the above comparison between roughening films and smoothening films, the characteristics of columnar films tend to resemble those of roughening films; however the scaling with roughness height and with J is different.

We note that the effect on specular reflectivity of substrate roughness acting in combination with any of the other three roughness models may be modeled by multiplying the specular reflectivity by a Debye-Waller factor. (More precisely, this represents the uncorrelated superposition of an invariant roughness profile of the identical films kind with one of the other types of roughness). Such a combination of identical films and roughening films has been termed "partially correlated" films by Elson et al. (1980).

EFFECT OF ROUGHNESS - REFLECTION INTO SPECULAR BEAM

UR
LLE

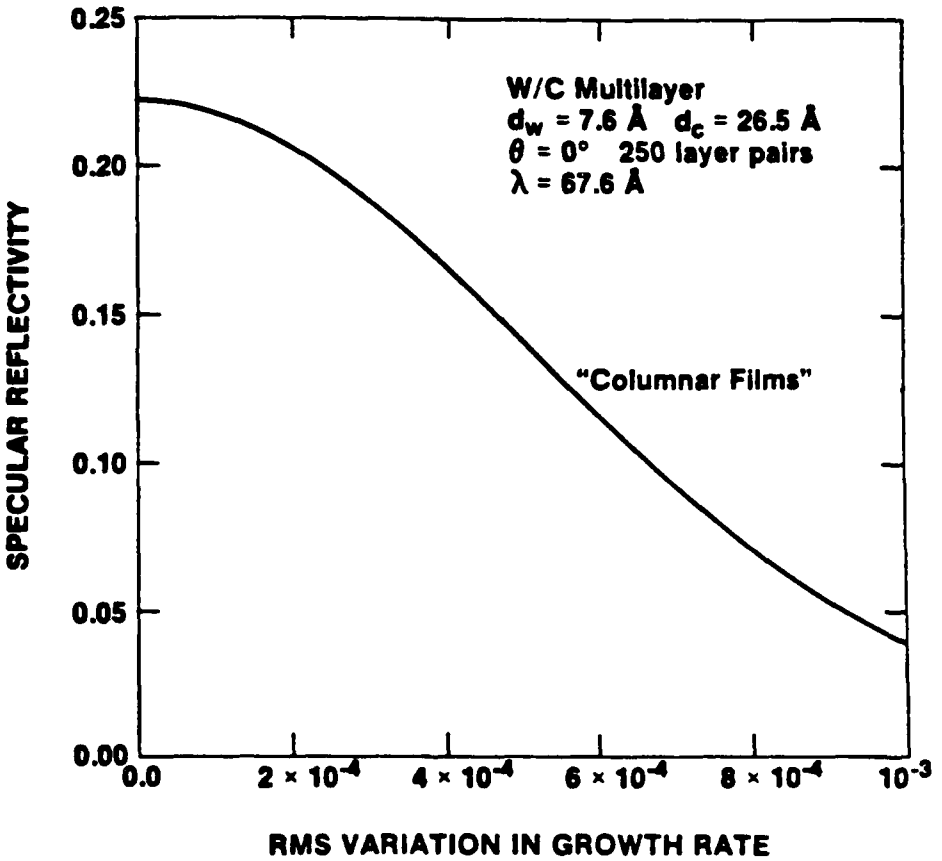

X362

Figure IV-2-4

Part B) Future Work

Our analysis suggests that different kinds of defects in x-ray multilayers may produce characteristic signatures in the reflecting properties. Such signatures might enable one to evaluate the reflecting structure present in a particular multilayer.

We will now summarize these characteristic properties.

Accumulating random thickness errors (one-dimensional) will produce no diffuse beam, but will produce a significant anomolous broadening of the bandwidth as the 2d-spacing is decreased. (However, this broadening will be relative to the trend of eq. II-3-21). Non-accumulating one-dimensional errors will likewise produce no diffuse beam, but will produce a smaller change in bandwidth than accumulating errors, particularly at longer wavelengths.

Smoothening films will have a very similar effect on reflectivity to non-accumulating thickness errors; the main difference being that smoothening films will also generate a diffusely scattered beam of low intensity, but in practice this weak and spatially dispersed beam might be masked by background.

Roughening films will have the same total reflectivity as will accumulating one-dimensional errors, but the fraction of this intensity in the specular beam will steadily decrease as the number of layers is increased.

If absorption has reached the steady-state with roughening films, the diffuse radiation will equal the specular radiation at a relatively small roughness height; in other words, as 2d-spacing is reduced, the diffuse and specular beams will become equal at a point where the total reflected radiation has decreased only slightly. In contrast, with smoothening films the two will become equal only when the overall reflectivity is very much less than that of a defect-free (large 2d-spacing) structure.

Our analysis suggests that non-accumulating defects of all kinds will have very similar properties. If we consider the progression of such defects from the case of interpenetrating rough features having transverse widths small compared to a wavelength (interlayer diffusion), through the case of roughness intermediate in transverse scale between the mirror substrate and the radiation wavelength (smoothening films), and on to the case where entire interfaces are randomly displaced relative to the substrate (non-accumulating thickness errors), then throughout the progression we find that the coherent beam remains virtually unchanged, and that the incoherent beam remains of low intensity, while it changes from an evanescent wave to a diffuse beam, and finally to a weak component in the Bragg direction. The low strength of the incoherent component would make the different non-accumulating errors difficult to distinguish in practice.

Identical films are different from the other kinds of roughness in that the total power in the diffuse and specular beams is unaffected by the roughness.

Columnar films appear to have qualitatively similar properties to roughening films (our examination of columnar films is less complete than that of the other roughness models). However, the scaling of roughening films and columnar films with the total number of layers J is different; thus to distinguish the two kinds of defects one could compare the constancy as J is changed of best-fit values for sigma determined with the two models (say by changing the 2d-spacing).

We do not wish to downplay the difficulties associated with the measurements suggested by the above characteristics. Any method involving measurement of an incoherent component of radiation that is scattered very close to the specular beam will call for careful experimental technique and judicious interpretation (for example, in a practical case the specular beam will probably be in the near-field rather than the far field).

We should mention the possibility of direct measurement of any roughness that may be present. At the point where they cause a substantial degradation in multilayer reflectivity, roughness of the kinds considered would produce 2 - 10Å RMS roughness in the upper interfaces of a multilayer with a 2d-spacing of $\sim$ 100Å.

Such roughness heights are at the periphery of what is measurable with present technology, depending very much on the transverse scale length of the roughness (Stedman, 1981, Price, 1982).

We also note that an experimental investigation based on qualitative signatures such as those above will be considerably more difficult if the structure contains more than one kind of defect in significant

proportions.

An obvious motivation for such a study is the possibility that the results would suggest changes in the fabrication procedures that could lower the magnitude of the defects.

Another possibility is that a detailed understanding of the structural defects present would permit compensation to be made in the design of the multilayers. Modest gains in performance might be obtained in the presence of accumulating errors, or with non-accumulating errors under low absorption conditions, by choosing a structure that produces a comparatively large reflectivity from comparatively few layers. Such a structure would cause too large an absorption to provide optimal reflectivity with a large number of layers if no disorder were present; however it might provide the largest reflectivity possible in the presence of disorder.

Our work also suggests that examination of new multilayer materials may prove fruitful. Table II-2-1 (and a more lengthy version that lists multiple possibilities at each wavelength) suggests materials combinations that are worth investigating.

Bibliography

T.W. Barbee (1982), "Sputtered Layered Synthetic Microstructure (LSM) Dispersion Elements", in Low Energy X-Ray Diagnostics - 1981, D.T. Attwood and B.L. Henke, Eds. (AIP, 1982), 131-45.

T.W. Barbee and D.C. Keith (1979), "Layered Synthetic Microstructures - Application as X-Ray Dispersion Elements", Stanford SSRL Report No. 79/02, 185-94.

B.W. Batterman and H. Cole (1964), "Dynamical Diffraction of X-Rays by Perfect Crystals", Rev. Mod. Phys. 36, 681-717.

P.W. Baumeister (1962), "Applications of Thin Film Coatings", in Optical Design, MIL-HDBK-141, Defense Supply Agency, Washington, D.C., chptr. 20.

P.W. Baumeister (1981), "Theory of Rejection Filters with Ultranarrow Bandwidths", J. Opt. Soc. Am. 71, 604-6.

J.H. Bechtel (1975), "Heating of Solid Targets with Laser Pulses", J. Appl. Phys. 46, 1585-93.

V.A. Bhagavatula and B. Yaakobi, "Direct Observation of Population Inversions Between Al+11 Levels in a Laser Produced Plasma", Opt. Commun. 24-3, 331-4.

M. Born and E. Wolf (1975), Principles of Optics, (Pergamon, Great Britain).

P. Bousquet et al. (1981), "Scattering from Multilayer Thin Films: Theory and Experiment", J. Opt. Soc. Am. 71, 1115-23.

J. Bremer and L. Kaihola (1980), "An X-Ray Resonator Based on Successive Reflections ...", Appl. Phys. Lett. 37, 360-2.

A. Broers and E. Spiller (1982a), "A Comparison of ... Electron Micrographs ... with X-Ray Interference Measurements of ... Roughness", in Scanning Electron Microscopy, (SEM Inc., AMF O'Hare), 201-8.

A. Broers and E. Spiller (1982b), "On the Problem of Coating Samples for High-Resolution Low-Loss Surface SEM", in Microbeam Analysis, D.B. Wittry, Ed., (San Fransisco Press, San Fransisco), 36-42.

A. Burek (1976), "Crystals for Astronomical Spectroscopy", Space Sci. Instrum. 2, 55-104.

C.K. Carniglia (1979), "Scalar Scattering Theory for Multilayer Optical Coatings", Opt. Eng. 18, 104-15.

C.K. Carniglia and J.H. Apfel (1980), "Maximum Reflectance of Multilayer Dielectric Mirrors in the Presence of Slight Absorption", J. Opt. Soc. Am. 70, 523-34.

Y.G. Conturie (1982), "Development of an XUV Amplifier", Ph.D. Thesis, University of Rochester, New York.

CRC Handbook of Tables for Applied Engineering Science (1973), (CRC Press, Cleveland).

W. Deubner (1930), Ann. der Phys. 5, 261, quoted by (Barbee, 1982).

J.B. Dinklage (1967), "X-Ray Diffraction by Multilayered Thin-Film Structures and Their Diffusion", J. Appl. Phys. 38, 3781-5.

J.M. Eastman (1978), "Scattering by All-Dielectric Multilayer Bandpass Filters and Mirrors for Lasers", in Physics of Thin Films, vol. 10, 167-226.

J.M. Elson (1977), "Infrared Light Scattering from Surfaces Covered with Multiple Dielectric Overlayers", Appl. Opt. 16, 2872-81.

J.M. Elson et al. (1979), "Scattering from Optical Surfaces", in Applied Optics and Optical Engineering, Vol. VII, R.R. Shannon and J.C. Wyant, Eds.

J.M. Elson et al. (1980), "Light Scattering from Multilayer Optics: Comparison of Theory and Experiment", Appl. Opt. 19, 669-79.

A. Franks (1977), "X-Ray Optics", Sci. Prog. Oxf. 64, 371-422.

S.V. Gaponov et al. (1981), "Long-Wave X-Ray Radiation Mirrors", Opt. Commun. 38, 7-9.

J.W. Goodman (1968), Introduction to Fourier Optics, (McGraw Hill, New York).

R.P. Haelbich and C. Kunz (1976), "Multilayer Interference Filters for the XUV Range ...", Opt. Commun. 17, 287-92.

R.P. Haelbich, A. Segmuller, and E. Spiller (1979), "Smooth Multilayer Films Suitable for X-Ray Mirrors", Appl. Phys. Lett. 34, 184-6.

B.L. Henke (1982a), "Low Energy X-Ray Spectroscopy with Crystals and Multilayers", in Low Energy X-Ray Diagnostics - 1981, D.T. Attwood and B.L. Henke, Eds. (AIP, 1982), 85-96.

B.L. Henke (1982b), "Low Energy X-Ray Interactions: ...", in Low Energy X-Ray Diagnostics - 1981, D.T. Attwood and B.L. Henke, Eds. (AIP, 1982), 146-55.

B.L. Henke et al. (1982), "Low Energy X-Ray Interaction Coefficients: Photoabsorption, Scattering and Reflection", Atomic Data and Nuclear Data Tables 27, 1-144.

A. Herpin (1947), Compt. Rendu. 225, 182. (In French.)

W. Heitler (1954), The Quantum Theory of Radiation, (Oxford Press, Oxford).

R. Hopkins (1981), Private Communication.

R.W. James (1965), The Optical Principles of the Diffraction of X-Rays, (Cornell University Press, Ithaca, NY).

P. Kirkpatrick and A. Baez (1948), "Formation of Optical Images by X-Rays", J. Opt. Soc. Am. 38, 766-74.

Z. Knittl (1976), Optics of Thin Films, (Wiley, New York).

H. Koeppe (1929), Dissertation Giessen, quoted by (Barbee, 1982).

H. Kogelnik (1976), "Filter Response of Nonuniform Almost Periodic Structures", Bell Syst. Tech. J., 55, 109-26.

P. Lee (1981), "X-Ray Diffraction in Multilayers", Opt. Commun. 37, 59-64.

I. Lovas et al. (1982), "Design and Assembly of a ... Microscope for X-Rays", in High Resolution Soft X-Ray Optics, E. Spiller, Ed. (SPIE, 1982), 90-7.

A.P. Lukirskii et al. (1964), "Reflection Coefficients for Radiation in the Wavelength Range from 23.6A to 113A ...", Opt. Spectry. 16, 168-72.

A.P. Lukirskii et al. (1965), "Reflection of X-Rays ...", Opt. Spectry. 19, 237-41.

F. Miller (1935), "A Simplification of Prins' Formula ...", Phys. Rev. 47, 209-12.

A. Papoulis (1965), Probability, Random Variables, and Stochastic Processes, (McGraw-Hill, New York).

R.H. Price (1982), "X-Ray Microscopy Using Grazing Incidence Reflecting Optics", in Low Energy X-Ray Diagnostics - 1981, D.T. Attwood and B.L. Henke, Eds. (AIP, 1982), 189-99.

M.C. Richardson (1981), Private Communication.

L.I. Schiff (1955), Quantum Mechanics, (International Student Edition, McGraw-Hill, Mexico).

J. Shellan et al. (1978), "Statistical Analysis of Bragg Reflectors", J. Opt. Soc. Am. 68, 18-27.

E. Spiller (1972), "Low Loss Reflecting Multilayers Using Absorbing Materials", Appl. Phys. Lett. 20, 365-7.

E. Spiller (1976), "Reflecting Multilayer Coatings for the Far UV Range", Appl. Opt. 15, 2333-8.

E. Spiller (1982a), Private Communication.

E. Spiller (1982b), "Evaporated Multilayer Dispersion Elements for Soft X-Rays", in Low Energy X-Ray Diagnostics - 1981, D.T. Attwood and B.L. Henke, Eds. (AIP, 1982), 24-30.

E. Spiller et al. (1980), "Controlled Fabrication of Multilayer Soft X-Ray Mirrors", Appl. Phys. Lett. 37, 1048-50.

M. Stedman (1982), "New Design for Mirror Bending Block", in Reflecting Optics for Synchrotron Radiation, M. Howells, Ed. (SPIE, 1982), 69-74.

J.H. Underwood and T.W. Barbee (1981), "Layered Synthetic Microstructures as Bragg Diffractors for X-Rays and Extreme Ultraviolet: Theory and Predicted Performance", Appl. Opt. 20, 3027-34.

A.V. Vinogradov and B. Ya Zeldovich (1977), "X-Ray and Far UV Multilayer Mirrors: Principles and Possibilities", Appl. Opt. 16, 89-93.

E. Williams (1982), Private Communication.

Appendix 1 - Perturbation Solution for the Unit Cell of an X-Ray Multilayer

Born and Wolf (1975) show that the characteristic matrix solution for the unit cell of an x-ray multilayer (in P polarization) can be obtained by solving eqs. II-1-4,5 subject to the boundary conditions of eq. II-1-6. (These equations assume that the magnetic permeability is one at x-ray frequencies). The case of S polarization will be treated later.

As discussed in sec. II-1-B, our solution will be first order in the parameter Δ, first order in the product $\varphi \cdot \Delta$, and will retain all orders of the parameter φ. In fact, the results derived in this appendix will also retain terms of order $\varphi^n \cdot \Delta$, where n may be any integer. However, the analysis of sec. II-4 (where these terms become important) will only be performed to order $\varphi \cdot \Delta$.

The calculation of the characteristic matrix elements tends to be somewhat repetitive, so we will include few intermediate steps after calculating the first one or two of these elements.

The vacuum (i.e. $\Delta = 0$) solutions to eq. II-1-4 are

$$U_1(z) = (-1)^{\frac{m-1}{2}} \frac{\cos\left(k_0 \cos\theta \cdot z - \frac{\varphi}{2}\right)}{\cos\theta} \qquad (A\text{-}1\text{-}1)$$

$$U_2(z) = (-1)^{\frac{m+1}{2}} \sin\left(k_0 \cos\theta \cdot z - \frac{\varphi}{2}\right)$$

for the odd orders, and

$$U_1(z) = (-1)^{\frac{m}{2}}\, i\, \frac{\sin\left(k_0 \cos\theta \cdot z - \frac{\varphi}{2}\right)}{\cos\theta} \qquad (A\text{-}1\text{-}2)$$

$$U_2(z) = (-1)^{\frac{m}{2}}\, \cos\left(k_0 \cos\theta \cdot z - \frac{\varphi}{2}\right)$$

for the even orders.

If we set

$$\frac{d(\ln\epsilon(z))}{dz} = \frac{d\Delta(z)}{dz} + O(\Delta^2) \qquad (A\text{-}1\text{-}3)$$

in eq. II-1-4, and then substitute eqs. A-1-1,2 into all terms of the differential equation that are first order in Δ, we obtain

$$\frac{d^2U_1}{dz^2} + k_0^2\cos^2\theta \cdot U_1 = (-1)^{\frac{m+1}{2}}\, \frac{2ik_0}{\cos\theta}\cos\left(k_0\cos\theta\cdot z - \frac{\varphi}{2}\right) + (-1)^{\frac{m+1}{2}}\, 2ik_0\, \frac{d\Delta(z)}{dz}\sin\left(k_0\cos\theta\cdot z - \frac{\varphi}{2}\right)$$

$$\frac{d^2U_2}{dz^2} + k_0^2\cos^2\theta \cdot U_2 = (-1)^{\frac{m-1}{2}}\, 2k_0^2\,\Delta(z)\sin\left(k_0\cos\theta\cdot z - \frac{\varphi}{2}\right) + (-1)^{\frac{m+1}{2}}\, 2k_0\cos\theta\, \frac{d\Delta(z)}{dz}\cos\left(k_0\cos\theta\cdot z - \frac{\varphi}{2}\right) \qquad (A\text{-}1\text{-}4)$$

for the odd orders, and

$$\frac{d^2U_1}{dz^2} + k_o^2\cos^2\theta\cdot U_1 = -(-1)^{\frac{m}{2}}\frac{2ik_o^2}{\cos\theta}\Delta(z)\sin\left(k_o\cos\theta\cdot z-\frac{\varphi}{2}\right)$$

$$+(-1)^{\frac{m}{2}}\,2ik_o\frac{d\Delta(z)}{dz}\cos\left(k_o\cos\theta\cdot z-\frac{\varphi}{2}\right)$$

$$\frac{d^2U_2}{dz^2} + k_o^2\cos^2\theta\cdot U_2 = -(-1)^{\frac{m}{2}}\,2k_o^2\Delta(z)\cos\left(k_o\cos\theta\cdot z-\frac{\varphi}{2}\right)$$

$$-(-1)^{\frac{m}{2}}\,2k_o\cos\theta\frac{d\Delta(z)}{dz}\sin\left(k_o\cos\theta\cdot z-\frac{\varphi}{2}\right) \qquad (A-1-5)$$

for the even orders.

These are harmonic oscillator equations with known driving functions. The well-known Green's function for such equations is

$$G(z,z') = H(z-z')\frac{\sin\left(k_o\cos\theta\cdot(z-z')\right)}{k_o\cos\theta} \qquad (A-1-6)$$

Our solution can now be expressed as the sum of a solution to the homogeneous equation plus the integral of the the driving function multiplied by the Green's function.

However, the required homogeneous solution will not in general be the vacuum solution of eqs. A-1-1,2; in general the amplitudes of the homogeneous solutions must be altered by terms of order $1 + \Delta$, in order that their sum with the Green's function solution satisfy the boundary conditions to order Δ.

Our solution for U_1 should therefore be of the form

$$U_1(z) = (-1)^{\frac{m-1}{2}} i \frac{A}{\cos\theta} \cos\left(k_0 \cos\theta \cdot z - \frac{\varphi}{2}\right)$$

$$+ (-1)^{\frac{m+1}{2}} \frac{2ik_0}{\cos\theta} \int_{z_1}^{z} dz' \Delta(z') \cos\left(k_0 \cos\theta \cdot z' - \frac{\varphi}{2}\right) \sin\left(k_0 \cos\theta (z - z')\right)$$

$$+ (-1)^{\frac{m+1}{2}} \frac{2i}{\cos\theta} \int_{z_1}^{z} dz' \frac{d\Delta(z')}{dz'} \sin\left(k_0 \cos\theta \cdot z' - \frac{\varphi}{2}\right) \sin\left(k_0 \cos\theta (z - z')\right)$$

(A-1-7)

for the odd orders, and

$$U_1(z) = (-1)^{\frac{m}{2}} i \frac{A}{\cos\theta} \sin\left(k_0 \cos\theta \cdot z - \frac{\varphi}{2}\right)$$

$$- (-1)^{\frac{m}{2}} \frac{2ik_0}{\cos\theta} \int_{z_1}^{z} dz' \Delta(z') \sin\left(k_0 \cos\theta \cdot z' - \frac{\varphi}{2}\right) \sin\left(k_0 \cos\theta (z - z')\right)$$

$$+ (-1)^{\frac{m}{2}} \frac{2i}{\cos\theta} \int_{z_1}^{z} dz' \frac{d\Delta(z')}{dz'} \cos\left(k_0 \cos\theta \cdot z' - \frac{\varphi}{2}\right) \sin\left(k_0 \cos\theta (z - z')\right)$$

(A-1-8)

for the even orders, with the constant A (which is of order $1 + \Delta$) still to be determined.

We determine A by finding the solution for the subsidiary field V that is defined in eq. II-1-5.

Differentiating eq. A-1-7, and employing an integration by parts on the $d\Delta(z')/dz'$ term, we find for the odd orders:

$$\frac{dU_1}{dz} = (-1)^{\frac{m+1}{2}} A k_0 \sin\left(k_0 \cos\theta \cdot z - \frac{\varphi}{2}\right)$$

$$+ (-1)^{\frac{m+1}{2}} \frac{2ik_0}{\cos\theta} \int_{z_1}^{z} dz' \Delta(z') \cos\left(k_0 \cos\theta \cdot z' - \frac{\varphi}{2}\right) \cos\left(k_0 \cos\theta (z - z')\right)$$

$$+ (-1)^{\frac{m+1}{2}} 2ik_0 \left[\Delta(z') \sin\left(k_0 \cos\theta \cdot z' - \frac{\varphi}{2}\right) \cos\left(k_0 \cos\theta \cdot (z - z')\right) \right]_{z'=z_1}^{z'=z}$$

$$+ (-1)^{\frac{m-1}{2}} 2ik_0^2 \cos\theta \int_{z_1}^{z} dz' \Delta(z') \cos\left(k_0 \cos\theta \cdot z' - \frac{\varphi}{2}\right) \cos\left(k_0 \cos\theta (z - z')\right)$$

$$+ (-1)^{\frac{m-1}{2}} 2ik_0^2 \cos\theta \int_{z_1}^{z} dz' \Delta(z') \sin\left(k_0 \cos\theta \cdot z' - \frac{\varphi}{2}\right) \sin\left(k_0 \cos\theta (z - z')\right) \qquad (A\text{-}1\text{-}9)$$

or

$$\frac{dU_1}{dz} = (-1)^{\frac{m+1}{2}} k_0 \sin\left(k_0 \cos\theta \cdot z - \frac{\varphi}{2}\right) \left[A + 2\Delta(z) \right]$$

$$+ (-1)^{\frac{m+1}{2}} 2ik_0 \Delta(z_1) \cos\left(\left(k_0 \cos\theta \cdot z - \frac{\varphi}{2}\right) + \frac{m\pi}{2} \right)$$

(continued on next page)

$$+(-1)^{\frac{m+1}{2}}\,2ik_0^2\left(\frac{1}{\cos\theta}-\cos\theta\right)\int_{z_1}^{z}dz'\Delta(z')\cos\left(k_0\cos\theta\cdot z-\frac{\varphi}{2}\right)\cos\left(k_0\cos\theta(z-z')\right)$$

$$+(-1)^{\frac{m-1}{2}}\,2ik_0^2\cos\theta\int_{z_2}^{z}dz'\Delta(z')\sin\left(k_0\cos\theta\cdot z'-\frac{\varphi}{2}\right)\sin\left(k_0\cos\theta(z-z')\right)$$

(A-1-10, continued)

so that

$$\frac{dU_1}{dz}=(-1)^{\frac{m+1}{2}}k_0\sin\left(k_0\cos\theta\cdot z-\frac{\varphi}{2}\right)\left[A+2\left(\Delta(z)-\Delta(z_1)\right)\right]$$

$$+(-1)^{\frac{m+1}{2}}\frac{2ik_0^2}{\cos\theta}\sin^2\theta\int_{z_1}^{z}dz'\Delta(z')\cos\left(k_0\cos\theta\cdot z'-\frac{\varphi}{2}\right)\cos\left(k_0\cos\theta(z-z')\right)$$

$$+(-1)^{\frac{m-1}{2}}\,2ik_0^2\cos\theta\int_{z_1}^{z}dz'\Delta(z')\sin\left(k_0\cos\theta\cdot z'-\frac{\varphi}{2}\right)\sin\left(k_0\cos\theta(z-z')\right)$$

(A-1-11)

Similarly, we find for the even orders

$$\frac{dU_1}{dz}=(-1)^{\frac{m}{2}}ik_0\cos\left(2k_0\cos\theta\cdot z-\frac{\varphi}{2}\right)\left[A+2\left(\Delta(z)-\Delta(z_1)\right)\right]$$

$$-(-1)^{\frac{m}{2}}\frac{2ik_0^2}{\cos\theta}\sin^2\theta\int_{z_1}^{z}dz'\Delta(z')\sin\left(k_0\cos\theta\cdot z'-\frac{\varphi}{2}\right)\cos\left(k_0\cos\theta(z-z')\right)$$

$$-(-1)^{\frac{m}{2}}\,2ik_0^2\cos\theta\int_{z_1}^{z}dz'\Delta(z')\cos\left(k_0\cos\theta\cdot z'-\frac{\varphi}{2}\right)\sin\left(k_0\cos\theta\cdot(z-z')\right)$$

(A-1-12)

Our origin is at z = 0. Making use of eqs. II-1-11,12, we have at $z = z_1$ that $dU_1/dz = ik_0 A$ (for all orders), and also

$$V_1(z_1) = -\frac{i}{k_0 \epsilon(z_1)} \frac{dU_1}{dz} = \frac{A}{\epsilon(z_1)} \qquad (A-1-13)$$

Given the boundary condition on V_1 in eq. II-1-6, we must have

$$A = \epsilon(z_1) = 1 + 2\Delta(z_1) + O(\Delta^2) \qquad (A-1-14)$$

Therefore, to first order in Δ, we have

$$V_1(z) = (-1)^{\frac{m+1}{2}} \sin\left(k_0 \cos\theta \cdot z - \frac{\varphi}{2}\right)$$

$$+ (-1)^{\frac{m+1}{2}} \frac{2k_0}{\cos\theta} \left\{ \sin^2\theta \int_{z_1}^{z} dz' \Delta(z') \cos\left(k_0 \cos\theta \cdot z' - \frac{\varphi}{2}\right) \cos\left(k_0 \cos\theta (z - z')\right) \right.$$

$$\left. - \cos^2\theta \int_{z_1}^{z} dz' \Delta(z') \sin\left(k_0 \cos\theta \cdot z' - \frac{\varphi}{2}\right) \sin\left(k_0 \cos\theta (z - z')\right) \right\} \qquad (A-1-15)$$

for the odd orders, and

$$V_1(z) = (-1)^{\frac{m}{2}} \cos\left(k_0 \cos\theta \cdot z - \frac{\varphi}{2}\right)$$

$$- (-1)^{\frac{m}{2}} \frac{2k_0}{\cos\theta} \left\{ \sin^2\theta \int_{z_1}^{z} dz' \Delta(z') \sin\left(k_0 \cos\theta \cdot z' - \frac{\varphi}{2}\right) \cos\left(k_0 \cos\theta (z - z')\right) \right.$$

$$\left. - \cos^2\theta \int_{z_1}^{z} dz' \Delta(z') \cos\left(k_0 \cos\theta \cdot z' - \frac{\varphi}{2}\right) \sin\left(k_0 \cos\theta (z - z')\right) \right\} \qquad (A-1-16)$$

for the even orders.

Next we employ the trigonometric identity

$$\sin^2\theta \cos a \cos b - \cos^2\theta \sin a \sin b \equiv \frac{1}{2}\cos(a+b) - \frac{1}{2}\cos 2\theta \cos(a-b) \qquad (A-1-17)$$

in the odd order case and

$$\sin^2\theta \sin a \cos b + \cos^2\theta \cos a \sin b \equiv \frac{1}{2}\sin(a+b) - \frac{1}{2}\cos 2\theta \sin(a-b)$$

for the even orders. We obtain for the odd orders

$$V_1(z) = (-1)^{\frac{m+1}{2}} \sin\left(k_0 \cos\theta \cdot z - \frac{\varphi}{2}\right)$$
$$+ (-1)^{\frac{m+1}{2}} \frac{k_0}{\cos\theta} \cos\left(k_0 \cos\theta \cdot z - \frac{\varphi}{2}\right) \int_{z_1}^{z} dz' \Delta(z')$$
$$- (-1)^{\frac{m-1}{2}} \frac{k_0 \cos 2\theta}{\cos\theta} \int_{z_1}^{z} dz' \Delta(z') \cos\left(2k_0 \cos\theta z' - \left(k_0 \cos\theta z + \frac{\varphi}{2}\right)\right) \qquad (A-1-19)$$

and for the even orders

$$V_1(z) = (-1)^{\frac{m}{2}} \cos\left(k_0 \cos\theta \cdot z - \frac{\varphi}{2}\right)$$
$$- (-1)^{\frac{m}{2}} \frac{k_0}{\cos\theta} \sin\left(k_0 \cos\theta \cdot z - \frac{\varphi}{2}\right) \int_{z_1}^{z} dz' \Delta(z')$$

(continued on next page)

$$+(-1)^{\frac{m}{2}}\frac{k_0\cos 2\theta}{\cos\theta}\int_{z_1}^{z}dz'\Delta(z')\sin\left(2k_0\cos\theta\cdot z'-(k_0\cos\theta\cdot z+\frac{\varphi}{2})\right)$$

(A-1-20, continued)

Since our origin is at z = 0, we have using eq. II-1-11 that at $z = z_2$,

$$\sin\left(k_0\cos\theta\cdot z-\frac{\varphi}{2}\right)=(-1)^{\frac{m-1}{2}}\cos\varphi$$

$$\cos\left(k_0\cos\theta\cdot z-\frac{\varphi}{2}\right)=(-1)^{\frac{m-1}{2}}\sin\varphi$$

$$\cos\left(2k_0\cos\theta\cdot z'-(k_0\cos\theta\cdot z+\frac{\varphi}{2})\right)=(-1)^{\frac{m-1}{2}}\sin(2k_0\cos\theta\cdot z')$$

(A-1-21)

for the odd orders, so that

$$V_1(z_2)=-\cos\varphi-\mu\sin\varphi+p \qquad \text{(A-1-22)}$$

where the quantities μ and p are defined by eq. II-1-15. In a similar way, we obtain for the even orders

$$V_1(z_2)=\cos\varphi+\mu\sin\varphi+p \qquad \text{(A-1-23)}$$

The approximation

$$\cos\varphi + \mu\sin\varphi \cong \cos\varphi\cos\mu + \sin\mu\sin\varphi = \cos(\varphi-\mu)$$

$$= \cos t \qquad (A\text{-}1\text{-}24)$$

has error terms that are of second or higher order in Δ; the substitution is therefore permissable under our approximation scheme.

We can therefore write eqs. A-1-22,23 as

$$V_1(z_2) = (-1)^m \cos t + p + O(\Delta^2) \qquad (A\text{-}1\text{-}25)$$

We now simplify our solution for U_1 . Substituting eq. A-1-14 into eq. A-1-7 (odd orders) and integrating the $d\Delta(z)/dz$ term by parts, we obtain

$$U_1(z) = (-1)^{\frac{m-1}{2}} \frac{i}{\cos\theta} (1+2\Delta(z_1)) \cos(k_0 \cos\theta \cdot z - \frac{\varphi}{2})$$

$$+ (-1)^{\frac{m+1}{2}} \frac{2ik_0}{\cos^2\theta} \int_{z_1}^{z} dz' \Delta(z') \cos(k_0 \cos\theta z - \frac{\varphi}{2}) \sin(k_0 \cos\theta (z-z'))$$

$$+ (-1)^{\frac{m+1}{2}} \frac{2i}{\cos\theta} \left[\Delta(z') \sin(k_0 \cos\theta z' - \frac{\varphi}{2}) \sin(k_0 \cos\theta (z-z')) \right]_{z'=z_1}^{z'=z}$$

$$+ (-1)^{\frac{m-1}{2}} 2ik_0 \int_{z_1}^{z} dz' \Delta(z') \cos(k_0 \cos\theta z' - \frac{\varphi}{2}) \sin(k_0 \cos\theta (z-z'))$$

$$+ (-1)^{\frac{m+1}{2}} 2ik_0 \int_{z_1}^{z} dz' \Delta(z') \sin(k_0 \cos\theta z' - \frac{\varphi}{2}) \cos(k_0 \cos\theta (z-z')) \qquad (A-1-26)$$

or

$$U_1(z) = (-1)^{\frac{m-1}{2}} \frac{i}{\cos\theta} \left\{ (1+2\Delta(z_1)) \cos(k_0 \cos\theta z - \frac{\varphi}{2}) - 2\Delta(z_1) \sin(\frac{m\pi}{2} + (k_0 \cos\theta z - \frac{\varphi}{2})) \right\}$$

$$+ (-1)^{\frac{m+1}{2}} \frac{2ik_0}{\cos^2\theta} \sin^2\theta \int_{z_1}^{z} dz' \Delta(z') \cos(k_0 \cos\theta z' - \frac{\varphi}{2}) \sin(k_0 \cos\theta (z-z'))$$

$$+(-1)^{\frac{m+1}{2}}\,2ik_0\int_{z_1}^{z}dz'\,\Delta(z')\sin\left(k_0\cos\theta z'-\frac{\varphi}{2}\right)\cos\left(k_0\cos\theta\,(z-z')\right)$$

(A-1-27, continued)

Similarly, for the even orders we obtain

$$U_1(z)=(-1)^{\frac{m}{2}}\,\frac{i}{\cos\theta}\left\{(1+2\Delta(z_1))\sin\left(k_0\cos\theta z-\frac{\varphi}{2}\right)\right.$$
$$\left.-2\Delta(z_1)\sin\left(\frac{mx}{2}+\left(k_0\cos\theta z-\frac{\varphi}{2}\right)\right)\right\}$$

$$-(-1)^{\frac{m}{2}}\,\frac{2ik_0}{\cos^2\theta}\sin^2\theta\int_{z_1}^{z}dz'\,\Delta(z')\sin\left(k_0\cos\theta z'-\frac{\varphi}{2}\right)\sin\left(k_0\cos\theta\,(z-z')\right)$$

$$+(-1)^{\frac{m}{2}}\,2ik_0\int_{z_1}^{z}dz'\,\Delta(z')\cos\left(k_0\cos\theta z'-\frac{\varphi}{2}\right)\cos\left(k_0\cos\theta\,(z-z')\right)$$

(A-1-28)

Using the trigonometric identity

$$\sin^2\theta\sin a\sin b+\cos^2\theta\cos a\sin b=\frac{1}{2}\sin(a+b)-\frac{1}{2}\cos 2\theta\sin(a-b)$$

(A-1-29)

for the odd orders, we obtain

$$U_1(z)=(-1)^{\frac{m-1}{2}}\,\frac{i}{\cos\theta}\left\{\cos\left(k_0\cos\theta z-\frac{\varphi}{2}\right)+(-1)^{\frac{m+1}{2}}\,\frac{k_0}{\cos\theta}\sin\left(k_0\cos\theta z-\frac{\varphi}{2}\right)\int_{z_1}^{z}dz'\,\Delta(z')\right.$$
$$\left.+(-1)^{\frac{m+1}{2}}\,\frac{k_0\cos 2\theta}{\cos\theta}\int_{z_1}^{z}dz'\sin\left(2k_0\cos\theta z'-\left(k_0\cos\theta z-\frac{\varphi}{2}\right)\right)\right\}$$

(A-1-30)

which at $z = z_2$ reduces to

$$U_1(z_2) = \frac{i}{\cos\theta}\left(\sin\varphi - \mu\cos\varphi + r\right) \qquad (A\text{-}1\text{-}31)$$

(the parameter r is defined in eq. II-1-15). Under our approximation scheme U_1 can be written

$$U_1(z_2) = \frac{i}{\cos\theta}\left(\sin t + r\right) \qquad (A\text{-}1\text{-}32)$$

Similarly, for the even orders we find

$$U_1(z_2) = \frac{i}{\cos\theta}\left(-\sin t + r\right) \qquad (A\text{-}1\text{-}33)$$

so that our final solution for U_1 is

$$U_1 = \frac{i}{\cos\theta}\left((-1)^m \sin t + r\right) \qquad (A\text{-}1\text{-}34)$$

We now follow similar steps to obtain solutions for U_2 and V_2.

The sum of the homogeneous solution and the Green's function solution is, according to eqs. A-1-4,5,6

$$U_2(z) = (-1)^{\frac{m+1}{2}} B \sin\left(k_0 \cos\theta \cdot z - \frac{\varphi}{2}\right)$$

$$+ (-1)^{\frac{m-1}{2}} \frac{2k_0}{\cos\theta} \int_{z_1}^{z} dz' \Delta(z') \sin\left(k_0 \cos\theta z' - \frac{\varphi}{2}\right) \sin\left(k_0 \cos\theta (z - z')\right)$$

$$+ (-1)^{\frac{m+1}{2}} 2 \int_{z}^{z} dz' \frac{d\Delta(z')}{dz'} \cos\left(k_0 \cos\theta z' - \frac{\varphi}{2}\right) \sin\left(k_0 \cos\theta (z - z')\right)$$

(A-1-35)

for the odd orders (where B is a constant of order $1 + \Delta$), and

$$U_2(z) = (-1)^{m/2} B \cos\left(k_0 \cos\theta z - \frac{\varphi}{2}\right)$$

$$- (-1)^{\frac{m}{2}} \frac{2k_0}{\cos\theta} \int_{z_1}^{z} dz' \Delta(z') \cos\left(k_0 \cos\theta z' - \frac{\varphi}{2}\right) \sin\left(k_0 \cos\theta (z - z')\right)$$

$$- (-1)^{\frac{m}{2}} 2 \int_{z_1}^{z} dz' \frac{d\Delta(z')}{dz'} \sin\left(k_0 \cos\theta z' - \frac{\varphi}{2}\right) \sin\left(k_0 \cos\theta (z - z')\right)$$

(A-1-36)

for the even orders.

In this case, we can see immediately that

$$U_2(z_1) = B \qquad (A\text{-}1\text{-}37)$$

so that eq. II-1-6 is satisfied if we set B = 1.

Integrating the last term in the odd order solution (eq. A-1-35) by parts, we then have

$$\begin{aligned} U_2(z) = {} & (-1)^{\frac{m+1}{2}} \sin\left(k_0 \cos\theta z - \frac{\varphi}{2}\right) \\ & + (-1)^{\frac{m-1}{2}} \frac{2k_0}{\cos\theta} \int_{z_1}^{z} dz\, \Delta(z') \sin\left(k_0 \cos\theta z' - \frac{\varphi}{2}\right) \sin\left(k_0 \cos\theta (z-z')\right) \\ & + (-1)^{\frac{m+1}{2}} 2\left[\Delta(z') \cos\left(k_0 \cos\theta z' - \frac{\varphi}{2}\right) \sin\left(k_0 \cos\theta (z-z')\right)\right]_{z'=z_1}^{z'=z} \\ & + (-1)^{\frac{m+1}{2}} 2k_0 \cos\theta \int_{z_1}^{z} dz' \Delta(z') \sin\left(k_0 \cos\theta z' - \frac{\varphi}{2}\right) \sin\left(k_0 \cos\theta (z-z')\right) \\ & + (-1)^{\frac{m+1}{2}} 2k_0 \cos\theta \int_{z_1}^{z} dz' \Delta(z') \sin\left(k_0 \cos\theta z' - \frac{\varphi}{2}\right) \cos\left(k_0 \cos\theta (z-z')\right) \end{aligned} \qquad (A\text{-}1\text{-}38)$$

which, after algebraic manipulation and the use of the identity

$$\sin^2\theta \sin a \sin b - \cos^2\theta \cos a \cos b = -\frac{1}{2}\cos(a+b) - \frac{1}{2}\cos 2\theta \cos(a-b) \qquad (A\text{-}1\text{-}39)$$

reduces to

$$U_2(z) = (-1)^{\frac{m+1}{2}} \sin\left(k_0 \cos\theta z - \frac{\varphi}{2}\right)$$

$$+ (-1)^{\frac{m+1}{2}} \frac{k_0}{\cos\theta} \cos\left(k_0 \cos\theta z - \frac{\varphi}{2}\right) \int_{z_1}^{z} dz' \Delta(z')$$

$$+ (-1)^{\frac{m+1}{2}} \frac{k_0}{\cos\theta} \cos 2\theta \int_{z_1}^{z} dz' \Delta(z') \cos\left(2k_0 \cos\theta z' - \left(k_0 \cos\theta z + \frac{\varphi}{2}\right)\right)$$

(A-1-40)

Similarly, we find that the even order equation eq. A-1-36 reduces to

$$U_2(z) = (-1)^{m/2} \cos\left(k_0 \cos\theta z - \frac{\varphi}{2}\right)$$

$$-(-1)^{\frac{m}{2}} \frac{k_0}{\cos\theta} \sin\left(k_0 \cos\theta z - \frac{\varphi}{2}\right) \int_{z_1}^{z} dz' \Delta(z')$$

$$-(-1)^{\frac{m}{2}} \frac{k_0}{\cos\theta} \cos 2\theta \int_{z_1}^{z} dz' \Delta(z') \sin\left(2k_0 \cos\theta z' - \left(k_0 \cos\theta z + \frac{\varphi}{2}\right)\right)$$

(A-1-41)

At $z = z_2$, we find that for all orders

$$U_2(z_2) = (-1)^m \cos\varphi - p \qquad (A\text{-}1\text{-}42)$$

We obtain V_2 by taking dU_2/dz , to obtain

$$\frac{dU_2}{dz} = (-1)^{\frac{m+1}{2}} k_0 \cos\theta \cos\left(k_0 \cos\theta z - \frac{\varphi}{2}\right)\left[1 + 2\Delta(z)\right]$$

$$+ (-1)^{\frac{m-1}{2}} k_0^2 \sin\left(k_0 \cos\theta z - \frac{\varphi}{2}\right) \int_{z_1}^{z} dz' \Delta(z')$$

$$+ (-1)^{\frac{m+1}{2}} k_0^2 \cos 2\theta \int_{z_1}^{z} dz' \Delta(z') \sin\left(2k_0 \cos\theta z' - \left(k_0 \cos\theta z + \frac{\varphi}{2}\right)\right)$$

(A-1-43)

for the odd orders, where we have used the identity

$1 + \cos 2\theta = 2\cos^2\theta$.

At $z = z_2$, we find to our usual approximation

$$V_2(z_2) = i\cos\theta\,(\sin t - \tau) \qquad (A\text{-}1\text{-}44)$$

Similarly, we find for the even orders

$$V_2(z_2) = i\cos\theta(-\sin t - \tau) \qquad (A\text{-}1\text{-}45)$$

Combining our results to this point, we find that the characteristic matrix for the Kth cell in P-polarization is

$$\begin{pmatrix} E_{y,K+1} \\ H_{x,K+1} \end{pmatrix} = \begin{pmatrix} (-1)^m \cos t_K - p_K & i\cos\theta\left((-1)^m \sin t_K - \tau_K\right) \\ \frac{i}{\cos\theta}\left((-1)^m \sin t_K + \tau_K\right) & (-1)^m \cos t_K + p_K \end{pmatrix} \begin{pmatrix} E_{y,K} \\ H_{x,K} \end{pmatrix}$$

$$(A\text{-}1\text{-}46)$$

The case of S polarization is somewhat simpler to solve than that of P polarization.

Born and Wolf (1975) show that the characteristic matrix solution for S polarization is

$$\begin{pmatrix} E_x(z_1) \\ H_y(z_1) \end{pmatrix} = \begin{pmatrix} V_1(z_2) & -U_1(z_2) \\ -V_2(z_2) & U_2(z_2) \end{pmatrix} \begin{pmatrix} E_x(z_2) \\ H_y(z_2) \end{pmatrix} \qquad (A\text{-}1\text{-}47)$$

where the boundary conditions of eq. II-1-6 apply as in the P case, but now

$$\frac{d^2 U_{1,2}}{dz^2} + k_o^2 \left(\epsilon(z) - \sin^2\theta\right) U_{1,2} = 0 \qquad (A\text{-}1\text{-}48)$$

$$V_{1,2} = -\frac{i}{k_o} \frac{dU_{1,2}}{dz}$$

The vacuum solutions are

$$U_1(z) = (-1)^{\frac{m-1}{2}} \frac{i}{\cos\theta} \cos\left(k_o \cos\theta z - \frac{\varphi}{2}\right) \qquad (A\text{-}1\text{-}49)$$

$$U_2(z) = (-1)^{\frac{m+1}{2}} \sin\left(k_o \cos\theta z - \frac{\varphi}{2}\right)$$

for the odd orders, and

$$U_1(z) = (-1)^{\frac{m}{2}} \frac{i}{\cos\theta} \sin\left(k_0 \cos\theta z - \frac{\varphi}{2}\right)$$

$$U_2(z) = (-1)^{\frac{m}{2}} \cos\left(k_0 \cos\theta z - \frac{\varphi}{2}\right) \qquad (A\text{-}1\text{-}50)$$

for the even orders.

Using the perturbation method, eq. A-1-48 becomes

$$\frac{d^2U_1}{dz^2} + k_0^2 \cos^2\theta \cdot U_1 = (-1)^{\frac{m+1}{2}} \frac{2ik_0^2\Delta(z)}{\cos\theta} \cos\left(k_0 \cos\theta z - \frac{\varphi}{2}\right)$$

$$\frac{d^2U_2}{dz^2} + k_0^2 \cos^2\theta \cdot U_2 = (-1)^{\frac{m-1}{2}} 2k_0^2\Delta(z) \sin\left(k_0 \cos\theta z - \frac{\varphi}{2}\right) \qquad (A\text{-}1\text{-}51)$$

for the odd orders.

We will find that in the case of S polarization, we can dispense with the constants A and B that were required to satisfy the boundary conditions in the P case.

Our solution for U_1 in odd orders is therefore

$$U_1(z) = (-1)^{\frac{m-1}{2}} \frac{i}{\cos\theta} \cos\left(k_0 \cos\theta z - \frac{\varphi}{2}\right)$$

$$+ (-1)^{\frac{m+1}{2}} \frac{2ik_0}{\cos^2\theta} \int_{z_1}^{z} dz' \Delta(z') \cos\left(k_0 \cos\theta z' - \frac{\varphi}{2}\right) \sin\left(k_0 \cos\theta (z - z')\right) \qquad (A\text{-}1\text{-}52)$$

Using the identity

$$\cos a \sin b = \frac{1}{2} \sin(a+b) - \frac{1}{2} \sin(a-b) \qquad (A\text{-}1\text{-}53)$$

we get

$$U_1(z) = (-1)^{\frac{m-1}{2}} \frac{i}{\cos\theta} \cos\left(k_0 \cos\theta z - \frac{\varphi}{2}\right)$$

$$+ (-1)^{\frac{m+1}{2}} \frac{ik_0}{\cos^2\theta} \sin\left(k_0 \cos\theta z - \frac{\varphi}{2}\right) \int_{z_1}^{z} dz' \Delta(z') \qquad (A\text{-}1\text{-}54)$$

$$+ (-1)^{\frac{m-1}{2}} \frac{ik_0}{\cos^2\theta} \int_{z_1}^{z} dz' \Delta(z') \sin\left(2k_0 \cos\theta z' - \left(k_0 \cos\theta z + \frac{\varphi}{2}\right)\right)$$

which at $z = z_1$ becomes

$$U_1(z) = \frac{i}{\cos\theta}(\sin\varphi - \mu\cos\varphi - r) = \frac{i}{\cos\theta}(\sin t - r) + O(\Delta^2) \qquad (A\text{-}1\text{-}55)$$

Similarly, we find for the even orders

$$U_1(z) = \frac{i}{\cos\theta}(-\sin t - r) \qquad (A\text{-}1\text{-}56)$$

We note that in the case of S polarization, the parameter r in the above equations is defined with the factor P set equal to one (see eq. II-1-5).

To obtain V_1, we differentiate eq. A-1-54 with respect to z to obtain after cancellation

$$\frac{dU_1}{dz} = (-1)^{\frac{m+1}{2}} i k_0 \sin\left(k_0\cos\theta z - \frac{\varphi}{2}\right)$$

$$+(-1)^{\frac{m+1}{2}} \frac{k_0^2}{\cos\theta}\cos\left(k_0\cos\theta z - \frac{\varphi}{2}\right)\int_{z_1}^{z} dz'\Delta(z')$$

$$+(-1)^{\frac{m+1}{2}} \frac{k_0^2}{\cos\theta}\int_{z_1}^{z} dz'\Delta(z')\cos\left(2k_0\cos\theta z' - \left(k_0\cos\theta z + \frac{\varphi}{2}\right)\right) \qquad (A\text{-}1\text{-}57)$$

for the odd orders. (Note that dU_1/dz at $z = z_1$ is ik_o, so that $V_1(z_1) = 1$ as required by eq. II-1-6).

At $z = z_2$ we find

$$V_1(z_2) = -\frac{i}{k_o}\frac{dU_1}{dz} = -\cos t - p \qquad (A-1-58)$$

and similarly for the even orders we obtain

$$V_1(z_2) = \cos t + p \qquad (A-1-59)$$

The solution for U_2 in odd orders is

$$U_2(z) = (-1)^{\frac{m+1}{2}} \sin\left(k_o \cos\theta z - \frac{\varphi}{2}\right)$$

$$+(-1)^{\frac{m+1}{2}} \frac{k_o}{\cos\theta} \cos\left(k_o \cos\theta z - \frac{\varphi}{2}\right)\int_{z_1}^{z} dz'\Delta(z')$$

$$+(-1)^{\frac{m-1}{2}} \frac{k_o}{\cos\theta}\int_{z_1}^{z} dz'\Delta(z')\cos\left(2k_o\cos\theta z' - \left(k_o\cos\theta\cdot z + \frac{\varphi}{2}\right)\right)$$

$$(A-1-60)$$

which reduces to

$$U_2(z_2) = -\cos t + p \qquad (A\text{-}1\text{-}61)$$

at $z = z_2$. For the even orders we obtain

$$U_2(z_2) = \cos t + p \qquad (A\text{-}1\text{-}62)$$

For V_2 we obtain

$$V_2(z) = -\frac{i}{k_0}\frac{dU_2}{dz} = (-1)^{\frac{m-1}{2}}\cos\theta\cos\left(k_0\cos\theta z - \frac{\varphi}{2}\right)$$

$$+ (-1)^{\frac{m+1}{2}}\sin\left(k_0\cos\theta z - \frac{\varphi}{2}\right)\int_{z_1}^{z} dz'\,\Delta(z')$$

$$+ (-1)^{\frac{m+1}{2}}\int_{z_1}^{z} dz'\,\Delta(z')\sin\left(2k_0\cos\theta z' - \left(k_0\cos\theta z + \frac{\varphi}{2}\right)\right)$$

$$(A\text{-}1\text{-}63)$$

for the odd orders, which becomes

$$V_2(z_2) = i\cos\theta\,(\sin t + \tau) \qquad (A\text{-}1\text{-}64)$$

at $z = z_2$. In the even orders,

$$V_2(z_2) = i\cos\theta\,(-\sin t + r) \qquad (A\text{-}1\text{-}65)$$

The characteristic matrix equation under S polarization is thus

$$\begin{pmatrix} E_{x,\,k+1} \\ \\ H_{y,\,k+1} \end{pmatrix} = \begin{pmatrix} (-1)^m \cos t_k - p_k & -\frac{i}{\cos\theta}\left((-1)^m \sin t_k - r_k\right) \\ \\ -i\cos\theta\left((-1)^m \sin t_k + r_k\right) & (-1)^m \cos t_k + p_k \end{pmatrix} \begin{pmatrix} E_{x,k} \\ \\ H_{y,k} \end{pmatrix}$$

$$(A\text{-}1\text{-}66)$$

This S matrix and the P matrix of eq. A-1-47 are not equal at $\theta = 0$. This is a consequence of the definitions in sec. II-1-B;

$$\vec{E} = E_x \hat{x} \qquad (A\text{-}1\text{-}67)$$

in S polarization, while

$$\vec{H} = H_x \hat{x} \qquad (A\text{-}1\text{-}68)$$

in P polarization. (See fig. II-1-2). Under these definitions it is impossible to rotate the coordinate axes in such a way that the S case at normal incidence is transformed into the P case (so long as the z axis is required to point towards the substrate).

However, as discussed in sec. II-1-B it is convenient to modify eqs. A-1-47,66 in order to facilitate calculations at angles off normal incidence.

If we define

$$\mathcal{E} \equiv E_x$$
$$\mathcal{H} \equiv H_y / \cos\theta \qquad (A\text{-}1\text{-}69)$$

in S polarization, then we can set

$$\mathcal{E} \equiv (1+\rho)\,A$$
$$\mathcal{H} \equiv (1-\rho)\,A \qquad (A\text{-}1\text{-}70)$$

for all θ (see fig. II-1-2). Here A is some K-dependent field amplitude. Because of the plus sign that appears in the first of eq. A-1-70, these definitions satisfy the usual thin film convention where ρ is real and positive if the reflected electric field component parallel to the interface is in phase with the incident component.

If we now convert eq. A-1-66 into an equation involving these new field quantities we obtain eq. II-1-14. In the remainder of the text it is this matrix solution that is referred to as the characteristic matrix solution.

It would be convenient to be able to employ eq. A-1-14 in the case of P polarization as well (with eq. A-1-70 still obtaining).

In order to have eq. II-1-14 apply to P as well as S polarization at normal incidence, the equation must remain consistent with eq. A-1-70 when the coordinate axes are rotated to bring x from its original direction along the incident E field into a direction aligned with the incident H field.

From fig. II-1-2, we therefore require

$$\mathcal{E} = -E_y / \cos\theta$$

$$\mathcal{H} = H_x \qquad (A\text{-}1\text{-}71)$$

in P polarization.

Appendix 2 - Difference Equation for Amplitude Reflectivity

In this appendix we use a well-known procedure to convert the matrix solution that propagates the field components from cell to cell into a difference equation that propagates the amplitude reflectivity from cell to cell.

In the x-ray case the difference equation is a Ricatti equation under our usual set of approximations.

Combining eq. A-1-70 with eq. II-1-14:

$$\begin{pmatrix} 1+\rho_{k+1} \\ 1-\rho_{k+1} \end{pmatrix} \cdot A_{k+1} = \begin{pmatrix} (-1)^m \cos t_k - \rho_k & i((-1)^m \sin t_k + r_k) \\ i((-1)^m \sin t_k - r_k) & (-1)^m \cos t_k + \rho_k \end{pmatrix} \begin{pmatrix} 1+\rho_k \\ 1-\rho_k \end{pmatrix} A_k \qquad (A-2-1)$$

so that

$$\frac{1+\rho_{k+1}}{1-\rho_{k+1}} = \frac{(-1)^m \cos t_k - \rho_k + (-1)^m i \sin t_k + i r_k + (-1)^m \cos t_k \rho_k - \rho_k \rho_k - i(-1)^m \sin t_k \rho_k - i r_k \rho_k}{(-1)^m \cos t_k + \rho_k + (-1)^m i \sin t_k - i r_k - (-1)^m \cos t_k \rho_k - \rho_k \rho_k + i(-1)^m \sin t_k \rho_k - i r_k \rho_k} \qquad (A-2-2)$$

or, after manipulation

$$\rho_{k+1} = \frac{(-1)^m e^{-it_k}\rho_k + (ir_k - p_k)}{(-1)^m e^{it_k} - (ir_k + p_k)} \qquad (A-2-3)$$

Neglecting terms of order Δ^2 :

$$\rho_{k+1} \cong \frac{(-1)^m e^{-it_k}\rho_k + (ir_k - p_k)}{(-1)^m e^{it_k}} \left(1 + (ir_k + p_k)(-1)^m e^{-it_k}\right)$$

$$= \left(e^{-2it_k}\rho_k + (-1)^m (ir_k - p_k)\right)\left(1 + (ir_k + p_k)(-1)^m e^{-it_k}\right) \qquad (A-2-4)$$

which reduces to eq. II-1-20 if the cross-term of order Δ^2 is neglected.

Appendix 3 - Reflectivity of a Periodic Multilayer with J Cells

Here we solve the difference equation

$$\rho_{K+1} = \rho_K - 2it\rho_K - (ir-\rho) - (ir+\rho)\rho_K^2 \qquad (A-3-1)$$

in the case of constant coefficients. When the coefficients are constant, there is no disadvantage in converting eq. A-3-1 to a differential equation, so as to obtain eq. II-1-25. With constant coefficients this equation is separable, and so

$$\int_0^{\rho_J} \frac{d\rho}{(ir+\rho)\rho^2 + 2it\rho + (ir-\rho)} = -\int_1^{J-1} dK \qquad (A-3-2)$$

The upper subscript of the integral on the right side has the value J-1 so as to follow the enumeration scheme established in sec. II-1-B. The reflectivity of the substrate has been taken to be zero; however our results are easily extended to the more general case.

Using

$$\int \frac{dx}{a+bx+cx^2} = \frac{1}{\sqrt{-w}} \ln\left(\frac{b+2cx-\sqrt{-w}}{b+2cx+\sqrt{-w}}\right) \qquad (A-3-3)$$

where $w \equiv 4ac - b^2$, we obtain

$$\ln\left(\frac{it+(ir+p)\rho_J - iS}{it+(ir+p)\rho_J + iS}\right) = -2iS(J-1) \qquad (A-3-4)$$

where

$$S \equiv \sqrt{t^2 - r^2 - p^2} = \frac{1}{2}\sqrt{-w} \qquad (A-3-5)$$

Solving, we find

$$\rho_J = \frac{1}{ir+p}\left(\frac{-t^2+s^2}{(it-is)-(it+is)e^{2is(J-1)}}\right)\left(e^{2is(J-1)}-1\right) \qquad (A-3-6)$$

From eq. II-2-12,

$$\frac{it+is}{it-is} = \rho_\infty^2 \frac{r-ip}{r+ip} \qquad (A-3-7)$$

so that

$$\rho_J = \frac{s^2-t^2}{(ir+p)(it-is)}\left(\frac{e^{2is(J-1)}}{1-\rho_\infty^2\frac{r-ip}{r+ip}e^{2is(J-1)}}\right) \qquad (A-3-8)$$

From eq. II-2-11

$$\frac{s^2-t^2}{(ir+p)(it-is)} = -\rho_\infty \qquad (A-3-9)$$

so that eq. II-2-13 is obtained.

Appendix 4 - Sufficient Criterion for the Bragg Condition

In sec. II-2-B we found that a necessary condition for the satisfaction of the Bragg condition $\mathrm{Re}(\delta) = 0$ was that the shift in the phase thickness of the cell from π radians be given by

$$\varphi = \mu' - \frac{r'r'' + p'p''}{\mu''} \qquad (A-4-1)$$

We now show that eq. A-4-1 is also a sufficient condition; as discussed in sec. II-2-B this is the same as showing that when $\mathrm{Im}(\delta^2)$ equals zero, $\mathrm{Re}(\delta^2)$ must automatically be less than zero.

According to eq. II-2-4 we therefore need to show that

$$t'^2 - t''^2 - (r^2 + p^2)' < 0 \qquad (A-4-2)$$

if

$$t' = \frac{r'r'' + p'p''}{t''} \qquad (A-4-3)$$

Since

$$t'^2 - t''^2 - (r^2 + p^2)'$$

$$= \frac{r'^2 r''^2 + p'^2 p''^2 + 2r'r''p'p''}{t''^2} - t''^2 - r'^2 + r''^2 - p'^2 + p''^2$$

$$= (r''^2 + p''^2 - t''^2)\left(1 + \frac{r'^2}{t''^2} + \frac{p'^2}{t''^2}\right) - \left(\frac{r''p' - p''r'}{t''}\right)^2$$

(A-4-4)

it is sufficient to show that

$$r''^2 + p''^2 < t''^2 \qquad \text{(A-4-5)}$$

because the second term in parentheses in the last part of eq. A-4-4 is always positive, and the third term is positive after being squared.

Using the definitions of eqs. II-1-15, we rewrite eq. A-4-5:

$$\left\{\left[\int_{-\frac{d}{2}}^{\frac{d}{2}} dz\, \Delta''(z) \cos(2k_0 \cos\theta z)\right]^2\right.$$

(continued on next page)

$$+ \left[\int_{-\frac{d}{2}}^{\frac{d}{2}} dz\, \Delta''(z) \sin(2k_o \cos\theta z) \right]^2 \Bigg\} < \left[\int_{-\frac{d}{2}}^{\frac{d}{2}} dz\, \Delta''(z) \right]^2$$

(A-4-6, continued)

Using the Schwartz inequality (Goodman, 1968)

$$\left(\left| \int AB \right|^2 \right) < \left(\int |A|^2 \right) \cdot \left(\int |B|^2 \right) \qquad (A\text{-}4\text{-}7)$$

with

$$A \equiv \sqrt{\Delta''(z)}\,, \qquad B \equiv \sqrt{\Delta''(z)}\, \cos(2k_o \cos\theta z) \qquad (A\text{-}4\text{-}8)$$

we have

$$\left[\int_{-\frac{d}{2}}^{\frac{d}{2}} dz\, \Delta''(z) \cos(2k_o \cos\theta z) \right]^2 <$$

$$\left[\int_{-\frac{d}{2}}^{\frac{d}{2}} dz\, \Delta''(z) \right] \cdot \left[\int_{-\frac{d}{2}}^{\frac{d}{2}} dz\, \Delta''(z) \cos^2(2k_o \cos\theta z) \right] \qquad (A\text{-}4\text{-}9)$$

Similarly,

$$\left[\int_{-\frac{d}{2}}^{\frac{d}{2}} dz\,\Delta''(z)\sin\left(2k_0\cos\theta z\right)\right]^2 <$$

$$\left[\int_{-\frac{d}{2}}^{\frac{d}{2}} dz\,\Delta''(z)\right]\cdot\left[\int_{-\frac{d}{2}}^{\frac{d}{2}} dz\,\Delta''(z)\sin^2\left(2k_0\cos\theta z\right)\right] \qquad (A-4-10)$$

Adding gives

$$r''^2 + p''^2 < t''^2 \qquad (A-4-11)$$

which is the desired result.

Appendix 5 - Comparison of Absorption Correction to Dispersion Correction

In this appendix we show that the absorption correction must always be smaller than the dispersion correction, so long as the real part of the unit decrement is negative throughout the unit cell. This means that the absorption correction will be less than the dispersion correction except in regions of strong anomalous dispersion, since it is only in such regions that the decrement can have a positive real part.

It will be sufficient to show that the absorption-induced contribution to the total refractive phase-shift is less than the contribution from dispersion, i.e. that

$$\frac{\tau'\tau'' + p'p''}{\mu'\mu''} < 1 \qquad (A\text{-}5\text{-}1)$$

(see eq. II-2-36).

If the decrement has a negative real part everywhere, both numerator and denominator on the left side are negative. If, on the other hand, the decrement can have a positive real part, then the dispersion correction may become arbitrarily small, and it is even possible for the denominator of eq. A-5-1 to be zero. We will assume that both numerator and denominator in eq. A-5-1 are negative.

From the definitions of eqs. II-1-15, we can write the left side as

$$\left\{ \iint_{-d/2}^{d/2} dz_1\, dz_2\, \Delta'(z_1)\, \Delta''(z_2) \cos(2k_0 \cos\theta z_1) \cos(2k_0 \cos\theta z_2) + \iint_{-d/2}^{d/2} dz_1\, dz_2\, \Delta'(z_1)\, \Delta''(z_2) \sin(2k_0 \cos\theta z_1) \sin(2k_0 \cos\theta z_2) \right\} \Bigg/ \left\{ \iint_{-d/2}^{d/2} dz_1\, dz_2\, \Delta'(z_1)\, \Delta''(z_2) \right\} \qquad (A-5-2)$$

which equals

$$\left\{ \iint_{-d/2}^{d/2} dz_1\, dz_2\, \Delta'(z_1)\, \Delta''(z_2) \cos(2k_0 \cos\theta (z_1 - z_2)) \right\} \Bigg/ \left\{ \iint_{-d/2}^{d/2} dz_1\, dz_2\, \Delta'(z_1)\, \Delta''(z_2) \right\} \qquad (A-5-3)$$

Under our assumptions, $\Delta'(z_1)\,\Delta''(z_2)$ is always negative, and so

$$\frac{r'r'' + p'p''}{\mu'\mu''} < 1 \qquad (A-5-4)$$

because

$$\left|\cos\left(2k_0 \cos\theta\,(z_1 - z_2)\right)\right| \leqslant 1 \qquad (A-5-5)$$

Since there is a linear relation between phase thickness and d-spacing or the reciprocal of wavelength, eq. A-5-4 implies that the absorption-induced shift in either of these quantities is less than the dispersion induced shift.

According to eq. II-2-35 the relation between angular shift and phase shift is

$$\Delta\theta = \sqrt{\tan^2\theta_B + \frac{2\varphi_{Opt}}{\pi}} - \tan\theta_B \qquad (A-5-6)$$

which is non-linear near normal incidence. However, eq. A-5-6 is still a monotonic function of φ, so that the greater portion of φ_{Opt} that is due to

dispersion can be taken to imply that the greatest contribution to the angular shift is also due to dispersion.

Appendix 6 - Algorithm for Calculating β_{0pt}

In this appendix we present an algorithm for solving the transcedental equation

$$\tan \beta_{0pt} = \beta_{0pt} + W \qquad (A-6-1)$$

where

$$W \equiv \frac{\pi \Delta_L''}{\Delta_H'' - \Delta_L''} \qquad (A-6-2)$$

We will first present a two fold method for obtaining initial estimates of β_{0pt}.

In the multilayer designs of greatest interest there is significant contrast in absorption between the two constituent materials, making the parameter W fairly small.

In this case β_{0pt} is also small, and we can set

$$\tan \beta_{0pt} \cong \beta_{0pt} + \frac{\beta_{0pt}^3}{3} + \frac{2\beta_{0pt}^5}{15} \qquad (A-6-3)$$

If we neglect the last term on the right, substitute into eq. A-6-1, solve for β_{opt}, and then substitute our solution back into the previously neglected fifth order term in eq. A-6-3, we get after again solving for β_{opt}

$$\beta_{opt} \cong \sqrt[3]{3W - \frac{2 \cdot 3^{5/3}}{5} W^{5/3}} \qquad (A-6-4)$$

We can keep this from diverging rapidly at large W by making the substitution in the last term

$$W \Rightarrow \frac{W}{1+W} \qquad (A-6-5)$$

to obtain

$$\beta_{opt} \cong \sqrt[3]{3W - 2.496 \left(\frac{W}{1+W}\right)^{5/3}} \qquad (A-6-6)$$

Fig. A-6-1 shows a plot of this seed function (which we will refer to as the "small-W" seed function).

In an exhaustive search for multilayer materials combinations (such as that presented in sec. II-2-C), one might wish to calculate β_{opt} in cases where W will not be small. In such cases the small-W seed is not very accurate. If we define

$$V \equiv \frac{\pi}{2} - \beta_{opt} \qquad (A-6-7)$$

and set on the assumption that v is small

$$\tan \beta_{opt} \cong \frac{1}{V} \qquad (A-6-8)$$

eq. A-6-1 becomes a quadratic whose solution is

$$\beta_{opt} = \frac{\pi}{2} - V = \frac{1}{2}\left[\pi - (W + \frac{\pi}{2}) + \sqrt{(W+\frac{\pi}{2})^2 - 4}\right] \qquad (A-6-9)$$

This large-W seed formula is also plotted in fig. A-6-1.

We now present two iteration methods that rapidly converge to the exact solution from these initial seeds.

When W is small, we use Newton-Raphson iteration, so that

$$\beta_{i+1} = \beta_i - \frac{(\tan\beta_i - \beta_i - W)}{\frac{d}{d\beta}(\tan\beta_i - \beta_i - W)} = \beta_i - \frac{\tan\beta_i - \beta_i - W}{\sec^2\beta_i - 1} \qquad (A-6-10)$$

For large W, we use the iteration scheme

$$\beta_{i+1} = \arctan(\beta_i + W) \qquad (A-6-11)$$

This scheme is quite convenient to use with a pocket calculator (if it has inverse trig keys).

The two seed formulae have equal departures from the true solution at the transition point W = 0.656. The search program described in sec. II-2-C uses this W value to separate the two regions in which the different formulas are applied. A slight increase in computational speed could have been obtained in the program if the dividing value of W had taken into account the longer time needed to evaluate eq. A-6-6 in comparison with eq. A-6-9.

The point W = 0.656 also turns out to be approximately the point at which the two iteration equations A-6-10 and A-6-11 require equal numbers of steps; of course the precise transition point is dependent on the desired final accuracy.

Fig. A-6-1 shows a plot of the improvement on the seed guess that is achieved after one iteration; the W=0.656 point was used to decide between the two iteration schemes as well as between the two seed formulas.

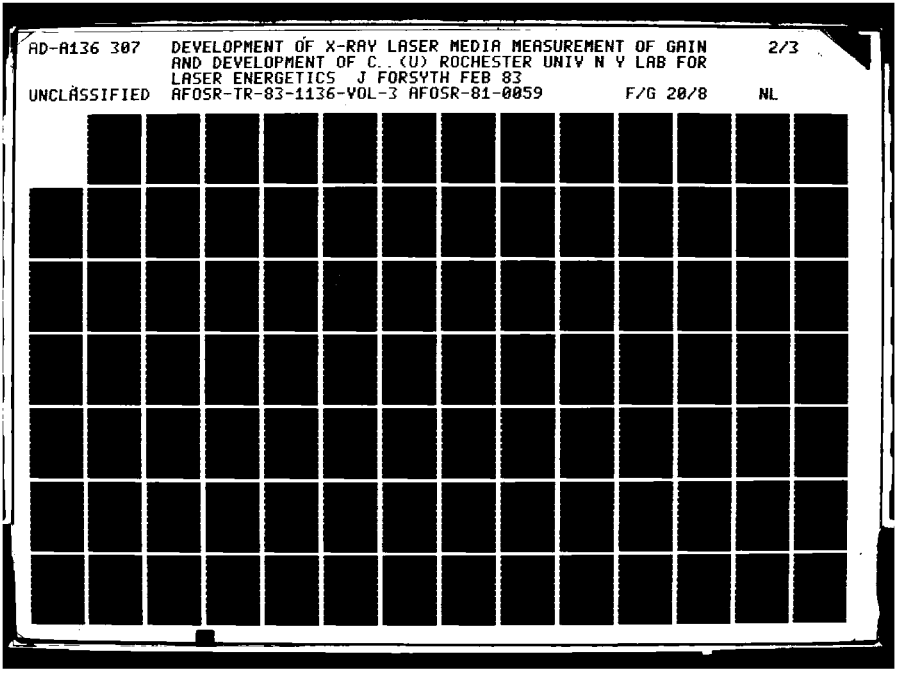
AD-A136 307 DEVELOPMENT OF X-RAY LASER MEDIA MEASUREMENT OF GAIN AND DEVELOPMENT OF C..(U) ROCHESTER UNIV N Y LAB FOR LASER ENERGETICS J FORSYTH FEB 83
2/3
UNCLASSIFIED AFOSR-TR-83-1136-VOL-3 AFOSR-81-0059 F/G 20/8 NL

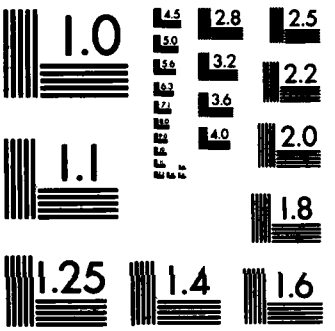

MICROCOPY RESOLUTION TEST CHART
NATIONAL BUREAU OF STANDARDS-1963-A

ALGORITHMS FOR OBTAINING $\beta_{Optimum}$

UR LLE

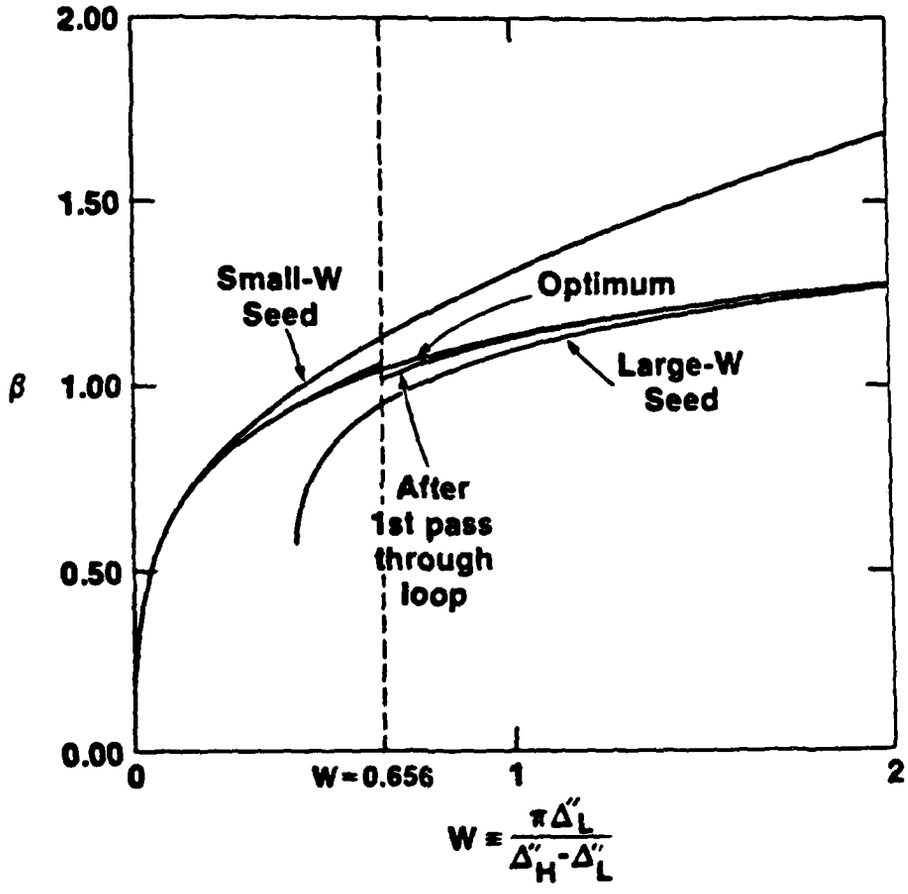

X352

Figure A-6-1

Appendix 7 - Peak Reflectivity of Periodic Multilayers

In this appendix we calculate the reflectivity of a periodic multilayer operating at the Bragg condition.

According to eqs. II-2-11 and 26, we must calculate

$$R_{Peak} = \frac{|s + t|^2}{|r - ip|^2} \qquad (A-7-1)$$

evaluated at $Re(\delta) = 0$. Using eq. II-2-30,

$$\delta'' = \sqrt{t''^2 - t'^2 + (r^2 + p^2)'}$$

$$= \sqrt{\mu''^2 - \frac{((r^2+p^2)'')^2}{4\mu''^2} + (r^2+p^2)'} \qquad (A-7-2)$$

Thus, with some manipulation, we find

$$|s + t|^2 = t'^2 + \delta''^2 + t''^2 + 2t''\delta''$$

(continued on next page)

$$= 2\mu''^2 + \tau'^2 + p'^2 - \tau''^2 - p''^2$$

$$- 2\sqrt{\mu''^4 - (\tau'\tau'' + p'p'')^2 + \mu''^2(\tau'^2 + p'^2 - \tau''^2 - p''^2)}$$

(A-7-3, continued)

Using

$$|\tau - ip|^2 = (\tau' + p'')^2 + (\tau'' - p')^2$$

$$= |\tau|^2 + |p|^2 + 2(\tau'p'' - \tau''p')$$

(A-7-4)

we obtain eq. II-2-45.

Appendix 8 - Demonstration that the Periodic Multilayer has an Extremum Reflectivity

Let v_1 , v_2 , ... v_{J-1} be the numerical values of the (not necessarily equal) changes that are made in some structural parameter of each of the J-1 cells of a periodic multilayer whose structure is initially optimized in accordance with the formulas of sec. II-2-B.

Since variations in structure must ultimately represent variations in real physical quantities, the v_K can be assumed to be real.

To show that the reflectivity is an extremum with respect to the v_K , we show that in lowest order the intensity reflectance $|\rho_J|^2$ is not changed by the v_K variations. We will only consider the steady-state regime where the formulas of sec. II-2-B apply.

In lowest order

$$\tau_K = \tau_o + \dot{\tau}_o V_K$$

$$p_K = p_o + \dot{p}_o V_K \qquad (A-8-1)$$

$$t_K = t_o + \dot{t}_o V_K$$

where the dot represents differentiation with respect to the physical parameter under consideration.

We now follow a standard perturbation method for ordinary differential equations (Schiff, 1968)

Let

$$\rho_{s,k} \equiv \rho_0 + \rho_{1,k} \qquad (A\text{-}8\text{-}2)$$

where

$$\rho_0 \equiv (1 - 2it_0)\rho_0 - (ir_0 - p_0) - (ir_0 + p_0)\rho_0^2 \qquad (A\text{-}8\text{-}3)$$

and

$$\rho_{1,k+1} \equiv (1 - 2it_0)\rho_{1,k} - 2i\dot{t}_0 V_k \rho_0$$

$$- 2ir_0 \rho_0 \rho_{1,k} - i\dot{r}_0 V_k (1 + \rho_0^2)$$

$$- 2p_0 \rho_0 \rho_{1,k} + \dot{p}_0 V_k (1 - \rho_0^2)$$

$$(A\text{-}8\text{-}4)$$

ρ_o is thus the ideal reflectivity, which is assumed to be in steady-state.

The total solution $\rho_{s,\kappa}$ will satisfy the (first order in φ and Δ) equation

$$\rho_{s,\kappa+1} = (1-2it_\kappa)\rho_{s,\kappa} - (i\tau_\kappa - p_\kappa) - (i\tau_\kappa + p_\kappa)\rho_{s,\kappa}^2 \qquad (A-8-5)$$

to within first order in the v_κ.

From eq. II-2-3,

$$\delta_o = -t_o - \tau_o\rho_o + ip_o\rho_o \qquad (A-8-6)$$

so that eq. A-8-4 becomes

$$\rho_{1,\kappa+1} = (1+2i\delta_o)\rho_{1,\kappa} - \left[2i\dot{t}_o\rho_o + i\dot{\tau}_o(1+\rho_o^2) - \dot{p}_o(1-\rho_o^2)\right] \qquad (A-8-7)$$

This equation is linear, so its solution is

$$\rho_{1,J} = -(1-2\delta_o'')^{J-1}\sum_{\kappa=1}^{J-1}\frac{i\left[2\dot{t}_o + \dot{\tau}_o(\rho_o + \frac{1}{\rho_o}) - i\dot{p}_o(\rho_o - \frac{1}{\rho_o})\right]\rho_o V_\kappa}{(1-2\delta_o'')^\kappa} \qquad (A-8-8)$$

where we have set

$$i\delta_o = -\delta_o^* \qquad (A-8-9)$$

since the multilayer's unit cell thickness is assumed to have been optimized, making $Re(\delta_o) = 0$.

From eqs. II-2-41 and 11, we have for a periodic multilayer optimized with respect to each of the parameters represented by the v_κ:

$$Im\left[2\dot{t}_o + (\dot{r}_o - i\dot{p}_o)\rho_o + (\dot{r}_o + i\dot{p}_o)\,1/\rho_o\right]$$

$$= Im\left[2\dot{t}_o + \dot{r}_o\left(\rho_o + \frac{1}{\rho_o}\right) - i\dot{p}_o\left(\rho_o - \frac{1}{\rho_o}\right)\right]$$

$$= 0 \qquad (A-8-10)$$

Let the quantity in brackets in eq. A-8-10 then be denoted α, with $Im(\alpha)=0$.

Since

$$R_J \equiv \left|\rho_o + \rho_{1,J}\right|^2 = R_o + 2Re\left(\rho_o^* \rho_{1,J}\right) + \left|\rho_{1,J}\right|^2$$

$$(A-8-11)$$

we can set

$$R_J \cong R_0 + 2\,\mathrm{Re}\left(\rho_0^* \rho_{1,J}\right) \qquad (A-8-12)$$

to first order in v_K.

Since

$$\rho_0^* \rho_{1,J} = -\left(1-2S_0''\right)^{J-1} \sum_{K=1}^{J-1} \frac{i\alpha R_0 v_K}{\left(1-2S_0''\right)^K} \qquad (A-8-13)$$

and since α is real,

$$\mathrm{Re}\left(\rho_0^* \rho_{1,J}\right) = 0 \qquad (A-8-14)$$

so that the reflectivity is an extremum with respect to the v_K.

Appendix 9 - Two-by-Two Optimization of X-Ray Multilayers

In this appendix we show how to calculate those thicknesses for the uppermost pair of layers in an x-ray multilayer that will maximize the reflectivity of the entire multilayer stack, given that the preceeding stack has a reflectivity ρ_K.

As discussed in sec. II-1-B we must include terms of order $\varphi \cdot \Delta$ in this calculation. It will therefore prove convenient to carry out the initial part of the calculation in terms of the parameters

$$\beta_{H,K} \equiv \frac{2\pi}{\lambda} \cos\theta \, d_{H,K}$$

$$\beta_{L,K} \equiv \frac{2\pi}{\lambda} \cos\theta \, d_{L,K} \qquad (A\text{-}9\text{-}1)$$

rather than the parameters φ and β. While the parameter β_H appearing in eq. II-2-15 is formally the same as that defined in eq. A-9-1, we will not, for the first part of the analysis in this appendix, be using "zeroth" order approximations (such as, for example, eq. II-2-43). The greater accuracy that we are using at present will be indicated by the use of the H subscript on the parameter β. In contrast the unsubscripted parameter β may be regarded as a division parameter with radian units, rather than as a precise phase thickness.

STRUCTURE OF UNIT CELL IN A BILAYER REFLECTOR
(Non-Centrosymmetric Geometry)

UR
LLE

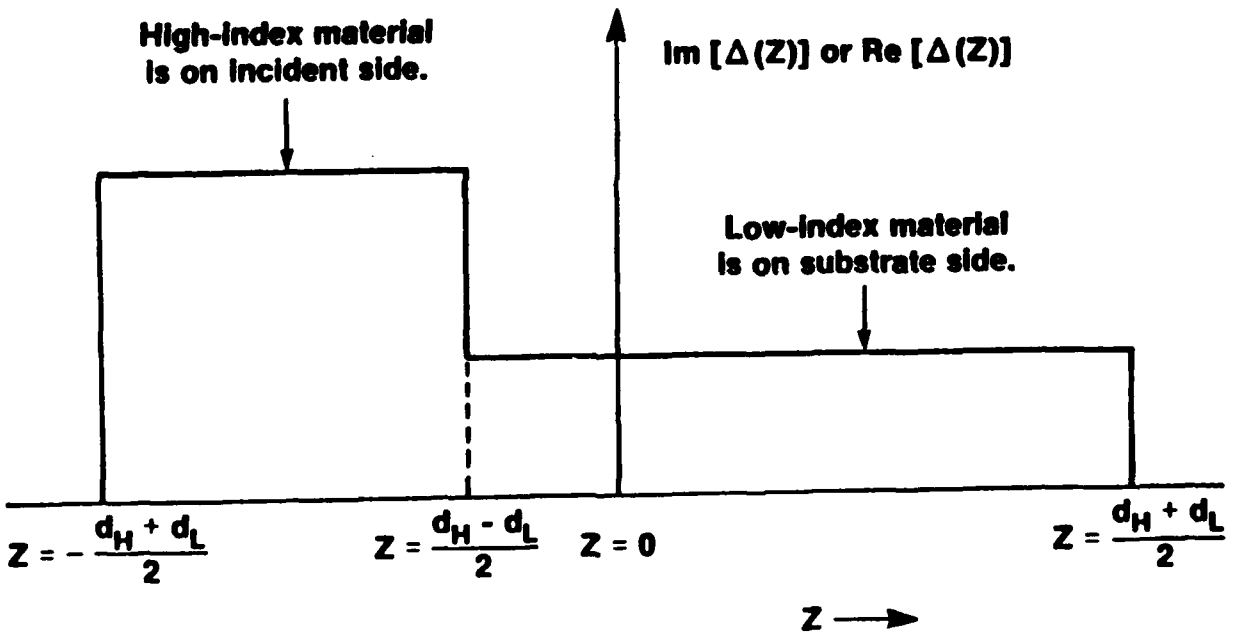

X351

Figure A-9-1

From fig. A-9-1 and the definitions of eqs. II-1-15, we have

$$\gamma_K = (\Delta_H \sin\beta_{H,K} \cos\beta_{L,K} + \Delta_L \cos\beta_{H,K} \sin\beta_{L,K})\, P(\theta) \sec^2\theta$$

$$\rho_K = (-\Delta_H \sin\beta_{H,K} \sin\beta_{L,K} + \Delta_L \sin\beta_{H,K} \sin\beta_{L,K})\, P(\theta) \sec^2\theta$$

$$\mu_K = (\Delta_H \beta_{H,K} + \Delta_L \beta_{L,K}) \sec^2\theta \qquad (A\text{-}9\text{-}2)$$

Eq. A-9-2 differs from eq. II-2-15 due to the inclusion of terms of order φ^2 and $\varphi \cdot \Delta$, and also due to the non-centrosymmetric geometry of fig. A-9-1.

The amplitude recursion equation eq. II-1-20 becomes

$$\rho_{K+1} = e^{-2it_K} \rho_K - i(\Delta_L \sin\beta_{L,K}\, e^{i\beta_{H,K}} + \Delta_H \sin\beta_{H,K}\, e^{-i\beta_{L,K}}) \times e^{-it_K} P(\theta) \sec^2\theta$$

$$- i(\Delta_L \sin\beta_{L,K}\, e^{-i\beta_{H,K}} + \Delta_H \sin\beta_{H,K}\, e^{i\beta_{L,K}}) \times e^{-3it_K} \rho_K^2 P(\theta) \sec^2\theta \qquad (A\text{-}9\text{-}3)$$

We now differentiate ρ_{K+1} with respect to the phase thickness of the final low index layer. Writing $\tilde{n}_{L,H} \equiv 1 + \Delta_{L,H}\sec^2\theta$:

$$\dot{\rho}_{K+1} = 2i\tilde{n}_L e^{-2it_K}\rho_K + \tilde{n}_L\left(\Delta_L \sin\beta_{L,K}\, e^{i\beta_{H,K}} + \Delta_H \sin\beta_{H,K}\, e^{-i\beta_{L,K}}\right) e^{-it_K} P(\theta)\sec^2\theta$$

$$- i\left(\Delta_L \cos\beta_{L,K}\, e^{i\beta_{H,K}} - i\,\Delta_H \sin\beta_{H,K}\, e^{-i\beta_{L,K}}\right) e^{-it_K} P(\theta)\sec^2\theta$$

$$+ 3\tilde{n}_L\left(\Delta_L \sin\beta_{L,K}\, e^{-i\beta_{H,K}} - i\,\Delta_H \sin\beta_{H,K}\, e^{-i\beta_{L,K}}\right) e^{-3it_K}\rho_K^2 P(\theta)\sec^2\theta$$

$$- i\left(\Delta_L \cos\beta_{L,K}\, e^{-i\beta_{H,K}} + i\,\Delta_H \sin\beta_{H,K}\, e^{i\beta_{L,K}}\right) e^{-3it_K}\rho_K^2 P(\theta)\sec^2\theta$$

(A-9-4)

Neglecting terms of order Δ^2 :

$$\dot{\rho}_{K+1} = 2ie^{-2it_K}\rho_K\Big[1 + \Delta_L\sec^2\theta - \frac{i}{2}\left(\Delta_L \sin\beta_{L,K}\, e^{i\beta_{H,K}} + \Delta_H \sin\beta_{H,K}\, e^{-i\beta_{L,K}}\right)\frac{e^{it_K}}{\rho_K} P(\theta)\sec^2\theta$$

$$- \frac{1}{2}\left(\Delta_L \cos\beta_{L,K}\, e^{i\beta_{H,K}} - i\,\Delta_H \sin\beta_{H,K}\, e^{-i\beta_{L,K}}\right)\frac{e^{it_K}}{\rho_K} P(\theta)\sec^2\theta$$

$$- \frac{3}{2} i\left(\Delta_L \sin\beta_{L,K}\, e^{-i\beta_{H,K}} + \Delta_H \sin\beta_{H,K}\, e^{i\beta_{L,K}}\right) e^{-it_K}\rho_K P(\theta)\sec^2\theta$$

$$- \frac{1}{2}\left(\Delta_L \cos\beta_{L,K}\, e^{-i\beta_{H,K}} + i\,\Delta_H \sin\beta_{H,K}\, e^{i\beta_{L,K}}\right) e^{-it_K}\rho_K P(\theta)\sec^2\theta\Big]$$

(A-9-5)

To maximize R_{K+1}, we require that $\mathrm{Re}\left(\dot{\rho}_{K+1}/\rho_{K+1}\right) = 0$. Writing

$$\rho_{K+1} = e^{-2it_K}\rho_K\left(1 - i\left(\Delta_L \sin\beta_{L,K}\, e^{i\beta_{H,K}} + \Delta_H \sin\beta_{H,K}\, e^{-i\beta_L}\right)\frac{e^{it_K}}{\rho_K}\,P(\theta)\sec^2\theta\right.$$

$$\left. - i\left(\Delta_L \sin\beta_{L,K}\, e^{-i\beta_{H,K}} + \Delta_H \sin\beta_{H,K}\, e^{i\beta_{L,K}}\right)e^{-it_K}\rho_K\,P(\theta)\sec^2\theta\right) \qquad (A\text{-}9\text{-}6)$$

we obtain after neglecting terms of order Δ^2:

$$0 = \mathrm{Im}\left[\Delta_L + \frac{i}{2}\left(\Delta_L \sin\beta_{L,K}\, e^{i\beta_{H,K}} + \Delta_H \sin\beta_{H,K}\, e^{-i\beta_{L,K}}\right)\frac{e^{it_K}}{\rho_K}\,P(\theta)\right.$$

$$- \frac{i}{2}\left(\Delta_L \sin\beta_{L,K}\, e^{-i\beta_{H,K}} + \Delta_H \sin\beta_{H,K}\, e^{i\beta_{L,K}}\right)e^{-it_K}\rho_K\,P(\theta)$$

$$- \frac{i}{2}\left(\Delta_L \cos\beta_{L,K}\, e^{i\beta_{H,K}} - i\,\Delta_H \sin\beta_{H,K}\, e^{-i\beta_{L,K}}\right)\frac{e^{it_K}}{\rho_K}\,P(\theta)$$

$$\left. - \frac{i}{2}\left(\Delta_L \cos\beta_{L,K}\, e^{-i\beta_{H,K}} + i\,\Delta_H \sin\beta_{H,K}\, e^{i\beta_{L,K}}\right)e^{-it_K}\rho_K\,P(\theta)\right] \qquad (A\text{-}9\text{-}7)$$

or

or

$$0 = Im\left[\Delta_L + i\Delta_H P(\theta)\sin\beta_{H,K}\left(\frac{1}{\rho_K e^{-it_K} e^{i\beta_{L,K}}} - \rho_K e^{-it_K} e^{i\beta_{L,K}}\right)\right.$$

$$\left. -\frac{1}{2}\Delta_L P(\theta)\left(\frac{1}{\rho_K e^{-it_K} e^{-i(\beta_{H,K}-\beta_{L,K})}} + \rho_K e^{-it_K} e^{-i(\beta_{H,K}-\beta_{L,K})}\right)\right] \qquad (A-9-8)$$

Similarly, differentiating with respect to $\beta_{H,K}$:

$$\dot{\rho}_{K+1} = 2i\tilde{n}_H e^{-2it_K}\rho_K + \tilde{n}_H\left(\Delta_L \sin\beta_{L,K} e^{i\beta_{H,K}} + \Delta_H \sin\beta_{H,K} e^{-i\beta_{L,K}}\right) e^{-it_K} P(\theta)\sec^2\theta$$

$$= i\left(i\Delta_L \sin\beta_{L,K} e^{i\beta_{H,K}} + \Delta_H \cos\beta_{H,K} e^{-i\beta_{L,K}}\right) e^{-it_K} P(\theta)\sec^2\theta$$

$$+3\tilde{n}_H\left(\Delta_L \sin\beta_{L,K} e^{-i\beta_{H,K}} + \Delta_H \sin\beta_{H,K} e^{i\beta_{L,K}}\right) e^{-3it_K}\rho_K^2 P(\theta)\sec^2\theta$$

$$-i\left(-i\Delta_L \sin\beta_{L,K} e^{-i\beta_{H,K}} + \Delta_H \cos\beta_{H,K} e^{i\beta_{L,K}}\right) e^{-3it_K}\rho_K^2 P(\theta)\sec^2\theta$$

$$(A-9-9)$$

which leads to the condition

$$0 = Im\left\{\Delta_H\left[1 - \frac{P(\theta)}{2}\left(\rho_K e^{-it_K} e^{i(\beta_{H,K}+\beta_{L,K})} + \frac{1}{\rho_K e^{-it_K} e^{i(\beta_{H,K}+\beta_{L,K})}}\right)\right]\right\}$$

$$(A-9-10)$$

We will now convert back to the parameters φ and β in order to facilitate comparison with earlier results. For reasons discussed in sec. II-1-B, it is only necessary to retain terms of order $\varphi \cdot \Delta$ prior to performing the differentiations necessary for the optimization. Therefore at this stage in the calculation we can follow a procedure similar to that used in optimizing the periodic case, and neglect terms of order $\varphi \cdot \Delta$ when optimizing β .

To obtain an optimization condition for the parameter β , we therefore use the "zeroth" order relations

$$\beta_{L,K} \cong \pi - \beta_K , \qquad \beta_{H,K} - \beta_{L,K} \cong 2\beta_K - \pi \tag{A-9-11}$$

where we have set $\varphi_K = 0$.

Substituting into eq. A-9-8,

$$0 = Im\left\{ \Delta_L \left[1 + \frac{P(\theta)}{2} \left(\rho_K e^{-2i\beta_K} + \frac{1}{\rho_K e^{-2i\beta_K}} \right) \right] + iP(\theta)\Delta_H \sin\beta_K \left(\rho_K e^{-i\beta_K} - \frac{1}{\rho_K e^{-i\beta_K}} \right) \right\} \tag{A-9-12}$$

or re-arranging

$$0 = Im\left\{ \Delta_L + \frac{\Delta_H P(\theta)}{2} \left(\rho_K + \frac{1}{\rho_K} \right) - \frac{1}{2}(\Delta_H - \Delta_L) \left(\rho_K e^{-2i\beta_K} + \frac{1}{\rho_K e^{-2i\beta_K}} \right) \right\} \tag{A-9-13}$$

Similarly, using the relation $\beta_{u,\kappa} + \beta_{\ell,\kappa} = \pi - \varphi_\kappa$, eq. A-9-10 becomes an optimization condition for the parameter φ_κ which is accurate to order $\varphi \cdot \Delta$:

$$0 = Im\left\{\Delta_u\left[1 + \frac{P(\theta)}{2}\left(\rho_\kappa e^{i\mu_\kappa} e^{-2i\varphi_\kappa} + \frac{1}{\rho_\kappa e^{i\mu_\kappa} e^{-2i\varphi_\kappa}}\right)\right]\right\} \qquad (A-9-14)$$

Eqs. A-9-13,14 are of the form

$$Im\left\{A \cdot C \cdot e^{iB} \cdot e^{ix} + \frac{C}{A \cdot e^{iB} \cdot e^{ix}} + D\right\} = 0 \qquad (A-9-15)$$

with x the unknown.

Introducing the notation $v_\varphi \equiv \arg(G)$ for the arguments of the various complex parameters, we have

$$0 = Im\left\{|A| \cdot |C| \cdot e^{i(B+x+V_A+V_C)} + \frac{|C|}{|A|} e^{-i(B+x+V_A-V_C)}\right\} + D''$$

(continued on next page)

$$= D'' + |C| \left(|A| - \frac{1}{|A|}\right) \sin\left(B + x + V_A\right) \cos\left(V_C\right) + |C| \left(|A| + \frac{1}{|A|}\right) \cos\left(B + x + V_A\right) \sin\left(V_C\right)$$

(A-9-16, continued)

or

$$0 = \frac{\left(|A|^2 - 1\right) \sin\left(B + x + V_A\right) \cos V_C}{\sqrt{\cos^2 V_C \left(1 - |A|^2\right)^2 + \sin^2 V_C \left(1 + |A|^2\right)^2}} + \frac{\left(|A|^2 + 1\right) \cos\left(B + x + V_A\right) \sin V_C}{\sqrt{\cos^2 V_C \left(1 - |A|^2\right)^2 + \sin^2 V_C \left(1 + |A|^2\right)^2}} + \frac{D'' |A| / |C|}{\sqrt{\cos^2 V_C \left(1 - |A|^2\right)^2 + \sin^2 V_C \left(1 + |A|^2\right)^2}}$$

(A-9-17)

Letting

$$\cos w \equiv \frac{-\left(|A|^2 - 1\right) \cos V_C}{\sqrt{\cos^2 V_C \left(1 - |A|^2\right)^2 + \sin^2 V_C \left(1 + |A|^2\right)^2}}$$

$$\sin w \equiv \frac{\left(|A|^2 + 1\right) \sin V_C}{\sqrt{\cos^2 V_C \left(1 - |A|^2\right)^2 + \sin^2 V_C \left(1 + |A|^2\right)^2}}$$

(A-9-18)

so that

$$\tan w = \frac{1+|A|^2}{1-|A|^2} \tan V_c \qquad (A-9-19)$$

and using

$$\cos^2 V_c (1-|A|^2)^2 + \sin^2 V_c (1+|A|^2)^2 = 1+|A|^4 - 2\cos(2V_c)|A|^2 \qquad (A-9-20)$$

we have

$$0 = \cos(B+x+V_A)\sin w - \sin(B+x+V_A)\cos w + \frac{D''|A|}{|C|\sqrt{1+|A|^4-2\cos(2V_c)|A|^2}} \qquad (A-9-21)$$

or

$$w - B - x - V_4 = -\arcsin\left(\frac{D''|A|}{|C|\sqrt{1+|A|^4-2\cos(2V_c)|A|^2}}\right) \qquad (A-9-22)$$

so that

$$x = -B - V_A + \arctan\left(\frac{1+|A|^2}{1-|A|^2}\tan V_C\right)$$

$$+ \arcsin\left(\frac{D''|A|}{|C|\sqrt{1+|A|^4-2\cos(2V_C)|A|^2}}\right) \qquad (A-9-23)$$

Applying this result to eq. A-9-14 we find that φ_k is given by

$$\varphi_k = \frac{1}{2}\left\{\mu'_k + V_\rho - \arctan\left(\frac{1+\mathcal{R}_k}{1-\mathcal{R}_k}\tan V_H\right)\right.$$

$$\left. - \arcsin\left(\frac{2\sqrt{\mathcal{R}_k}\sin V_H}{|P(\theta)|\sqrt{1+\mathcal{R}_k^2-2\mathcal{R}_k\cos(2V_H)}}\right)\right\} \qquad (A-9-24)$$

Eq. II-4-8 can be obtained from eq. A-9-13 if we use the identity

$$\mathrm{Im}\left[\Delta_H\left(\rho_k+\frac{1}{\rho_k}\right)\right] = \sqrt{\frac{|\Delta_H|^2}{R_k}}\left[(1+R_k)\sin V_H\cos V_\rho-(1-R_k)\cos V_H\sin V_\rho\right]$$

$$= \sqrt{\frac{|\Delta_H|^2\left(1+R_k^2-2R_k\cos(2V_H)\right)}{R_k}}\sin(h-V_\rho) \qquad (A-9-25)$$

where

$$h \equiv \arctan\left(\frac{1+R_H}{1-R_H}\tan V_H\right) \qquad (A-9-26)$$

Substituting into eq. A-9-23:

$$\beta_R = \frac{1}{2}\left\{\pi + \arcsin\left[\sqrt{|\Delta_H - \Delta_L|^2\,(1+R^2-2R\cos(2V_q))}\;\times\right.\right.$$

$$\left.\left.\left(2\Delta_L''\sqrt{R} + P(\theta)\sqrt{|\Delta_H|^2\,(1+R^2-2R\cos(V_H))}\;A\right)\right] + f(V_p, R, V_q)\right\}$$

where $\quad A \equiv \sin\left(f(V_p, R, V_H)\right)$

$$f(V_1, G, V_2) \equiv V_1 - \arctan\left[\frac{1+G}{1-G}\tan V_2\right]$$

(A-9-27)

We have found from numerical tests that the correct results are obtained if the standard lowest order returns to the inverse trigonometric functions are used in eqs. A-9-24 and 27; the equations have been written in a form that yields this result.

Appendix 10 - Effect of Accumulating Thickness Errors Outside the Steady-State Regime

In this appendix we calculate $< R_s >$ outside the steady-state regime for multilayers that contain accumulating thickness errors.

We first obtain an approximate K-dependent solution to eq. II-5-12. The fourth term on the right of eq. II-5-12 is small compared to the constant second term, and attains its largest magnitude only as the steady-state is approached.

In the steady-state, this term is given by eq. II-5-23. If we substitute for the fourth term the approximate expression

$$< \tilde{\rho}_K^2 > = \frac{- < \Delta\varphi^2 > < \rho_K >^2}{- i\tilde{\delta}_\infty + 2 < \Delta\varphi^2 >} \qquad (A\text{-}10\text{-}1)$$

then this term will go to the correct limit in the large K regime where it is numerically most significant. In addition, the term will correctly go to zero when K is small, or when $< \Delta\varphi^2 >$ becomes large. (In eq. A-10-1, the subscript on $\tilde{\delta}_\infty$ indicates that eq. II-5-15 is to be evaluated in the steady-state).

Eqs. II-5-12 and A-10-1 complete the statistical treatment of the terms in eq. II-5-5. As discussed above, the principle advantage of the difference equation formulation lies in performing this statistical treatment, and it is now easiest to proceed by converting eq. II-5-12 to a differential equation.

Using

$$\langle \rho_{n+1} \rangle - \langle \rho_n \rangle = \frac{d\langle \rho \rangle}{dK} \cdot \Delta K + O\left(\frac{d^2 \langle \rho \rangle}{dK^2} \right)$$

$$= \frac{d\langle \rho \rangle}{dK} + O\left(\langle \Delta \varphi^2 \rangle^2\right) + O\left(\langle \varphi \rangle^2\right) + O(\varphi \cdot \Delta) + O(\Delta^2)$$

(A-10-2)

eq. II-5-12 can be written under our approximation scheme:

$$\frac{d\langle \rho \rangle}{dK} = -2\left(i\langle t \rangle + \langle \Delta \varphi^2 \rangle\right)\langle \rho \rangle - (ir - \rho)$$

$$-(ir + \rho)\left(1 - \frac{\langle \Delta \varphi^2 \rangle}{-i\bar{s}_\infty + 2\langle \Delta \varphi^2 \rangle}\right)\langle \rho \rangle^2 \qquad \text{(A-10-3)}$$

Since the reflectivity of the substrate is small, the exact boundary condition applied to eq. A-10-3 becomes unimportant if the multilayer contains more than a few layers. For simplicity we will set $\langle \rho \rangle = 0$ at

the substrate.

The solution of eq. A-10-3 is straightforward, and is similar to that presented in Appendix 3 for the defect-free case. We find

$$\langle \rho_y \rangle = \frac{1}{2c}\left(\frac{b^2+4D^2}{(b-2iD)-(b+2iD)e^{2iD(J-1)}}\right)\left(e^{2iD(J-1)}-1\right) \qquad (A\text{-}10\text{-}4)$$

where

$$a \equiv (ir+p)$$

$$b \equiv 2\left(i\langle t\rangle + \langle \Delta\varphi^2\rangle\right)$$

$$c \equiv (ir+p)\left(\frac{-i\tilde{\delta}_\infty + \langle \Delta\varphi^2\rangle}{-i\tilde{\delta}_\infty + 2\langle \Delta\varphi^2\rangle}\right) \qquad (A\text{-}10\text{-}5)$$

and

$$D \equiv \sqrt{-\left(i\langle t\rangle + \langle \Delta\varphi^2\rangle\right)^2 - (r^2+p^2)\left(\frac{-i\tilde{\delta}_\infty + \langle \Delta\varphi^2\rangle}{-i\tilde{\delta}_\infty + 2\langle \Delta\varphi^2\rangle}\right)} \qquad (A\text{-}10\text{-}6)$$

After manipulation, eq. A-10-4 reduces to

$$\langle \rho_j \rangle = \frac{\langle \rho_\infty \rangle \left(1 - e^{2iD(j-1)}\right)}{1 - \left(\frac{\gamma - ip}{\gamma + ip}\right)\left(\frac{-i\tilde{\delta}_\infty - \langle \Delta\varphi^2 \rangle}{-i\tilde{\delta}_\infty + 2\langle \Delta\varphi^2 \rangle}\right)\langle \rho_\infty \rangle^2 e^{2iD(j-1)}} \qquad (A\text{-}10\text{-}7)$$

Here $\langle \rho_\infty \rangle$ is the steady-state solution of eq. II-5-35.

In order to find $< R_k >$ we must now solve eq. II-5-22 outside the steady state regime. As a linear difference equation, eq. II-5-22 has the formal solution

$$<|\tilde{\rho}_J|^2> = 4<\Delta\rho^2> e^{-4\left[(J-1)\mu'' + Re\left((i\tau+p)\sum_{k=1}^{J-1}<\rho_k>\right)\right]}$$

$$\times \sum_{K'=1}^{J-1} |<\rho_{K'}>|^2 e^{4\left[K'\mu'' + Re\left((i\tau+p)\sum_{K''=1}^{K'}<\rho_{K''}>\right)\right]}$$

(A-10-8)

Eq. A-10-8 can easily be evaluated numerically using eq. II-5-35, but an analytic solution that is quite accurate can also be obtained.

We first find an approximate expression for $|<\rho_{K'}>|^2$ to use in the summation. In the soft x-ray regime, $<\rho_\infty>^2$ tends to be somewhat small compared to one, so that the denominator of eq. A-10-7 is approximately unity, and

$$|<\rho_{K'}>|^2 \cong \left|<\rho_\infty>\left(1 - e^{2iD(K'-1)}\right)\right|^2 \qquad (A-10-9)$$

(Eq. A-10-9 is compared to eq. A-10-7 in fig. A-10-1).

Eq. A-10-9 is quite accurate when K' is large, since the neglected term in the denominator of eq. A-10-7 is then small. To improve the fractional accuracy of eq. A-10-9 when K' is small, we re-normalize to $K' = J$ (where J is the index of the left-hand side of eq. A-10-8) to obtain

$$|<\rho_{K'}>|^2 \cong \left| \frac{<\rho_J>}{(1 - e^{2iD(J-1)})} \left(1 - e^{2iD(K'-1)}\right) \right|^2 \qquad (A\text{-}10\text{-}10)$$

The large K' terms dominate the sum over K' in eq. A-10-8 since $|<\rho_{K'}>|^2$ is most significant in that case. For this reason we make the approximations

$$(ir+p) \sum_{K=1}^{J-1} <\rho_K> \cong (ir+p)(J-1)<\rho_{J-1}>$$

$$\cong (ir+p)(J-1)<\rho_J> \qquad (A\text{-}10\text{-}11)$$

and

$$(ir+p) \sum_{K''=1}^{K'} <\rho_{K''}> \cong (ir+p)K'<\rho_J> \qquad (A\text{-}10\text{-}12)$$

TEST OF APPROXIMATE SOLUTION FOR $|<\rho_J>|^2$ TUNGSTEN-CARBON MULTILAYER

UR LLE

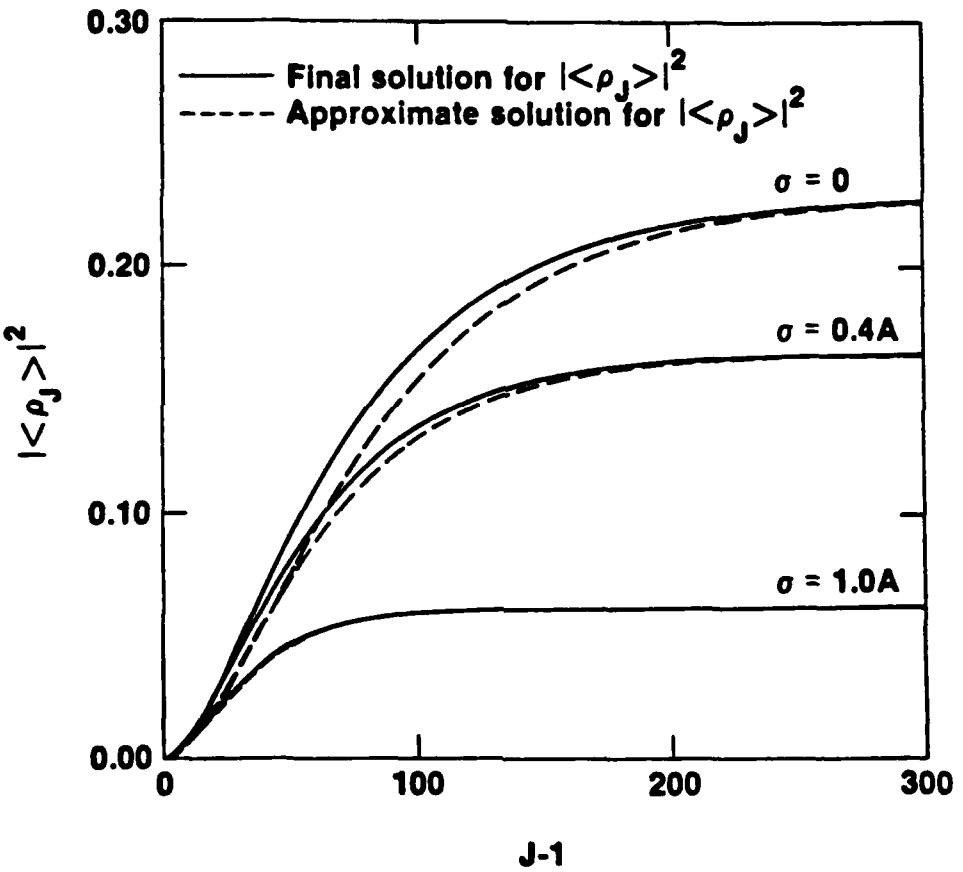

Plots are for a W/C multilayer reflecting 67.6Å radiation at normal incidence. d_W = 7.6Å, d_C = 26.5Å.

X356

Figure A-10-1

for the summations in the exponents on the right of eq. A-10-8. We note that these summation terms in the exponents tend to be small compared to the terms proportional to μ'' that preceed them.

Eq. A-10-8 is now reduced to the sum of four geometric series

$$\langle|\tilde{\rho}_J|^2\rangle = \frac{4\langle\Delta\varphi^2\rangle|\langle\rho_J\rangle|^2}{\left|1-e^{2iD(J-1)}\right|^2}\, e^{-4(J-1)\tilde{\delta}_J''}$$

$$\times \sum_{K'=1}^{J-1} e^{4K'\tilde{\delta}_J''}\left[1-e^{2i(K'-1)D}-e^{-2i(K'-1)D^*}+e^{-4(K'-1)D''}\right] \qquad (A\text{-}10\text{-}13)$$

Noting that terms of the form $\exp(\alpha)$, where α is of order Δ, can be set to 1, and using

$$\sum_{K'=1}^{J-1} e^{\alpha K'} = \frac{e^{\alpha J}-e^{\alpha}}{e^{\alpha}-1} \cong \frac{e^{\alpha J}-1}{\alpha} \qquad (A\text{-}10\text{-}14)$$

we find:

$$\langle|\tilde{\rho}_J|^2\rangle = \frac{2\langle\Delta\varphi^2\rangle|\langle\rho_J\rangle|^2}{\left|1-e^{2i(J-1)D}\right|^2}$$

(continued on next page)

$$\times \left[\frac{1 - e^{-4(J-1)\tilde{\delta}_J''}}{2\tilde{\delta}_J''} - \mathrm{Re}\left(\frac{e^{2i(J-1)D} - e^{-4(J-1)\tilde{\delta}_J''}}{\tilde{\delta}_J'' + iD/2} \right) \right.$$

$$\left. + \frac{e^{-4(J-1)D''} - e^{-4(J-1)}}{2\left(\tilde{\delta}_J'' - D''\right)} \right] \qquad \text{(A-10-14, continued)}$$

where $\langle \rho_J \rangle$ is determined from eq. A-10-7, and $\tilde{\delta}_J''$ from eq. II-5-15. $\langle R_J \rangle$ can then be determined with eq. II-5-36.

In order to show the accuracy of the assumptions made in eqs. A-10-8,15, we have compared in fig. A-10-2 an explicit numerical evaluation of the summation of eq. A-10-8 to the analytic expression of eq. A-10-15. Eq. A-10-7 is used in both cases to evaluate $\langle \rho_K \rangle$. Our usual $\lambda = 67.6A$ example is used.

RANDOM COMPONENT OF REFLECTED BEAM (TUNGSTEN-CARBON MULTILAYER CONTAINING THICKNESS ERRORS)

UR LLE

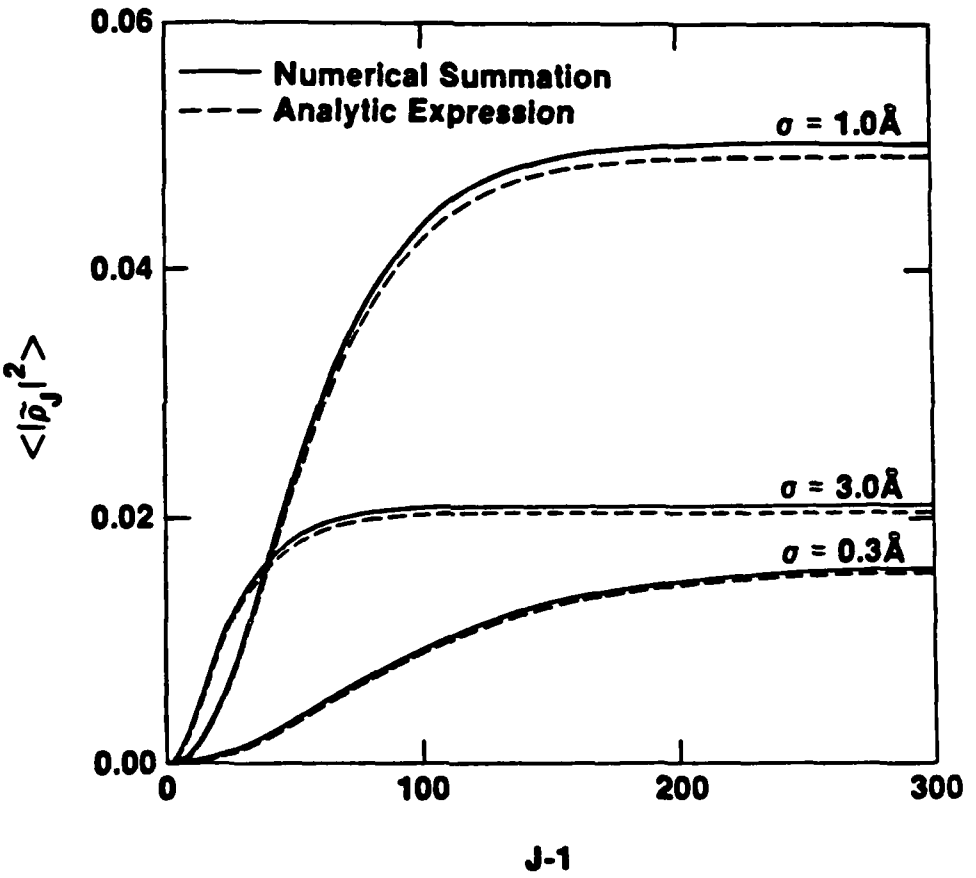

Plots are for a W/C multilayer reflecting 67.6Å radiation at normal incidence. d_W = 7.6Å, d_C = 26.5Å.

X358

Figure A-10-2

Appendix 11 - Phenomenological Solution for Multilayer Reflectivity in the Presence of Non-Accumulating Errors

In this appendix we calculate the reflectivity under a simplified model of non-accumulating random thickness errors in which the physical layer interfaces are taken to be randomly displaced in an uncorrelated way from their ideal positions.

We use a quasi-centrosymmetric cell decomposition, as shown in fig. A-11-1. Here $f_{L,K}$ and $f_{H,K}$ are the shifts in position of the L and H interfaces of the Kth cell.

Although we may speak of f_H as being the error in the Kth high index layer, it is more accurate to consider f_H to be the error in truncation of the Kth high index layer (and similarly for the low index layers).

The ISRM operator will attempt to perform these layer truncations at the appropriate points in the ISRM oscillations, and, if the multilayer contains more than a few layers, these oscillations will not be significantly influenced by any one individual layer error in the preceeding stack.

Thus, it is plausible to treat the f values as uncorrelated and as having zero mean. However, the more rigorous analysis of sec. II-6-B shows that this assumption is not strictly accurate.

From fig. A-11-1 and the defining equations in eq. II-1-15, we find after manipulation that the structural parameters in eq. II-1-20 are given by

$$i\tau - p = \left[i\tilde{\Delta}_L \sin\varphi_0 + \frac{\tilde{q}}{2}\left(e^{i\beta_{H,0}} e^{2i\xi_{L,K}} - e^{-i\beta_{H,0}} e^{2i\xi_{H,K}} \right) \right]$$

(continued on next page)

UNIT CELL DECOMPOSITION FOR NON-ACCUMULATING ERRORS – PHENOMENOLOGICAL TREATMENT

UR LLE

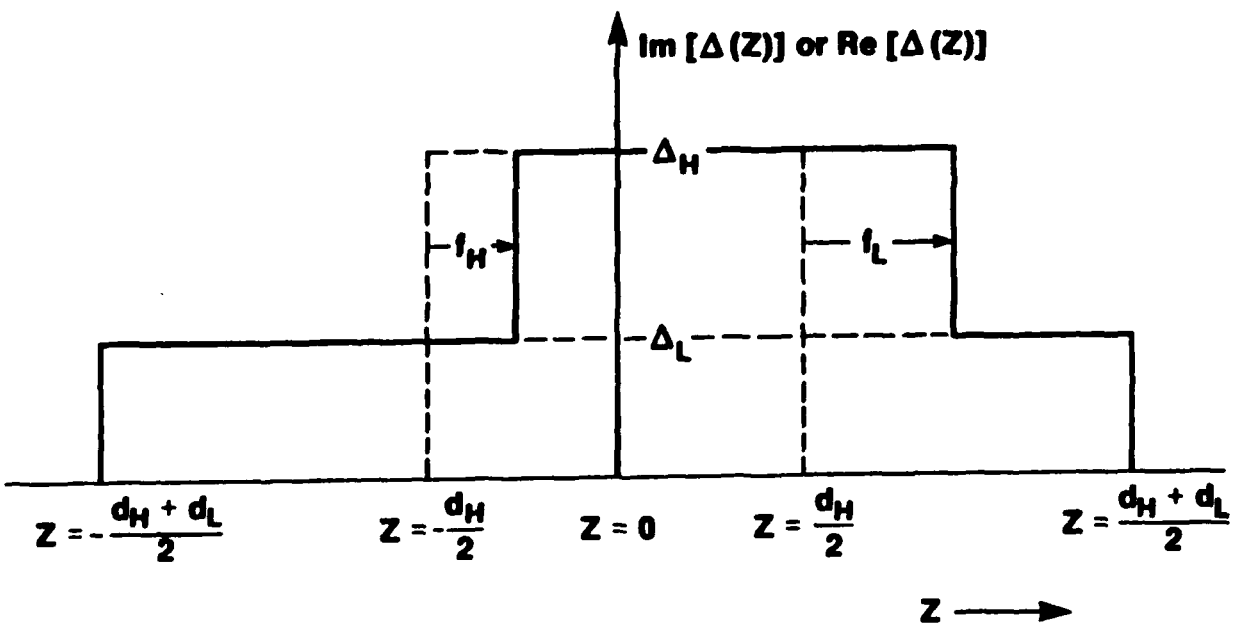

X360

Figure A-11-1

$$ir + p = \left[i\tilde{\Delta}_L \sin\varphi_0 + \frac{\tilde{q}}{2}\left(e^{i\beta_{H,0}} e^{-2i\xi_{H,K}} - e^{-i\beta_{H,0}} e^{-2i\xi_{L,K}}\right)\right]$$

$$\mu = \pi\tilde{\Delta}_L + \beta_{H,0}\,\tilde{q} + \tilde{q}\,(\xi_L - \xi_H)$$

(A-11-1, continued)

where

$$\xi_{H,K} \equiv \frac{2\pi}{\lambda}\cos\theta\, f_{H,K}$$

$$\xi_{L,K} \equiv \frac{2\pi}{\lambda}\cos\theta\, f_{L,K} \qquad (A\text{-}11\text{-}2)$$

Thus, eq. II-1-20 becomes in first order

$$\rho_{K+1} = e^{-2it_0} e^{2i\tilde{q}(\xi_{L,K} - \xi_{H,K})}\,\rho_K$$

$$- e^{-it_0} e^{i\tilde{q}(\xi_{L,K} - \xi_{H,K})}\left[\frac{\tilde{q}}{2}\left(e^{i\beta_{H,0}} e^{2i\xi_{L,K}} - e^{-i\beta_{H,0}} e^{2i\xi_{H,K}}\right) + i\tilde{\Delta}_L \sin\varphi_0\right]$$

$$- e^{-3it_0} e^{3i\tilde{q}(\xi_{L,K} - \xi_{H,K})}\,\rho_K^2\left[\frac{\tilde{q}}{2}\left(e^{i\beta_{H,0}} e^{-2i\xi_{H,K}} - e^{-i\beta_{H,0}} e^{-2i\xi_{L,K}}\right) + i\Delta_L \sin\varphi_0\right]$$

(A-11-3)

Taking expectation values, neglecting quadratic terms in $\tilde{\rho}$, and neglecting terms of order $\varphi \cdot \Delta$, yields eq. II-6-17.

We now derive an approximate expression for the incoherent reflectivity $\langle | \tilde{\rho} |^2 \rangle$ in order to show that our neglect of quadratic terms in $\tilde{\rho}$ is reasonable.

If we take the expectation value of eq. A-11-3 without neglecting terms of order $\varphi \cdot \Delta$ or Δ^2 (but neglecting terms of order $\varphi^2 \cdot \Delta$, and Δ^3), and then subtract from eq. A-11-3, we obtain the following equation for $\tilde{\rho}$

$$\tilde{\rho}_{n+1} = e^{-2it_0}\langle \rho_n \rangle \left[e^{2i\tilde{q}(\xi_{1,n} - \xi_{N,n})} - e^{-2\tilde{q}^2(\langle \xi_N^2 \rangle + \langle \xi_1^2 \rangle)} \right]$$

$$+ \tilde{\rho}_n e^{-2it_0} e^{2i\tilde{q}(\xi_{1,n} - \xi_{N,n})} - e^{-it_0} \frac{\tilde{q}}{2} \left[e^{i\beta_{N,0}} \left(e^{2i\xi_{1,n}} e^{i\tilde{q}(\xi_{1,n} - \xi_{N,n})} - e^{-2\langle \xi_1^2 \rangle (1+\tilde{q})} \right) \right.$$

$$\left. - e^{-i\beta_{N,0}} \left(e^{2i\xi_{N,n}} e^{i\tilde{q}(\xi_1 - \xi_N)} - e^{-2\langle \xi_N^2 \rangle (1-\tilde{q})} \right) \right]$$

$$- \langle \rho_n \rangle^2 \frac{\tilde{q}}{2} e^{-3it_0} \left[e^{i\beta_{N,0}} \left(e^{3i\tilde{q}(\xi_{1,n} - \xi_{N,n})} e^{-2i\xi_{N,n}} - e^{-2\langle \xi_N^2 \rangle (1+3\tilde{q})} \right) \right.$$

$$\left. - e^{-i\beta_{N,0}} \left(e^{-2i\xi_{1,n}} e^{3i\tilde{q}(\xi_{1,n} - \xi_{N,n})} - e^{-2\langle \xi_1^2 \rangle (1-3\tilde{q})} \right) \right]$$

(continued on next page)

$$-2e^{-3it_0}e^{3i\tilde{q}(\xi_{L,K}-\xi_{H,K})}\left[i\tilde{\Delta}_L\rho_0+\frac{\tilde{q}}{2}\left(e^{i\beta_{H,0}}e^{-2i\xi_{H,K}}-e^{-i\beta_{H,0}}e^{-2i\xi_L}\right)\right]\langle\rho_K\rangle\tilde{\rho}_K$$

$$-e^{-3it_0+3i\tilde{q}(\xi_{L,K}-\xi_{H,K})}\left[i\tilde{\Delta}_L\rho_0+\frac{\tilde{q}}{2}\left(e^{i\beta_{H,0}}e^{-2i\xi_{H,K}}-e^{-i\beta_{H,0}}e^{-2i\xi_{L,K}}\right)\right]\tilde{\rho}_K^2$$

$$e^{-3it_0}\left[i\tilde{\Delta}_L\rho_0+\frac{\tilde{q}}{2}\left(e^{i\beta_{H,0}}e^{-2\langle\xi_H^2\rangle}-e^{-i\beta_{H,0}}e^{-2\langle\xi_L^2\rangle}\right)\right]\langle\tilde{\rho}_K^2\rangle$$

(A-11-4, continued)

When we take the magnitude squared of this equation, we will find that the principal driving term for $\langle|\tilde{\rho}|^2\rangle$ is the magnitude squared of the third term.

Since our purpose in calculating $\langle|\tilde{\rho}|^2\rangle$ is to verify our basic assumption that $\langle|\tilde{\rho}|^2\rangle$ is a very small quantity, we will, for purposes of illustration, make the same simplifying assumption as was used in obtaining eq. II-6-23, namely that the L and H layer errors have equal RMS magnitudes; for a fixed total RMS error per cell we would not expect the relative proportion of the L and H errors to dramatically affect the result.

If we take the expectation value of the magnitude squared of this third term, neglecting terms of order Δ^4 (but retaining terms of order Δ^3), we obtain

$$\langle|\text{Term \#3}|^2\rangle = \frac{|\tilde{q}|^2}{2}\left[1-e^{-4\langle\xi^2\rangle(1+\tilde{q}')}+\tilde{q}''e^{-4\langle\xi^2\rangle}\sin(2\beta_{H,0})\right]$$

(A-11-5)

The lowest order terms in this result are of order Δ^2; to this order the term becomes

$$\langle |\text{Term \#3}|^2 \rangle = |\tilde{q}|^2 e^{-2\langle \xi^2 \rangle} \sinh(2\langle \xi^2 \rangle) \qquad (A\text{-}11\text{-}6)$$

We draw two conclusions from this result.

First, since the principal driving term is of order Δ^2, $\langle |\tilde{\rho}|^2 \rangle$ will be of the order of Δ^2 divided by the magnitude squared of the coefficient of $\tilde{\rho}$ in the second term, less unity. The latter has a magnitude squared that is of order Δ, so we can expect that $\langle |\tilde{\rho}|^2 \rangle$ will be of order Δ.

This means that we need only retain terms of order Δ^2 when squaring eq. A-11-4 if we wish to obtain a steady-state solution for $\langle |\tilde{\rho}|^2 \rangle$ that is accurate in lowest order.

Since eq. A-11-4 contains all terms of order Δ, it will be possible to obtain all terms of order Δ^2 after the equation is squared, since the lowest order terms in the equation are of order $\sqrt{\Delta}$.

Second, if we compare eq. A-11-6 with eq. A-11-5, we see that we can simplify eq. A-11-4 considerably before squaring it if we are only interested in terms of order Δ.

By considering each term in eq. A-11-4, we find that it can be written in lowest order as

$$\tilde{\rho}_{K+1} = -\frac{\tilde{q}}{2}\left[e^{i\beta_{N,0}}\left(e^{2i\xi_{L,K}} - e^{-2\langle\xi^2\rangle}\right) - e^{-i\beta_{N,0}}\left(e^{2i\xi_{N,K}} - e^{-2\langle\xi^2\rangle}\right)\right]$$

$$+ \tilde{\rho}_K e^{-2it_0} - \tilde{q}\langle\rho_K\rangle\,\tilde{\rho}_K\left[e^{-2i\xi_N} e^{i\beta_{N,0}} - e^{-2i\xi_L} e^{-i\beta_{N,0}}\right]$$

$$+ \langle\rho_K\rangle\, e^{-2it_0}\left(e^{2i\tilde{q}(\xi_{L,K} - \xi_{N,K})} - 1\right)$$

$$- \frac{\tilde{q}}{2}\left[e^{i\beta_{N,0}}\left(e^{-2i\xi_{N,K}} - e^{-2\langle\xi^2\rangle}\right) - e^{-i\beta_{N,0}}\left(e^{-2i\xi_{L,K}} - e^{-2\langle\xi^2\rangle}\right)\right]\langle\rho_K\rangle^2$$

(A-11-7)

Denoting the five terms in this equation as A, B, C, D, and E for simplicity, we find

$$\langle|A|^2\rangle = |\tilde{q}|^2 e^{-2\langle\xi^2\rangle} \sinh(2\langle\xi^2\rangle)$$

$$\langle AB^*\rangle = \langle A^*B\rangle = \langle AC^*\rangle = \langle A^*C\rangle = 0$$

$$\langle AD^*\rangle + \langle A^*D\rangle = -8\cos\beta_{N,0}|\tilde{q}|^2\langle\xi^2\rangle e^{-2\langle\xi^2\rangle}\,\mathrm{Re}(\langle\rho\rangle)$$

$$\langle AE^*\rangle + \langle A^*E\rangle = 2|\tilde{q}|^2\cos(2\beta_{N,0})\, e^{-6\langle\xi^2\rangle}\sinh(2\langle\xi^2\rangle)\,\mathrm{Re}(\langle\rho\rangle^2)$$

$$\langle|B|^2\rangle = \langle|\tilde{\rho}|^2\rangle\, e^{-4\mu_0''}$$

(continued on next page)

$$\langle BC^* \rangle + \langle B^* C \rangle = 4e^{-2\langle \xi^2 \rangle} \, \mathrm{Im}(r_0 \langle \rho \rangle) \langle |\tilde{\rho}|^2 \rangle$$

$$\langle BD^* \rangle = \langle B^* D \rangle = \langle BE^* \rangle = \langle B^* E \rangle = 0$$

$$\langle |C|^2 \rangle = -2|\tilde{q}|^2 \langle |\tilde{\rho}|^2 \rangle |\langle \rho \rangle|^2 \left(1 - e^{-4\langle \xi^2 \rangle} \cos(2\beta_{N,0})\right)$$

$$\langle CD^* \rangle = \langle C^* D \rangle = \langle CE^* \rangle = \langle C^* E \rangle = 0$$

$$\langle |D|^2 \rangle = 8|\tilde{q}|^2 \langle \xi^2 \rangle |\langle \rho \rangle|^2$$

$$\langle DE^* \rangle + \langle D^* E \rangle = -4 \cos\beta_{N,0} |\tilde{q}|^2 \langle \xi^2 \rangle e^{-2\langle \xi^2 \rangle} |\langle \rho \rangle|^2 \, \mathrm{Re}(\langle \rho \rangle)$$

$$\langle |E|^2 \rangle = |\tilde{q}|^2 |\langle \rho \rangle|^4 e^{-2\langle \xi^2 \rangle} \sinh(2\langle \xi^2 \rangle)$$

(A-11-8, continued)

If we solve for $\langle |\tilde{\rho}|^2 \rangle$ in the steady-state we obtain eq. II-6-19.

Appendix 12 - Effect of Interlayer Diffusion on Unit Cell Parameters

In sec. II-6 we have considered a model for interlayer diffusion in which the ideal sharp-interface structural profile of a periodic bilayer (shown in fig. II-2-1) is convolved with some smoothening function g(z).

Since the cell structure is centrosymmetric and the multilayer is periodic, we might regard the cosine transform that defines the parameter r in eq. II-1-15 as a Fourier transform, and conclude from the convolution theorem that the effect of diffusion will be to multiply r by the Fourier transform of g.

In this appendix we show that because $\Delta(z)$ is periodic, this conclusion is correct even though the parameter r is actually a truncated Fourier transform, to which the convolution theorem does not apply.

We let B denote the Fourier transform of $\Delta(z)$, where in our notation the Fourier transform is defined as

$$B = FT(\Delta) \equiv \int_{-\infty}^{\infty} dz\, e^{-2\pi i f z}\, \Delta(z) \qquad (A-12-1)$$

We denote convolution with an $*$, and use a prime to denote parameters that apply to the diffused multilayer. Then

$$\Delta'(z) = \Delta(z) * g(z) \qquad (A-12-2)$$

and

$$B' = BG \qquad (A\text{-}12\text{-}3)$$

where

$$G \equiv FT(g) \qquad (A\text{-}12\text{-}4)$$

If rect(z/d) $\equiv$ 1 for $|z| < d/2$, and zero otherwise, and if we define

$$A \equiv FT\left(\Delta(z)\,\mathrm{rect}\left(\frac{z}{d}\right)\right)$$

$$A' \equiv FT\left(\Delta'(z)\,\mathrm{rect}\left(\frac{z}{d}\right)\right) \qquad (A\text{-}12\text{-}5)$$

then

$$\tau = \frac{k_o}{\cos\theta} A\Big|_{f = 1/d}$$

(continued on next page)

$$q' = \frac{k_o}{\cos\theta} A' \Big|_{f = 1/d}$$

(A-12-6, continued)

Using the identity

$$\Delta(z) \equiv \Delta(z)\ \mathrm{rect}\left(\frac{z}{d}\right) * \mathrm{comb}\left(\frac{z}{d}\right) \qquad (A\text{-}12\text{-}7)$$

where

$$\mathrm{comb}(x) \equiv \sum_{-\infty}^{\infty} \delta(x-n) \qquad (A\text{-}12\text{-}8)$$

we have from eqs. A-12-5 and the definitions of B and B′

$$B = Ad\ \mathrm{comb}(fd)$$

$$B' = A'd\ \mathrm{comb}(fd) \qquad (A\text{-}12\text{-}9)$$

At frequencies where the comb function is non-zero, eqs. A-12-3 and 9 imply

$$A'\Big|_{fd=n} = AG\Big|_{fd=n} \qquad (A-12-11)$$

which, according to eq. A-12-6, is the desired result.

Appendix 13 - Analysis of the Ring Cavity

In this appendix we present an analysis of the ring cavity devised by Bremer and Kaihola (1980).

We first calculate the limiting throughput of a cavity made from grazing reflectors having a complex index of refraction n_s.

Let ξ be the angle of incidence to each surface. At each reflection

$$\rho_s = \frac{1-N}{1+N} \qquad (A-13-1)$$

where

$$N = N' + iN'' = \frac{n_s \cos\theta'}{\cos\left(\frac{\pi}{2} - \xi\right)} \qquad (A-13-2)$$

and

$$n_s \sin\theta' = \sin\left(\frac{\pi}{2} - \xi\right) \qquad (A-13-3)$$

so that as $\xi \Rightarrow 0$

$$N = \frac{\sqrt{n_B^2 - \cos^2 \xi}}{\sin \xi} \Rightarrow \frac{\sqrt{n_B^2 - 1}}{\xi} \qquad (A-13-4)$$

Since

$$R_s = \frac{1 - \dfrac{2N'}{1 + |N|^2}}{1 + \dfrac{2N'}{1 + |N|^2}} \qquad (A-13-5)$$

we have after manipulation

$$R_s \Rightarrow 1 - \frac{4\mathrm{Re}\left(\sqrt{n_B^2 - 1}\right)}{|n_B^2 - 1|}\xi \Rightarrow e^{-\frac{4\mathrm{Re}\left(\sqrt{n_B^2 - 1}\right)}{|n_B^2 - 1|}\xi}$$

$$(A-13-6)$$

The total number of reflections M is π/ξ , so

$$Q_s = R_s^M \Rightarrow e^{-\frac{4\pi}{Re\left(\sqrt{n_\beta^2 - 1}\right)}} \qquad (A-13-7)$$

By similar steps, we obtain for the P case

$$Q_p = \exp\left[-\frac{4\pi}{Re\left(\frac{\sqrt{n_\beta^2 - 1}}{n_\beta^2}\right)}\right] \qquad (A-13-8)$$

To first order in $\Delta_\beta \equiv n_\beta - 1$, eqs. A-13-7 and 8 both reduce to

$$Q_{s,p} \cong e^{-2\pi\left[\frac{1}{\sqrt{(\Delta_\beta')^2 + (\Delta_\beta'')^2}} + \frac{\Delta_\beta'}{(\Delta_\beta')^2 + (\Delta_\beta'')^2}\right]^{1/2}} \qquad (A-13-9)$$

If Δ_β'' is now treated as small compared to Δ_β' (a good approximation at shorter x-ray wavelengths), eq. III-2-6, first derived by Bremer and Kaihola (1980), is obtained.

The coefficient of the second order term for Δ_β in eq. A-13-7 differs from that of the second order term in eq. A-13-8 by a factor of 7; at very soft x-ray wavelengths (greater than 75Å or so) eq. A-13-9 therefore becomes inaccurate for certain materials.

We now obtain an approximate formula for the number of reflections $M_{1/2}$ required to approach the limiting throughput. To do so we must work to third order in ζ; for simplicity we retain only first order terms in Δ_β.

We must calculate

$$Q_{s,p} = \left(\frac{1-P}{1+P}\right)^{\pi/\zeta} \qquad (A-13-10)$$

where

$$P \equiv \frac{2N'}{1+|N|^2} \qquad (A-13-11)$$

and

$$N = \frac{\sqrt{n_\beta^2 - 1 + \sin^2\zeta}}{\sin\zeta} \qquad (A-13-12)$$

For $P \ll 1$, eq. A-13-10 reduces to

$$Q_{s,p} \cong \left[\frac{e^{-P - \frac{P^2}{2} - \frac{P^3}{3}}}{e^{P - \frac{P^2}{2} + \frac{P^3}{3}}} \right]^{\pi/\xi} = e^{-\frac{2\pi}{\xi} P - \frac{2\pi}{3\xi} P^3} \qquad (A\text{-}13\text{-}13)$$

We find after straightforward manipulations

$$P = \frac{\mathrm{Re}\left(\sqrt{2\Delta_B}\right)}{|\Delta_B|} \xi \left[1 - \frac{1}{2|\Delta_B|} \left(\frac{1}{2} + \frac{\Delta_B'}{|\Delta_B|} \right) \xi^2 \right] + O\left(\Delta_B^2\right) + O\left(\xi^4\right) \qquad (A\text{-}13\text{-}14)$$

Then from eq. A-13-13

$$Q_{s,p}(M) = Q(M \Rightarrow \infty) \cdot \exp\left[-2\pi^3 \frac{\mathrm{Re}\left(\sqrt{2\Delta_B}\right)}{|\Delta_B|} \right.$$

(continued on next page)

$$\cdot\left(\frac{1}{3}\left[\frac{\mathrm{Re}\left(\sqrt{2\Delta_0}\right)}{|\Delta_0|}\right]^2 - \left[\frac{1}{2|\Delta_0|}\left(\frac{1}{2} + \frac{\Delta_0'}{|\Delta_0|}\right)\right]\right)\Bigg]$$

(A-13-15, continued)

If

$$Q(M_{1/2}) \equiv \frac{1}{2}\, Q(M \Rightarrow \infty) \qquad (A\text{-}13\text{-}16)$$

then from eq. A-13-15

$$M_{1/2} = \sqrt{\frac{2\pi^3 b\left(b^2/3 - a\right)}{\ln 2}} \qquad (A\text{-}13\text{-}17)$$

where

$$a \equiv \frac{1}{2\sqrt{(\Delta_0')^2 + (\Delta_0'')^2}}\left[\frac{1}{2} + \frac{\Delta_0'}{\sqrt{(\Delta_0')^2 + (\Delta_0'')^2}}\right] \qquad (A\text{-}13\text{-}18)$$

and

$$b \equiv \left[\frac{1}{\sqrt{(\Delta_b')^2 + (\Delta_B'')^2}} - \frac{\Delta_B'}{(\Delta_B')^2 + (\Delta_B'')^2} \right] \qquad (A-13-19)$$

If eq. A-13-17 is expanded in powers of Δ_B'' / Δ_B' with only the first order term retained, eq. III-2-7 is obtained.

Appendix 14 - Scalar Model of Smoothening Films Roughness

Our formalism follows Eastman (1978), and treats the reflection from each interface using scalar scattering theory. In a nutshell, the theory makes the assumption that the near-field reflected amplitude above some rough feature has a phase aberration equal to twice the local roughness height, but is unaffected in magnitude. In essence we take the magnitude of the reflectance to be given by the undegraded Fresnel coefficient for the interface.

Eastman (1978) cites conditions that must obtain in order to apply this scalar model to reflection from the interfaces.

1) The slopes of the irregularities must be small enough that the Fresnel coefficients be constant. (This is a generalization of what Eastman says.)

2) The radii of curvature of the irregularities must be large compared to the wavelength.

Following Eastman, we will also assume that shadowing and multiple reflections between the rough features in a single interface are negligible. We also neglect bulk scattering. Carniglia (1981) discusses the conditions under which bulk scattering can be treated with a scalar approach.

When applying the scalar theory to the case of multiple interfaces, there is an additional requirement that we must impose that is considerably more stringent than the single-interface requirements above.

This requirement is that the transverse spreading that the beam undergoes as it is reflected from the finite-thickness multilayer, due either to diffraction from rough features, or to the transverse displacement that occurs following oblique reflection from underlying layers, be small compared to the width of a typical rough feature (so long as the beam remains within the structure). Each local region of the multilayer (i.e. the region in which the interfering partially reflected components of the beam are generated) can then be treated as one-dimensional, with the defects being essentially random thickness errors rather than roughness of varying height.

Quantitatively, the requirement that displacement due to oblique incidence be less than the width of a rough feature can be written

$$N \cdot d \cdot \tan\theta_o \ll l_T \qquad (A\text{-}14\text{-}1)$$

where l_T is the transverse autocorrelation length, θ_o is the angle of incidence, d is the period length, and N is either the number of layers, or the effective number of layers as limited by absorption or structural defects.

We now show that eq. A-14-1 is equivalent to a requirement that the angle between the diffusely scattered radiation and the specular beam be within the acceptance angle of the multilayer. Loosely speaking, we might describe this as a requirement that the multilayer must continue to be

highly reflecting despite any departures from the Bragg angle caused by the finite slopes of the rough features.

If Ψ is the angle at which radiation is diffracted away from the Bragg angle by a typical rough feature, then

$$\Psi \sim \frac{\lambda}{\ell_T \cos\theta_o} \qquad (A\text{-}14\text{-}2)$$

where θ_o is the angle of incidence. From eqs. II-3-16, 9, and 30

$$\delta\varphi_{FWHM} \cong 2\mu'' = \frac{2}{N} = \frac{2\pi d}{\lambda}\sin\theta_B \qquad (A\text{-}14\text{-}3)$$

Using eqs. A-14-2 and 3, and setting $\theta_o \cong \theta_B$, eq. A-14-1 becomes

$$\Psi \ll \delta\theta_{FWHM} \qquad (A\text{-}14\text{-}4)$$

Eq. A-14-1 involves only the transverse displacement that occurs due to oblique reflection from a multilayer of finite thickness. At normal incidence, the dominant transverse displacement will be that due to diffraction from rough features in the lower interfaces. Eq. A-14-4 can

be shown to express this normal incidence requirement as well.

Eq. A-14-4 can be shown to be more restictive than the single interface conditions 1 and 2 above. We consider condition 1, and show that

$$\left| \frac{1}{s} \frac{ds}{d\theta} \right| \ll \left| \frac{1}{\rho} \frac{d\rho}{d\theta} \right| \qquad (A-14-5)$$

where s is the single-interface reflectivity and ρ is the multilayer reflectivity, so that if eq. A-14-4 is satisfied,

$$\Psi \left| \frac{1}{s} \frac{ds}{d\theta} \right| \ll \delta\theta_{FWHM} \left| \frac{1}{s} \frac{ds}{d\theta} \right| \ll \delta\theta_{FWHM} \left| \frac{1}{\rho} \frac{d\rho}{d\theta} \right| \sim 1 \qquad (A-14-6)$$

For simplicity we consider S polarization; then

$$S = \frac{1-x}{1+x} \qquad (A-14-7)$$

where

$$x = \frac{n_1 \cos\theta_1}{n_N \cos\theta_N} \qquad (A-14-8)$$

with θ_L and θ_H given by Snell's law.

Then we find that in the x-ray regime

$$\left| \frac{1}{s} \frac{ds}{d\theta} \right| = 2\tan\theta_B \qquad (A\text{-}14\text{-}9)$$

From eq. II-2-11 we find

$$\left| \frac{1}{\rho} \frac{d\rho}{d\theta} \right| = \pi \left| \frac{1}{s} \right| \tan\theta_B \qquad (A\text{-}14\text{-}10)$$

Since $|s| \ll 1$, eqs. A-14-5 and 6 follow.

Now let a be a typical radius of curvature for an irregularity (condition 2). Clearly $l_T \leqslant 2a$ if we assume non-periodic roughness.

Then away from normal incidence, we require according to eq. A-14-1

$$N \cdot d \cdot \tan\theta_o \ll 2a \qquad (A\text{-}14\text{-}11)$$

or

$$\frac{a}{\lambda} \gg \frac{\sin\theta_B}{4\mu'' \cos^2\theta_B} \cong \frac{\sin\theta_o}{2\Delta''_H} \gg 1 \qquad (A\text{-}14\text{-}12)$$

Again it is straightforward to show that $\frac{a}{\lambda} \gg 1$ in the normal incidence regime as well.

Thus, the requirement that the region sampled by each ray in traversing the multilayer be transversely small compared to the width of a rough feature is a sufficient condition for requirements 1 and 2 above of the scalar scattering theory.

We note that since $\delta\theta_{FWHM}$ is likely to be of the order of the field of view in an imaging application, the scalar theory can be applied to roughness which scatters radiation within the field of view.

Given that a one-dimensional formalism can be used to make a scalar treatment of reflection from the rough interfaces, it is then necessary to calculate the statistical properties of the near-field radiation, and to propagate the radiation to the far-field.

We now briefly sketch the requirements of the statistical calculation and the far-field propagation. The formalism is essentially a recasting of that of Eastman (1978) into the notation of our difference equation.

If W_0 is the total power in the intercepted portion of an incident plane wave having propagation vector $\vec{k}_\alpha$, then the diffracted amplitude is given by

$$U = \frac{\cos\theta_0}{\lambda} \sqrt{\frac{W_0}{L^2 \cos\theta_0}} \iint_{-L/2}^{L/2} dx \cdot dy \; \rho_s(x,y) \; \frac{e^{ikr_0}}{r_0} \; e^{i\vec{k}_\alpha \cdot \vec{r}(x,y)} \qquad (A\text{-}14\text{-}13)$$

Here r_β is the distance from the point x,y to the observation point, and $\vec{r}$ (x,y) is the position vector of x,y. We have treated the multilayer as an LxL square, have set the obliquity factor to cos θ_o, and have set the incident amplitude to $(W_o / L^2 \cos\theta_o)^{1/2}$. The coordinate system is that shown in fig. IV-2-2.

In the far-field

$$U \cong \frac{\cos\theta_o}{\lambda r_\beta} \sqrt{\frac{W_o}{L^2 \cos\theta_o}} \iint_{-L/2}^{L/2} dx\,dy\, e^{-ikx\Delta\theta\cos\theta_o}\, e^{-iky\varphi}\, \rho_J(x,y) \qquad (A\text{-}14\text{-}14)$$

Eq. A-14-13 assumes that ρ_J is measured at a planar interface, as will be the case with our near-field analysis of smoothening films. The cases of roughening films and columnar films are discussed in Appendix 15.

If $L \gg l_T$, we would expect that

$$|u(\Delta\theta,\varphi)|^2 \cong \langle |u(\Delta\theta,\varphi)|^2 \rangle \qquad (A\text{-}14\text{-}15)$$

This assumption, that non-deterministic effects will average out when the structure contains a large number of rough features, breaks down in the

far-field at very fine scales; however we neglect the fine-scale speckle that in principle is present following reflection of an ideal monochromatic plane wave from a rough surface.

Then

$$|u|^2 \cong \frac{W_0 \cos\theta_0}{\lambda^2 r_\beta^2 L^2} \int_{-L/2}^{L/2} dx\,dx'\,dy\,dy'\, e^{-ik(x-x')\Delta\theta\cos\theta_0}\, e^{-ik(y-y')} \tag{A-14-16}$$

$$\cdot\left[\left|\langle\rho_j\rangle\right|^2 + 2\,\mathrm{Re}\left(\langle\tilde{\rho}_j(x,y)\langle\rho_j\rangle\rangle\right) + \langle\tilde{\rho}_j(x,y)\,\tilde{\rho}_j^*(x',y')\rangle\right]$$

which, since $\langle\tilde{\rho}\rangle \equiv 0$, becomes

$$|u|^2 = \frac{W_0 \cos\theta_0}{\lambda^2 L^2 r_\beta^2}$$

$$\cdot\left[\int_{-L/2}^{L/2} dx\,dx'\,dy\,dy'\, e^{-ik(x-x')\Delta\theta\cos\theta_0}\, e^{-ik(y-y')\varphi}\, \left|\langle\rho_j\rangle\right|^2\right.$$

$$\left. + \int_{-L/2}^{L/2} dx\,dx'\,dy\,dy'\, e^{-ik(x-x')\Delta\theta\cos\theta_0}\, e^{-ik(y-y')\varphi}\, \langle\tilde{\rho}_j(x,y)\,\tilde{\rho}_j^*(x',y')\rangle\right]$$

(A-14-17)

or from eq. A-14-14,

$$|u|^2 = |\langle u \rangle|^2 +$$

$$\frac{W_0 \cos\theta_0}{\lambda^2 r_\beta^2 L^2} \cdot \left[\iiiint_{-L/2}^{L/2} dx\, dx'\, dy\, dy'\, e^{-ik(x-x')\Delta\theta\cos\theta_0} e^{-ik(y-y')\varphi} \langle \tilde{\rho}_s(x,y)\, \tilde{\rho}_s^*(x',y') \rangle \right] \tag{A-14-18}$$

Since the argument of the transform in the first term of eq. A-14-17 is independent of x and y, $|\langle u \rangle|^2$ becomes a delta-function of the scattering angles $\Delta\theta$, φ.

Since this component is not spatially dispersed and has a deterministic phase, we can regard it as the specular reflectivity. The second term of eq. A-14-17 is therefore the diffuse beam.

Given our choice of normalization, eq. A-14-17 has the dimensions of power per unit projected area, i.e. $dW/dA_\perp$. In the coordinate system of fig. IV-2-2 we will have

$$dA_\perp = r_\beta^2\, d(\Delta\theta)\, d\varphi = r_\beta^2\, d\Omega \tag{A-14-19}$$

This will hold even near normal incidence. Thus, we can factor out the

incident power in eq. A-14-17, and write

$$\frac{1}{W_0}\frac{dW_{Reflected}}{d\Omega} = \left|\langle \rho_J \rangle\right|^2 \delta(\Omega)$$

$$+ \frac{\cos\theta_0}{\lambda^2 L^2} \int_{-L/2}^{L/2}\int_{-L/2}^{L/2} dx\,dx'\,dy\,dy'\, e^{-ik(x-x')\Delta\theta\cos\theta_0} e^{-ik(y-y')\varphi} \langle \tilde{\rho}_J(x,y)\tilde{\rho}_J^*(x',y')\rangle \qquad (A\text{-}14\text{-}20)$$

where the δ-function is centered at $\theta = \theta_0$, $\varphi = 0$.

Since the total near-field power is

$$W_{Reflected} = \frac{W_0}{L^2\cos\theta_0} \int_{-L/2}^{L/2}\int_{-L/2}^{L/2} d(x\cos\theta_0)\,dy \left|\rho_J(x,y)\right|^2 \qquad (A\text{-}14\text{-}21)$$

we have assuming $W \cong \langle W \rangle$

$$W_{Reflected} = W_0\left(\left|\langle \rho_J \rangle\right|^2 + \langle \left|\tilde{\rho}_J\right|^2 \rangle\right) \qquad (A\text{-}14\text{-}22)$$

Since $W_0 \left|\langle \rho_J \rangle\right|^2$ is the specular beam, we have that the total power in the diffuse beam is

$$W_{Diffuse} = \langle \left|\tilde{\rho}_J\right|^2 \rangle \qquad (A\text{-}14\text{-}23)$$

We will assume for simplicity that the roughness is isotropic, so that eqs. IV-2-3,4 hold.

Then, if $l_\tau << L$, we can convert the second term in eq. A-14-17 (diffuse beam) into a Fourier-Bessel transform (Goodman, 1968, pg. 11), to obtain eq. IV-2-5.

In the text, we have defined the far-field amplitude reflectance to be the (properly phased) quantity whose magnitude squared is the far-field power per unit area divided by the incident power per unit area. The latter is $W_0 / L^2 \cos \theta_0$, so eq. IV-2-1 (suitably modified for roughening films as discussed in appendix 15) then follows from eq. A-14-14.

We now use our difference equation formalism to determine the statistical properties of the near field reflectivity $\rho_J(x,y)$ in the presence of smoothening films.

In the simplest case, the local one dimensional structure with smoothening films can be taken to be that of a multilayer containing non-accumulating thickness errors. We apply the phenomenological model of sec. II-6, assuming for simplicity that the multilayer is periodic (it would not be very difficult to generalize the smoothening films case to aperiodic structures as was done in sec. II-6).

We note that this analysis uses the unit cell decomposition of fig. A-11-1, so that ρ_J is provided by the formalism at the fictitious planar interfaces that separate the cells.

Assuming Gaussian statistics, we then obtain eq. A-11-3 giving ρ_{n+1} in terms of ρ_n ; as discussed in sec. IV-2 the derivation is the same as in the one-dimensional case. If we take expectation values with terms of order $\varphi \cdot \Delta$ neglected, and solve for $\langle \rho \rangle$ in the steady-state, we obtain eq. IV-2-10 for the specular beam. By manipulations similar to those in appendix 3, we then obtain eq. IV-2-9 for the specular beam outside the steady-state.

Eq. IV-2-12 for the diffuse beam is based on a slightly different one-dimensional model for smoothening films; this revised model allows us to consider the effect of finite longitudinal autocorrelations.

To do so we must assume that in each cell the upper interface of the central layer replicates the roughness profile in the lower interface of that layer.

We then consider varying degrees of longitudinal correlation between the roughness of the upper interface and the roughness in the layers that are deposited on top of it.

Thus, referring to fig. A-11-1, we take $f_{H,K} = f_{L,K} \equiv f_K$, and following steps similar to those used to derive eq. A-11-3 in appendix 11, we obtain

$$\rho_{K+1}(x,y)$$

$$= e^{-2it_0}\rho_K(x,y) - \tilde{q}\,e^{2i\xi_K}\sin\beta_{H,0} - \tilde{q}\,e^{-2i\xi_K}\sin\beta_{H,0}\,\rho_K^2(x,y) \qquad (A-14-24)$$

where $\xi_K \equiv (2\pi/\lambda)\cos\theta_0 f_K$.

The steady-state solution is eq. II-6-23 (which also obtains if the profiles in the upper and lower interfaces are uncorrelated, but have equal RMS magnitudes).

Now, as a prelude to deriving eq. IV-2-13 for the diffusely reflected intensity in the presence of finite longitudinal autocorrelations, we consider a crude model in which there is a step-like longitudinal autocorrelation that extends over j cells (where j is an integer greater than zero).

The autocorrelation is step-like in the sense that

$$\xi_K = \xi_{K+1} = \cdots = \xi_{K+j} \qquad (A-14-25)$$

and

$$\langle \xi_k \xi_{k+i} \rangle = \begin{cases} 0 & \text{if } i > j \text{ or } i < 0 \\ \langle \xi^2 \rangle & \text{otherwise} \end{cases} \qquad (A\text{-}14\text{-}26)$$

Since $\Delta \ll 1$, we can use eq. A-14-24 to express ρ_{k+2} in terms of ρ_k as follows

$$\rho_{k+2} = e^{-2it_0}\rho_{k+1} - ir_0 e^{2i\xi_k} - ir_0 e^{-2i\xi_k}\rho_{k+1}^2 \qquad (A\text{-}14\text{-}27)$$

$$\cong e^{-4it_0}\rho_k - 2ir_0 e^{2i\xi_k} - 2ir_0 e^{-2i\xi_k}\rho_k^2$$

to order Δ, where r_0 is the defect-free value of the parameter r.

We will assume that j is sufficiently small that

$$|j\Delta| \ll 1 \qquad (A\text{-}14\text{-}28)$$

so that the group of cells within one longitudinal autocorrelation length has only a weak interaction with the incident beam.

Under this assumption we can coalesce the j cells into one by successive application of the steps in eq. A-14-27, to obtain

$$\rho_{\kappa+j} \cong e^{-2ijt_0}\rho_\kappa - ji\tau_0 e^{2i\xi_\kappa} - ji\tau_0 e^{-2i\xi_\kappa}\rho_\kappa^2 \qquad (A\text{-}14\text{-}29)$$

The only effect of the step-like longitudinal autocorrelation is to multiply all cellular parameters except ξ by j.

Because of the step-like autocorrelation, the identity expressed in eq. II-5-6 still obtains. Taking the expectation value of eq. A-14-29, we then obtain

$$\langle\rho_{\kappa+j}\rangle = e^{-2ijt_0}\langle\rho_\kappa\rangle - ji\tau_0 e^{-2\langle\xi^2\rangle} - ji\tau_0\langle\rho_\kappa\rangle^2 e^{-2\langle\xi^2\rangle} - ji\tau_0\langle\tilde{\rho}_\kappa^2\rangle e^{-2\langle\xi^2\rangle} \qquad (A\text{-}14\text{-}30)$$

assuming Gaussian statistics.

Subtracting from eq. A-14-29,

$$\tilde{\rho}_{\kappa+j} = \underbrace{e^{-2\dot{\jmath}\dot{t}_0}\tilde{\rho}_\kappa}_{A} \underbrace{- j\dot{\imath}\tau_0\left(e^{2i\xi_\kappa} - e^{-2\langle\xi^2\rangle}\right)}_{B} \underbrace{- j\dot{\imath}\tau_0\left(e^{-2i\xi_\kappa} - e^{-2\langle\xi^2\rangle}\right)}_{C}$$

$$\underbrace{-2j\dot{\imath}\tau_0 e^{-2i\xi_\kappa}\langle\rho_\kappa\rangle\tilde{\rho}_\kappa}_{D} \underbrace{- j\dot{\imath}\tau_0 e^{-2i\xi_\kappa}\tilde{\rho}_\kappa^2}_{E} \underbrace{- j\dot{\imath}\tau_0 e^{-2i\xi_\kappa}\langle\tilde{\rho}_\kappa^2\rangle}_{F} \qquad (A\text{-}14\text{-}31)$$

We label these terms alphabetically for convenience.

As in appendix 11, we expect $\tilde{\rho}$ to be of order $\sqrt{\Delta}$. Then

$$A \sim (1+\Delta)\tilde{\rho} \sim (1+\Delta)\sqrt{\Delta}\ ;\ B \sim \Delta\ ;\ C \sim \Delta\ ;$$

$$D \sim \Delta\tilde{\rho} \sim \Delta^{3/2}\ ;\ E \sim \Delta^2\ ;\ F \sim \Delta^2 \qquad (A\text{-}14\text{-}32)$$

Since our equation for $\tilde{\rho}$ contains no terms of zero order in Δ (i.e. no terms of order $\langle\rho\rangle$ or unity), and since it contains all terms first order in Δ, we can square it to obtain an equation for $\tilde{\rho}^2$ accurate to order Δ^2. We neglect all terms of higher order than Δ^2 in driving terms and coefficients of $|\tilde{\rho}|^2$, and take the expectation value. We find

$$\langle|\rho_{\kappa+j}|^2\rangle = e^{-4j\mu''}\langle|\tilde{\rho}_\kappa|^2\rangle + j^2|\tau_0|^2(1-e^{-4\langle\xi^2\rangle})$$

$$+ j^2|\tau_0|^2|\langle\rho_\kappa\rangle|^4(1-e^{-4\langle\xi^2\rangle})$$

(continued on next page)

$$- 2Re\left(2ji\tau_0 e^{-2\langle\xi^2\rangle} \langle\rho_K\rangle\right) \langle|\tilde{\rho}|^2\rangle$$

$$+ 2j^2 |\tau_0|^2 Re\left(\langle\rho_K\rangle^2\right)\left(e^{-8\langle\xi^2\rangle} - e^{-4\langle\xi^2\rangle}\right)$$

(A-14-33, continued)

In the steady-state

$$\langle|\tilde{\rho}|^2\rangle = j \frac{|\tau_0|^2}{2\tilde{S}} e^{-2\langle\xi^2\rangle} \sinh\left(2\langle\xi^2\rangle\right)$$

$$\times\left[1 - 2e^{-4\langle\xi^2\rangle} Re\left(\langle\rho\rangle^2\right) + |\langle\rho\rangle|^4\right]$$

(A-14-34)

where $\tilde{S}$ *is given by* eq. IV-2-11.

Under our assumed step-like longitudinal autocorrelation function, the diffuse beam scales linearly with the autocorrelation length j.

We now consider the effect of a non-step-like autocorrelation length. We first coalesce together the layers K through K + h, where h is a "large-small" integer assumed to be larger than the number of layers within one longitudinal autocorrelation length, but small compared to the reciprocal of Δ.

When we coalesce the h layers, we get

$$\rho_{K+h} = e^{-2iht_0}\rho_K - ir_0\sum_{q=K}^{K+h-1} e^{2i\xi_q} - ir_0\left(\sum_{q=K}^{K+h-1} e^{-2i\xi_q}\right)\rho_K^2 \qquad (A\text{-}14\text{-}35)$$

so that

$$\langle\rho_{K+h}\rangle = e^{-2iht_0}\langle\rho_K\rangle - ihr_0 e^{-2\langle\xi^2\rangle} - ihr_0 e^{-2\langle\xi^2\rangle}\langle\rho_K\rangle^2$$

$$-2ir_0\langle\rho_K\rangle\left\langle\sum_{q=K}^{K+h-1} e^{-2i\xi_q}\tilde{\rho}_K\right\rangle - ihr_0\left\langle\sum_{q=K}^{K+h-1} e^{-2i\xi_q}\tilde{\rho}_K^2\right\rangle \qquad (A\text{-}14\text{-}36)$$

and

$$\tilde{\rho}_{K+h} = e^{-2iht_0}\tilde{\rho}_K - ir_0\left[\sum_{q=K}^{K+h-1} e^{2i\xi_q} - he^{-2\langle\xi^2\rangle}\right]$$

$$-ir_0\left[\sum_{q=K}^{K+h-1} e^{-2i\xi_q} - he^{-2\langle\xi^2\rangle}\right]\langle\rho\rangle^2$$

$$-2ir_0\langle\rho_K\rangle\left[\sum_{q=K}^{K+h-1} e^{-2i\xi_q}\tilde{\rho}_K - \left\langle\sum_{q=K}^{K+h-1} e^{-2i\xi_q}\tilde{\rho}_K\right\rangle\right] \qquad (A\text{-}14\text{-}37)$$

In the soft x-ray region, we usually will have $\tau < t$ and $\langle \rho \rangle < 1$, so that $\tau \langle \rho \rangle / t \ll 1$; the final term of eq. A-14-37 is therefore the least sensitive. (The last term also vanishes when $\langle \rho \rangle$ attains its largest magnitude, as $\xi_q \Rightarrow 0$.)

We will assume that in this least sensitive term we can make the substitution made above with the step-like autocorrelation function, namely

$$\left\langle \sum_{q=K}^{K+h-1} e^{\pm 2i\xi_q} |\tilde{\rho}_K|^2 \right\rangle \cong \left\langle \sum_{q=K}^{K+h-1} e^{\pm 2i\xi_q} \right\rangle \left\langle |\tilde{\rho}_K|^2 \right\rangle$$

(A-14-38)

Then to order Δ^2 (dropping terms of order $\Delta^2 \tilde{\rho}$) we obtain eq. IV-2-12 with

$$A = \frac{1}{h} e^{4\langle \xi^2 \rangle} \left[\sum_{q=K}^{K+h-1} \sum_{q'=K}^{K+h-1} \left\langle e^{\pm 2i(\xi_q - \xi_{q'})} \right\rangle - h^2 e^{-4\langle \xi^2 \rangle} \right]$$

(A-14-39)

and

$$B = -\frac{1}{h} e^{4\langle \xi^2 \rangle}$$

(continued on next page)

$$\times \left[\sum_{q=K}^{K+h-1} \sum_{q'=K}^{K+h-1} \left\langle e^{\pm 2i(\xi_q + \xi_{q'})} \right\rangle - h^2 e^{-4\langle \xi^2 \rangle} \right]$$

(A-14-40, continued)

We now assume the Gaussian bivariate distribution of eq. IV-2-14, so that

$$A = \frac{1}{h} \sum_{q=K}^{K+h-1} \sum_{q'=K}^{K+h-1} e^{4C_L(s)\langle \xi^2 \rangle} - h \qquad (A-14-41)$$

and

$$B = h - \sum_{q=K}^{K+h-1} \sum_{q'\neq K}^{K+h-1} e^{-4C_L(s)\langle \xi^2 \rangle} \qquad (A-14-42)$$

Because of our assumption that h is large compared to the longitudinal autocorrelation length, these sums will effectively terminate as C_L (s) vanishes, and so A and B will be independent of the upper limits

on the summations. Eqs. IV-2-13 and 12 then follow.

If C_L (s) has a width $s_{\tau_{yp}}$, then the longitudinal autocorrelation length is given by $j \cong 2s_{\tau_{yp}} + 1$ (s cannot be negative), hence the appearance of the above expressions for A and B. The magnitude of the diffuse beam will now scale approximately linearly with $2s_{\tau_{yp}} + 1$, rather than exactly linearly with j as with the step-like longitudinal autocorrelation.

We now calculate $\langle \tilde{\rho}_j(x,y)\, \tilde{\rho}_j^*(x',y') \rangle$ in order to obtain the angular distribution of the diffusely scattered radiation.

Using eq. A-14-31 with j = 1, and assuming now that the statistics of the roughness are Gaussian bivariate in the transverse direction (eqs. IV-2-3,4), we find

$$
\begin{aligned}
\langle \tilde{\rho}_{\kappa+1}\, \tilde{\rho}_{\kappa+1}^{*\prime} \rangle = {} & e^{-4\mu''} \langle \tilde{\rho}_\kappa\, \tilde{\rho}_\kappa^{*\prime} \rangle \\
& + 2i\tau_0^* e^{-2\langle \xi^2 \rangle} \langle \tilde{\rho}_\kappa\, \tilde{\rho}_\kappa^{*\prime} \rangle \\
& + |\tau_0|^2 \left(e^{-4\langle \xi^2 \rangle (1+C(v))} - e^{-4\langle \xi^2 \rangle} \right) \langle \rho_\kappa^* \rangle^2 \\
& + |\tau_0|^2 \left(e^{-4\langle \xi^2 \rangle (1+C(v))} - e^{-4\langle \xi^2 \rangle} \right) \langle \rho_\kappa \rangle^2 \\
& + |\tau_0|^2 \left(e^{-4\langle \xi^2 \rangle (1-C(v))} - e^{-4\langle \xi^2 \rangle} \right) \\
& + |\tau_0|^2 \left(e^{-4\langle \xi^2 \rangle (1-C(v))} - e^{-4\langle \xi^2 \rangle} \right) |\langle \rho_\kappa \rangle|^4 \\
& - 2i\tau_0 e^{-2\langle \xi^2 \rangle} \langle \rho_\kappa \rangle \langle \tilde{\rho}_\kappa\, \tilde{\rho}_\kappa^{*\prime} \rangle
\end{aligned}
\qquad (A\text{-}14\text{-}43)
$$

The steady-state solution is eq. IV-2-15.

Appendix 15 - Analysis of Roughening Films and Columnar Films

This appendix first considers the effect of roughening films, i.e. roughness whose one-dimensional analogue is accumulating random thickness errors. With accumulating thickness errors the unit cell length is not constant, and the total thickness error in the multilayer increases in a random walk fashion as more layers are added.

Thus, in contrast to the situation with smoothening films, our formalism will provide the near-field reflectivity $\rho_j(x,y)$ along a rough surface, so $\rho_j(x,y)$ must be propagated to a flat plane before taking the Fourier transform.

If in fig. IV-2-2, $r_\beta(x,y,z(x,y))$ is the distance to the observation point, and $\vec{k}_\alpha$ the propagation vector for the incident plane-wave, then neglecting terms of quadratic and higher order in the scattering angles $\Delta\theta, \varphi$

$$\vec{k}_\alpha \cdot \vec{r} + k r_\beta = \text{Constant}$$

$$- k x \cos\theta_0 \, \Delta\theta - k y \varphi - 2k \cos\theta_0 h_j(x,y) + k h_j(x,y) \sin\theta_0 \, \Delta\theta \qquad (A-15-1)$$

where $\vec{r}$ is the position vector of a point on the rough upper interface (measured relative to an origin in the defect-free interfacial plane), and where

$$h_J(x,y) = \sum_{k=1}^{J-1} \Delta d_k(x,y) \approx -\frac{\lambda}{2\pi\cos\theta_0} \sum_{k=1}^{J-1} \Delta\varphi_k(x,y)$$

(A-15-2)

We can simplify eq. A-15-1 by neglecting the last term (although the analysis can if desired be worked without this simplification). The neglect is permissible because in cases of greatest interest, $\Delta\theta \sim \Psi \ll \delta\theta_{FWHM}$, $J \sim N \sim (\mu'')^{-1}$, and $\langle\Delta\varphi^2\rangle \sim \mu''$ (sec. II-5), so that $\langle h_J(x,y)\rangle \sim \sqrt{J\cdot\langle\Delta\varphi^2\rangle}\cdot\lambda \sim \lambda$, and from eq. II-3-21,

$$k\cdot h_J(x,y)\sin\theta_0\,\Delta\theta \sim 2.5\times10^{-6}\left(2d_{(\text{Å})}\right)^2 \ll 1 \qquad (A-15-3)$$

Then what we will call the "flat-field propagator" becomes

$$e^{-2ik\cos\theta_0 h_J(x,y)} = e^{2i\sum_{k=1}^{J-1}\Delta\varphi_k(x,y)}$$

(A-15-4)

We must now calculate the specular reflectivity by evaluating

$$\langle \rho_J \, e^{2i \sum_{K=1}^{J-1} \Delta\varphi_K} \rangle \qquad (A\text{-}15\text{-}5)$$

Assuming Gaussian statistics,

$$\langle \rho_J e^{2i \sum_{K=1}^{J-1} \Delta\varphi_K} \rangle = \langle \rho_J \rangle \, e^{-2(J-1)\langle \Delta\varphi^2 \rangle} - \langle \tilde{\rho}_J \, e^{2i \sum_{K=1}^{J-1} \Delta\varphi_K} \rangle \qquad (A\text{-}15\text{-}6)$$

To evaluate the second term, we begin with eq. II-5-13, combine the second and third terms into an exponential (valid to within the neglect of terms of order Δ^2 , $(\Delta\varphi)^3$), to obtain

$$\tilde{\rho}_{K+1} = e^{2i\tilde{S}_K} \, e^{-2i\Delta\varphi_K} \, \tilde{\rho}_K - 2\left(i\Delta\varphi_K + \Delta\varphi_K^2 - \langle \Delta\varphi^2 \rangle\right) \langle \rho_K \rangle - (i\tau + \rho)\left(\tilde{\rho}_K^2 - \langle \tilde{\rho}^2 \rangle\right) \qquad (A\text{-}15\text{-}7)$$

where $\tilde{\delta}_K$ is given by eq. II-5-15. Next, we multiply by the flat-field propagator of eq. A-15-4, and take expectation values

$$\langle \tilde{\rho}_{K+1} e^{2i\sum_{K'=1}^{K} \Delta\varphi_{K'}} \rangle = e^{2i\tilde{\delta}_K} \langle \tilde{\rho}_K e^{2i\sum_{K'=1}^{K-1} \Delta\varphi_{K'}} \rangle$$

$$- 2 \langle \left(i\Delta\varphi_K + \Delta\varphi_K^2 - \langle \Delta\varphi^2 \rangle \right) e^{2i\sum_{K'=1}^{K} \Delta\varphi_K} \rangle \langle \rho \rangle$$

$$- (ir+p) \left(\langle \tilde{\rho}_K^2 e^{2i\sum_{K'=1}^{K} \Delta\varphi_{K'}} \rangle - \langle \tilde{\rho}^2 \rangle e^{-2K\langle \Delta\varphi^2 \rangle} \right) \qquad (A\text{-}15\text{-}8)$$

where we have assumed that absorption is in steady-state, so that $\langle \rho_K \rangle = \langle \rho \rangle$ and $\langle \tilde{\rho}_K^2 \rangle = \langle \tilde{\rho}^2 \rangle$.

We now show that the sum of the two quantities in the final term is negligible. (This will require a fairly involved analysis.)

Using the identity of eq. II-5-6, we have (note the upper limit of K on the summation)

$$\langle \tilde{\rho}_K^2 e^{2i\sum_{K'=1}^{K} \Delta\varphi_{K'}} \rangle - \langle \tilde{\rho}^2 \rangle e^{-2K\langle \Delta\varphi^2 \rangle}$$

$$= e^{-2\langle \Delta\varphi^2 \rangle} U_K \qquad (A\text{-}15\text{-}9)$$

where

$$U_K \equiv V_K - \langle \tilde{\rho}^2 \rangle e^{-2(K-1)\langle \Delta\varphi^2 \rangle} \qquad (A\text{-}15\text{-}10)$$

and

$$V_K \equiv \langle \tilde{\rho}_K^2 \, e^{2i \sum_{K'=1}^{K-1} \Delta\varphi_{K'}} \rangle \qquad (A\text{-}15\text{-}11)$$

According to eq. A-15-9 we must now show that U_K is small, in order to justify neglect of the final term in eq. A-15-8.

If we square eq. A-15-7 neglecting terms of order Δ^2, $\varphi \cdot \Delta$, $(\Delta\varphi)^3$, and $\tilde{\rho}^3$, multiply by the flat-field propagator (upper subscript on summation set to K), and take the expectation value, we obtain

$$V_{K+1} = e^{4i\tilde{\delta}_K} e^{-2\langle \Delta\varphi^2 \rangle} V_K - 4\Delta\varphi_K^2 \langle \rho_K \rangle^2 e^{-2K\langle \Delta\varphi^2 \rangle}$$

$$- 4\langle \rho_K \rangle \langle \tilde{\rho}_K (i\Delta\varphi_K + 3\Delta\varphi_K^2 - \langle \Delta\varphi^2 \rangle) e^{2i \sum_{K'=1}^{K} \Delta\varphi_{K'}} \rangle$$

(A-15-12)

The last term of eq. A-15-12 can be shown as follows to be negligible. We have

$$\langle \tilde{\rho}_K e^{2i\sum_{K'=1}^{K} \Delta\varphi_{K'}} \left(i\Delta\varphi_K + 3\Delta\varphi_K^2 - \langle\Delta\varphi^2\rangle \right) \rangle$$

$$= W_K \cdot i \langle \Delta\varphi_K e^{2i\Delta\varphi_K} \rangle$$

$$+ W_K \cdot 3 \langle \Delta\varphi_K^2 e^{2i\Delta\varphi_K} \rangle$$

$$- W_K \langle\Delta\varphi^2\rangle e^{-2\langle\Delta\varphi^2\rangle}$$

$$= O\left((\Delta\varphi)^3\right) \cong 0 \qquad (A\text{-}15\text{-}13)$$

where

$$W_K \equiv \langle \tilde{\rho}_K e^{2i\sum_{K'=1}^{K-1} \Delta\varphi_{K'}} \rangle \qquad (A\text{-}15\text{-}14)$$

so that eq. A-15-12 becomes

$$V_{K+1} = e^{4i\tilde{\delta}_K} e^{-2\langle\Delta\varphi^2\rangle} V_K - 4\langle\Delta\varphi^2\rangle e^{-2K\langle\Delta\varphi^2\rangle} \langle\rho_K\rangle^2$$

$$(A\text{-}15\text{-}15)$$

If we square eq. A-15-7, take its expectation value, multiply by the expectation value of the flat-field propagator of eq. A-15-4, and subtract from eq. A-15-15, we find

$$U_{k+1} = e^{4i\tilde{\delta}_k} e^{-2\langle \Delta\varphi^2 \rangle} U_k$$

$$+ \delta \langle \Delta\varphi^2 \rangle \langle \tilde{\rho}_k^2 \rangle e^{-2(K-1)\langle \Delta\varphi^2 \rangle} \qquad (A\text{-}15\text{-}16)$$

where U_k is defined in eq. A-15-10.

If the absorption is in steady-state, we have (using eq. II-5-23 and the approximate solution for $\langle \rho \rangle$ in eq. II-5-28), that the last term can be written as

$$\delta \langle \Delta\varphi^2 \rangle \langle \tilde{\rho}^2 \rangle e^{-2(K-1)\langle \Delta\varphi^2 \rangle}$$

$$\equiv \frac{\delta \langle \Delta\varphi^2 \rangle^2 \rho_0^2 e^{-2(K-1)\langle \Delta\varphi^2 \rangle}}{\left(-i\tilde{\delta} + 2\langle \Delta\varphi^2 \rangle\right)\left(1 + \frac{\langle \Delta\varphi^2 \rangle}{i\langle t \rangle}\right)^2}$$

(A-15-17)

We now show that this term is quite small.

In the soft x-ray regime, we can set

$$-i\bar{\delta} \sim i\langle t \rangle \sim \mu'' \qquad (A\text{-}15\text{-}18)$$

Further, if absorption is in steady-state,

$$K - 1 \sim 1/\mu'' \qquad (A\text{-}15\text{-}19)$$

so to order of magnitude, the last term of eq. A-15-16 is

$$\frac{8}{3}\rho_0^2 \mu'' \cdot \frac{y^2 e^{-2y}}{(1+2y)(1+y)^2} \qquad (A\text{-}15\text{-}20)$$

where

$$y \equiv \langle \Delta\varphi^2 \rangle / \mu'' \qquad (A\text{-}15\text{-}21)$$

Considered as a function of y, eq. A-15-20 has a maximum value of $0.16\ \rho_0^2\ \mu''$ at y = 0.46; at other values of $\langle \Delta\varphi^2 \rangle$ or at significantly different values of K, the final term of eq. A-15-16 will be still smaller.

Thus, if we treat the final term of eq. A-15-16 as having this value in steady-state, we will obtain an upper bound on U_κ.

The steady-state value of U obtained from eq. A-15-16 will then be

$$U \sim \frac{0.16\,\rho_0^2\,\mu''}{4i\tilde{s} - 2\langle \Delta\varphi^2 \rangle} \sim \frac{0.16\,\rho_0^2\,\mu''}{4.9\,\mu''} \sim 0.03\,\rho_0^2 \ll 1 \qquad (A\text{-}15\text{-}22)$$

Thus, we neglect U in eq. A-15-8. The remaining terms of the equation are straightforward to evaluate. As a linear difference equation, it then has the solution

$$\langle \tilde{\rho}_\kappa\, e^{2i \sum_{\kappa'=1}^{\kappa-1} \Delta\varphi_{\kappa'}} \rangle$$

$$= 4\langle \Delta\varphi^2 \rangle\, e^{2i \sum_{\kappa'=1}^{\kappa-1} \tilde{s}_{\kappa'}} \sum_{\kappa''=1}^{\kappa-1} \langle \rho_{\kappa''} \rangle\, e^{-2i \sum_{\kappa'''=1}^{\kappa''} \tilde{s}_{\kappa'''}}\, e^{2i \sum_{\kappa'=1}^{\kappa''-1} \Delta\varphi_{\kappa'}} \qquad (A\text{-}15\text{-}23)$$

We now substitute from eq. A-10-9, with the additional approximation

$$D \cong i\langle \Delta\varphi^2 \rangle - \langle t \rangle \qquad (A\text{-}15\text{-}24)$$

which is most accurate when the $\tilde{\rho}_\kappa$ factor in the second term of eq. A-15-6 presently being evaluated is largest, i.e. when this second term is most important relative to the first. The substitution from eq. A-10-9 is also most accurate when $\tilde{\rho}$ becomes large relative to $\langle \rho \rangle$.

We obtain

$$\langle \tilde{\rho}_\kappa e^{2i\sum_{\kappa'=1}^{\kappa-1} \Delta\varphi_{\kappa'}} \rangle$$

$$= \langle \Delta\varphi^2 \rangle \langle \rho \rangle e^{2i\sum_{\kappa'=1}^{\kappa-1} \tilde{\delta}_{\kappa'}} \sum_{\kappa''=1}^{\kappa-1} e^{-2i\sum_{\kappa'''=1}^{\kappa''} \tilde{\delta}_{\kappa'''}} e^{-2(\kappa''-1)\langle \Delta\varphi^2 \rangle}$$

$$-4\langle \Delta\varphi^2 \rangle \langle \rho \rangle e^{2i\sum_{\kappa'=1}^{\kappa-1} \tilde{\delta}_{\kappa'}} \sum_{\kappa''=1}^{\kappa-1} e^{2(ir+p)\sum_{\kappa'''=1}^{\kappa''} \langle \rho_{\kappa'''} \rangle} e^{-4(\kappa''-1)\langle \Delta\varphi^2 \rangle}$$

(A-15-25)

We make separate approximations to evaluate each of the two terms on the right.

In the first term, we can set $\tilde{\delta}_{K'''} \cong \tilde{\delta}_{K}$. When $\langle \Delta\varphi^2 \rangle \gg \mu$, $\delta_{K'''} \cong -\langle t \rangle$ since $\langle \rho \rangle \ll 1$, on the other hand when $\langle \Delta\varphi^2 \rangle \lesssim \mu$, large K''' terms dominate the sum; thus, the substitution is accurate in either limit.

The exponential factor in front of the K'' summation in the second term of eq. A-15-25 is small when absorption is in steady-state, so that this second term is significant only when the first term in eq. A-15-6 is also small, i.e. when $\langle \Delta\varphi^2 \rangle \gg \mu$. The small K'' terms dominate in this case. We therefore set $\langle \rho_{K'''} \rangle \cong 0$.

In the K' summation in the second term of eq. A-15-25, we again use the approximations in eqs. A-10-9 and A-15-24

$$\sum_{K'''=1}^{K-1} \langle \rho_{K'} \rangle \cong \langle \rho \rangle \sum_{K'''=1}^{K-1} \left(1 - e^{-2(K'-1)(i\langle t \rangle + \langle \Delta\varphi^2 \rangle)}\right)$$

$$= (K-1)\langle \rho \rangle - \frac{1 - e^{-2(K-1)(i\langle t \rangle + \langle \Delta\varphi^2 \rangle)}}{2(i\langle t \rangle + \langle \Delta\varphi^2 \rangle)} \langle \rho \rangle$$

$$\cong \left[(K-1) - \frac{1}{2(i\langle t \rangle + \langle \Delta\varphi^2 \rangle)} \right] \langle \rho \rangle \qquad \text{(A-15-26)}$$

With these substitutions eq. A-15-25 becomes

$$W_{\kappa} = 2\langle\Delta\varphi^2\rangle\langle\rho\rangle\left[\frac{e^{2i(J-1)\tilde{\delta}} - e^{-2(J-1)\langle\Delta\varphi^2\rangle}}{i\tilde{\delta} + \langle\Delta\varphi^2\rangle}\right]$$

$$- \langle\rho\rangle e^{2i(J-1)\tilde{\delta}} e^{\frac{ir+\rho}{i\langle t\rangle + \langle\Delta\varphi^2\rangle}} \langle\rho\rangle$$

(A-15-27)

When this is combined with eq. A-15-6, eq. IV-2-2 is obtained.

We now calculate the diffusely scattered radiation.

The total fractional power in the diffuse beam is the near field reflectivity (eq. II-5-36) less the specular reflectivity (magnitude squared of eq. IV-2-2).

To calculate the angular distribution of the scattered radiation, it is easiest to calculate the angular distribution of the total radiated field, and then subtract the specular component.

Taking eq. II-5-5, multiplying by the flat-field propagator, and then multiplying by the conjugate at the primed coordinates,

$$\rho_{K+1}(x,y)\,\rho^{*}_{K+1}(x',y')\,e^{2i\sum_{K'=1}^{K}\left(\Delta\varphi_{K'}(x,y)-\Delta\varphi_{K'}(x',y')\right)}$$

$$= e^{-4\mu''}\,e^{-2i\left(\Delta\varphi_{K}(x,y)-\Delta\varphi_{K}(x',y')\right)}\,e^{2i\sum_{K'=1}^{K}\left(\Delta\varphi_{K'}(x,y)-\Delta\varphi_{K'}(x',y')\right)}$$

$$-(ir-p)\,\rho^{*}_{K}(x',y')\,e^{2i\sum_{K'=1}^{K}\left(\Delta\varphi_{K'}(x,y)-\Delta\varphi_{K'}(x',y')\right)}$$

$$-(-ir^{*}-p^{*})\,\rho_{K}(x,y)\,e^{2i\sum_{K'=1}^{K}\left(\Delta\varphi_{K'}(x,y)-\Delta\varphi_{K'}(x',y')\right)}$$

$$-(ir+p)\,\rho^{2}_{K}(x,y)\,\rho^{*}_{K}(x',y')\,e^{2i\sum_{K'=1}^{K}\left(\Delta\varphi_{K'}(x,y)-\Delta\varphi_{K'}(x',y')\right)}$$

$$-(-ir^{*}+p^{*})\,\rho^{*2}_{K}(x,y)\,\rho_{K}(x',y')\,e^{2i\sum_{K'=1}^{K}\left(\Delta\varphi_{K'}(x,y)-\Delta\varphi_{K'}(x',y')\right)}$$

(A-15-28)

The expectation value of the first term on the right is straightforward to evaluate. To evaluate the second pair of terms, we define

$$U_K \equiv \left\langle \rho_K(x,y)\, \rho_K^*(x',y')\, e^{2i\sum_{K'=1}^{K-1}\left(\Delta\varphi_{K'}(x,y) - \Delta\varphi_{K'}(x',y')\right)} \right\rangle$$

$$V_K(x,y;x',y') \equiv \left\langle \rho_K(x,y)\, e^{2i\sum_{K'=1}^{K}\left(\Delta\varphi_{K'}(x,y) - \Delta\varphi_{K'}(x',y')\right)} \right\rangle$$

(A-15-29)

Using

$$V_K^*(x,y;x',y') = \left\langle \rho_K^*(x,y)\, e^{-2i\sum_{K'=1}^{K}\left(\Delta\varphi_{K'}(x,y) - \Delta\varphi_{K'}(x',y')\right)} \right\rangle$$

$$= V_K^*\left((x-x')^2 + (y-y')^2\right) = V_K^*(x',y';x,y)$$

$$= \left\langle \rho_K^*(x',y')\, e^{-2i\sum_{K'=1}^{K}\left(\Delta\varphi_{K'}(x',y') - \Delta\varphi_{K'}(x,y)\right)} \right\rangle$$

$$= \left\langle \rho_K^*(x',y')\, e^{+2i\sum_{K'=1}^{K}\left(\Delta\varphi_{K'}(x,y) - \Delta\varphi_{K'}(x',y')\right)} \right\rangle$$

(A-15-30)

we have

$$\left\langle (i\tau+\rho)\, \rho_K^*(x',y')\, e^{2i\sum_{K'=1}^{K}\left(\Delta\varphi_{K'}(x,y) - \Delta\varphi_{K'}(x',y')\right)} \right\rangle$$

$$+ \left\langle (-i\tau^*+\rho^*)\, \rho_K(x,y)\, e^{2i\sum_{K'=1}^{K}\left(\Delta\varphi_{K'}(x,y) - \Delta\varphi_{K'}(x',y')\right)} \right\rangle$$

$$= 2\,\mathrm{Re}\left[(-i\tau^* - \rho^*)\, V_K(x,y;x',y')\right] \qquad \text{(A-15-31)}$$

The final, least sensitive terms in eq. A-15-28 remain to be evaluated. If we make the approximation

$$\left\langle \rho_K^2(x,y)\,\rho_K^*(x',y')\,e^{2i\sum_{K'=1}^{K}\left(\Delta\varphi_{K'}(x,y)-\Delta\varphi_{K'}(x',y')\right)}\right\rangle$$

$$\cong \left\langle \rho_K^2(x,y)\,\rho_K^*(x',y')\right\rangle \left\langle e^{2i\sum_{K'=1}^{K}\left(\Delta\varphi_{K'}(x,y)-\Delta\varphi_{K'}(x',y')\right)}\right\rangle \qquad (A\text{-}15\text{-}32)$$

then the result will be correct at $\langle\Delta\varphi^2\rangle \Rightarrow 0$ and will not cause difficulties at large $\langle\Delta\varphi^2\rangle$, where the term is small. Even in the intermediate region the error should be small at soft x-ray wavelengths.

Then assuming the Gaussian bivariate distribution of eqs. IV-2-3,4, eq. A-15-28 becomes

$$U_{K+1} = e^{-4\mu''}U_K - 2\mathrm{Re}\left((-i\tau^*-\rho^*)V_K\right)$$

$$-2e^{-4(K+1)\langle\Delta\varphi^2\rangle(1-C(v))}\mathrm{Re}\left[(i\tau+\rho)\left|\langle\rho\rangle\right|^2\langle\rho\rangle^*\right] \qquad (A\text{-}15\text{-}33)$$

To evaluate this we must find an approximate solution for $\mathcal{V}_K$. To do so we neglect the last, least sensitive term in eq. II-5-5, and multiply both sides by the product of the flat-field propagator at K + 1 with the conjugate propagator at the primed coordinates.

We obtain

$$\mathcal{V}_{K+1} \cong \rho_K(x,y)\, e^{-2i\langle t\rangle}\, e^{2i\sum_{K'=1}^{K-1}\left(\Delta\varphi_{K'}(x,y) - \Delta\varphi_{K'}(x',y')\right)}\, e^{2i\left(\Delta\varphi_{K+1}(x,y) - \Delta\varphi_{K+1}(x',y')\right)}\, e^{-2i\Delta\varphi_K(x,y)}$$

$$-(ir-\rho)\, e^{2i\sum_{K'=1}^{K+1}\left(\Delta\varphi_{K'}(x,y) - \Delta\varphi_{K'}(x',y')\right)} \qquad (A\text{-}15\text{-}34)$$

To evaluate the expectation of the first term, we use eq. II-5-6, so that

$$\langle \rho_K(x,y)\, e^{2i\sum_{K'=1}^{K-1}\left(\Delta\varphi_{K'}(x,y) - \Delta\varphi_{K'}(x',y')\right)}\rangle$$

$$= \langle \rho_K(x,y)\, e^{2i\sum_{K'=1}^{K-1}\left(\Delta\varphi_{K'}(x,y) - \Delta\varphi_{K'}(x',y')\right)}\rangle \cdot \frac{\langle e^{2i\left(\Delta\varphi_K(x,y) - \Delta\varphi_K(x',y')\right)}\rangle}{\langle e^{2i\left(\Delta\varphi_K(x,y) - \Delta\varphi_K(x',y')\right)}\rangle}$$

$$= \frac{\mathcal{V}_K}{e^{-4\langle\Delta\varphi^2\rangle(1-C(v))}} \qquad (A\text{-}15\text{-}35)$$

It is straightforward to evaluate the expectation value of the second term in eq. A-15-34. The equation now becomes a linear difference equation, whose formal solution, neglecting terms of order Δ^2, and $\varphi \cdot \Delta$ is

$$\nu_K = -(i\tau - p)\, e^{-K(i\langle t\rangle + 3\langle \Delta\varphi^2\rangle - 2C(v)\langle \Delta\varphi^2\rangle)}$$

$$\times (K-1)\,\mathrm{sinch}\left[(K-1)(i\langle t\rangle - \langle \Delta\varphi^2\rangle + 2C(v)\langle \Delta\varphi^2\rangle\right] \qquad (A\text{-}15\text{-}36)$$

(where the sinch-function is defined in eq. IV-2-8).

To partially compensate for our neglect of the final term in eq. II-5-5, we re-normalize

$$\nu_K \cong \frac{2\,\mathrm{sinch}\left[(K-1)(i\langle t\rangle - \langle \Delta\varphi^2\rangle + 2C(v)\langle \Delta\varphi^2\rangle)\right]}{\left(1 - 2\,\frac{\langle \Delta\varphi^2\rangle}{i\langle t\rangle + \langle \Delta\varphi^2\rangle}\,(1 - C(v))\right)} \langle \rho \rangle$$

$$\times\, e^{-K(i\langle t\rangle + 3\langle \Delta\varphi^2\rangle - 2C(v)\langle \Delta\varphi^2\rangle)} \qquad (A\text{-}15\text{-}37)$$

This is exact in the limits $\langle \Delta\varphi^2 \rangle \ll \mu$, $\langle \Delta\varphi^2 \rangle \gg \mu$, and $|x - x'| \Longrightarrow 0$, $K \gg \mu^{-1}$.

U_K is now the sum of five geometric series (including two conjugate pairs).

The solution is

$$U_K = -4\,\mathrm{Re}\left\{ \langle \rho \rangle \frac{e^{-2K(\mu'' + \langle \Delta\varphi^2 \rangle)}}{1 - 2\dfrac{\langle \Delta\varphi^2 \rangle (1 - C(v))}{i\langle t \rangle + \langle \Delta\varphi^2 \rangle}} (K-1)(-ir^* + \rho^*) \right.$$

$$\times \left[e^{2KC(v)\langle \Delta\varphi^2 \rangle} \operatorname{sinch}\left[2(K-1)\left(\mu'' - \langle \Delta\varphi^2 \rangle (1 - C(v))\right)\right] \right.$$

$$\left. \left. - e^{-K(\mu'' + i\langle t' \rangle)} \operatorname{sinch}\left[(K-1)(\mu'' - i\langle t' \rangle - \langle \Delta\varphi^2 \rangle)\right]\right]\right\}$$

$$- 2(K-1)\,\mathrm{Re}\left\{ (ir + \rho)\langle \rho \rangle^* \right\} |\langle \rho \rangle|^2 e^{-2K(\mu'' + \langle \Delta\varphi^2 \rangle (1 - C(v)))}$$

$$\times \operatorname{sinch}\left[2(K-1)\left(\mu'' - \langle \Delta\varphi^2 \rangle (1 - C(v))\right)\right] \qquad (A\text{-}15\text{-}38)$$

Eq. A-15-38 includes the specular beam as well as the diffuse beam. Since the approximations made in eq. IV-2-2 are slightly different from those made in eq. A-15-38, the best way to subtract out the specular component is to evaluate eq. A-15-38 as $v \Longrightarrow \infty$, and subtract the result from the finite-v equation. This results in eq. IV-2-7.

Note that in eq. IV-2-6 we have defined the quantity $\tilde{\rho}_j(x,y)$ to be given by eq. IV-2-6 for roughening films, and to be given by $\tilde{\rho}_j(x,y)$ for smoothening films, in order to unify our treatment of the two cases.

We now evaluate the specular reflectivity in the presence of columnar films. We treat the near-field beam as being reflected from a periodic multilayer whose Bragg detuning parameter φ is a random variable; as usual we assume a Gaussian distribution

$$P(\varphi) = \frac{1}{\pi\sqrt{2\pi\langle\Delta K^2\rangle}}\, e^{-(\varphi-\varphi_0)^2/2\pi^2\langle\Delta K^2\rangle} \qquad (A\text{-}15\text{-}39)$$

where $\Delta K(x,y)$ is the local variation in growth rate, i.e. $d(x,y) = \langle d\rangle(1 + \Delta K(x,y))$.

As in the case of roughening films, a flat-field propagator must be used, but now $\Delta\varphi(x,y)$ is independent of K. We therefore must evaluate

$$\langle \rho_{Far\ field}\rangle = \langle \rho_{Near\ field}\, e^{2i(J-1)(\varphi-\varphi_0)}\rangle = \int_{-\infty}^{\infty} d\varphi\, P(\varphi)\, e^{2i(J-1)(\varphi-\varphi_0)}\, \rho_J(\varphi) \qquad (A\text{-}15\text{-}40)$$

We will use the approximate expression for the reflectivity obtained by combining eqs. II-3-1 and 2,

$$\rho_J(\varphi) \cong \frac{\tau}{2(\varphi - \mu)} \left(1 - e^{-2i(J-1)(\varphi - \mu)}\right) \qquad (A\text{-}15\text{-}41)$$

From the first term of eq. A-15-41, we must evaluate

$$I_1 = \int_{-\infty}^{\infty} d\varphi \; e^{-(\varphi - \varphi_0)^2 / 2\pi^2 \langle \Delta K^2 \rangle} \; \frac{e^{2i(J-1)(\varphi - \varphi_0)}}{\varphi - \mu}$$

$$= -\int_{-\infty}^{\infty} d\Psi \; \frac{e^{-\Psi^2 / 2(J-1)^2 \langle \Delta K^2 \rangle}}{\Psi - \frac{(J-1)\langle t \rangle}{\pi}} \; e^{-2\pi i \Psi}$$

(A-15-42)

As the Fourier transform of a product, I_1 is the convolution of two transforms.

We find through straightforward manipulations that

$$I_1 = \pi i e^{-\langle t\rangle^2/2\pi^2\langle \Delta K^2\rangle} e^{-2i\langle t\rangle (J-1)}$$

$$\times \left[1 - \bar{\Phi}\left(-\sqrt{2\pi^2\langle \Delta K^2\rangle}\,(J-1) + \frac{i\langle t\rangle}{\sqrt{2\pi^2\langle \Delta K^2\rangle}}\right)\right]$$

(A-15-43)

where $\bar{\Phi}(w)$ is the complex error function as defined in the text.

The second term of eq. A-15-41 leads to a similar expression.

The sum of both terms is

$$\langle \rho\rangle = \frac{i r_0}{2} e^{-\langle t\rangle^2/2\pi^2\langle \Delta K^2\rangle} e^{-2i\langle t\rangle (J-1)}$$

$$\times \left[\bar{\Phi}\left(\frac{i\langle t\rangle}{\sqrt{2\pi^2\langle \Delta K^2\rangle}}\right)\right.$$

$$\left. - \bar{\Phi}\left(\frac{i\langle t\rangle}{\sqrt{2\pi^2\langle \Delta K^2\rangle}} - \sqrt{2\pi^2\langle \Delta K^2\rangle}\,(J-1)\right)\right]$$

(A-15-43)

In order to improve the accuracy we re-normalize to the exact defect-free solution of eq. II-2-11. Eq. IV-2-16 is then obtained.

Appendix 16 - Materials Combinations that Maximize Integrated Reflectivity

In this appendix we describe the results of a modification to the materials search program of sec. II-2-C; the modified program seeks to maximize integrated reflectivity (or collection solid angle) rather than peak reflectivity. The output routines in the search program have also been modified, in order to have printed out a number of possible materials pairs at each wavelength. To this end, the program prints several different lists of materials for each wavelength; fig. A-16-1 shows the detailed criteria on which the different lists are based.

An abbreviated tabulation of the materials selections (31 wavelengths) is given in table A-16-1. A fuller listing (125 wavelengths) is available upon request from the author. (Present address: IBM; Thomas J. Watson Research Center; P.O. Box 218; Yorktown Heights, NY 10598.)

The sorting parameter used by the program is the entry in table A-16-1 labeled "SOLID ANGLE", which more precisely is the quantity $8\pi R_{peak}\delta''$. This estimate of the collection solid angle (in steradians) applies to a multilayer-coated spherical reflector focussing collimated radiation. The multilayer reflection profile is assumed to be a Lorentzian function of phase thickness as in eq. II-3-1, except that to improve the accuracy we have set the FWHM equal to $2\delta''$ rather than $2\mu''$.

In addition, we assume that the coating's angle of peak reflectivity is sufficiently detuned from normal incidence that both sides of the reflection curve are realized at angles within 90° from the surface, and

Explanation of Different Entries at Each Wavelength

Best pair of materials at particular wavelength.

Second through fourth best pairs.

Second through sixth best pairs, with no previously selected materials allowed in pairs that follow.

Second through seventh best pairs, with no previously selected low index material allowed as low index material in following pairs.

Six best pairs containing carbon, or second through seventh such pairs if best overall pair contains carbon.

MINIMUM S ALLOWED IS 5

WAVELENGTH	SOLID ANGLE	R	N (AT NORMAL INCIDENCE)	G (R=0 / R=0.4)	ELEMENT - H	ELEMENT - L
126.00	2.3624043	.0300	8.9	.4474	RHODIUM	SILICON
126.00	2.3355276	.0339	9.0	.4457	RUTHENIUM	SILICON
126.00	1.6723551	.7672	11.5	.4366	MOLYBDENUM	SILICON
126.00	1.5303509	.5051	9.6	.4030	SILVER	SILICON
126.00	1.4201216	.7705	13.6	.4416	RUTHENIUM	STRONTIUM
126.00	.8933189	.4032	11.3	.4192	SILVER	CALCIUM
126.00	.7119008	.2961	10.5	.4400	BARIUM	MOLYBDENUM
126.00	.5215018	.2230	10.7	.4310	GOLD	PRASEODYMIUM
126.00	.4224630	.2266	13.5	.4241	PLATINUM	YTTRIUM
126.00	1.4481903	.7761	13.5	.4433	RHODIUM	STRONTIUM
126.00	1.3641634	.6757	12.4	.4849	RHODIUM	CALCIUM
126.00	1.1324930	.4139	9.2	.4420	BARIUM	RHODIUM
126.00	1.1252474	.4000	9.1	.4444	BARIUM	RUTHENIUM
126.00	1.1049286	.5001	13.6	.4956	RHODIUM	YTTRIUM
126.00	1.0710544	.6437	15.1	.4791	RHODIUM	BORON
126.00	1.0476124	.5755	13.8	.4962	RHODIUM	CERIUM
126.00	1.1125064	.7420	16.8	.4574	CARBON	SILICON
126.00	.8789213	.5503	15.7	.4920	RHODIUM	CARBON
126.00	.8661509	.5426	15.7	.4898	RUTHENIUM	CARBON
126.00	.6193521	.3028	12.1	.4287	SILVER	CARBON
126.00	.4147207	.2218	13.4	.4190	GOLD	CARBON
126.00	.3399269	.3247	24.0	.4774	MOLYBDENUM	CARBON

(By definition, the low index material in a pair is the material with the least absorption.)

Figure A-16-1

AD-A136 307 DEVELOPMENT OF X-RAY LASER MEDIA MEASUREMENT OF GAIN AND DEVELOPMENT OF C.. (U) ROCHESTER UNIV N Y LAB FOR LASER ENERGETICS J FORSYTH FEB 83 3/3

UNCLASSIFIED AFOSR-TR-83-1136-VOL-3 AFOSR-81-0059 F/G 20/8 NL

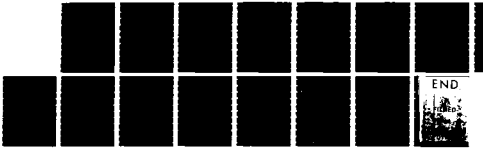

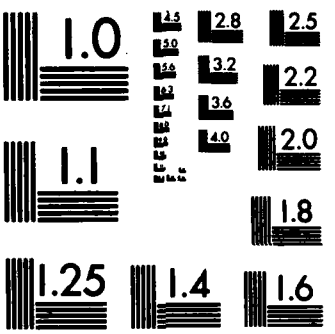

MICROCOPY RESOLUTION TEST CHART
NATIONAL BUREAU OF STANDARDS-1963-A

yet sufficiently close to normal incidence that polarization and obliquity effects can be neglected throughout the angular bandpass.

Because of the large acceptance angles that multilayers have at longer x-ray wavelengths, these approximations tend to hold only roughly. We have found by numerical integration that the "trigonometric efficiency factor", defined to be the resultant loss factor from all the above effects, is about 0.5 for the longer wavelengths in the table (assuming that the angle of peak reflectivity has also been numerically optimized).

For comparison's sake, the normal incidence factor of 8π is used by the search program at short wavelengths where normal incidence operation is impractical. The sorting parameter can also be regarded as an approximate index for the one-dimensional integral of reflectivity over angle (to within a different normalization constant).

The search program has excluded from consideration the same chemical elements as were excluded by the earlier program (sec. II-2-C). As before, structural defects were not considered. The optical constants used in the search are those of Henke et al. (1982).

We are indebted to E. Spiller (1982a) for useful discussion of these topics.

MINIMUM Z ALLOWED IS 5

WAVE-LENGTH	SOLID ANGLE (STERAD.)	R	N (AT NORMAL INCIDENCE)	GAMMA (DE / (DE + DL))	ELEMENT - E	ELEMENT - L
115.33	1.2459189	.7841	15.8	.4599	RHODIUM	STRONTIUM
115.33	1.2439364	.7754	15.7	.4551	RUTHENIUM	STRONTIUM
115.33	1.1312389	.6827	15.2	.4896	RUTHENIUM	CALCIUM
115.33	1.1233836	.6921	15.5	.4923	RHODIUM	CALCIUM
115.33	1.1312389	.6827	15.2	.4896	RUTHENIUM	CALCIUM
115.33	.8663727	.3809	11.0	.4601	SILVER	PRASEODYMIUM
115.33	.5302324	.2821	13.4	.4517	SILICON	MOLYBDENUM
115.33	.4617827	.2736	14.9	.4302	GOLD	YTTRIUM
115.33	.3461327	.2059	15.0	.4354	PLATINUM	CERIUM
115.33	1.1312389	.6827	15.2	.4896	RUTHENIUM	CALCIUM
115.33	1.0579488	.5781	13.7	.4860	PRASEODYMIUM	RUTHENIUM
115.33	1.0429040	.5871	14.1	.4822	PRASEODYMIUM	RHODIUM
115.33	.8960732	.6607	18.5	.4824	RUTHENIUM	BORON
115.33	.8663727	.3809	11.0	.4601	SILVER	PRASEODYMIUM
115.33	.7646700	.2509	8.2	.4948	SILICON	SILVER
115.33	.7350939	.3950	13.5	.4462	SILVER	YTTRIUM
115.33	.7208903	.5628	19.6	.4948	RUTHENIUM	CARBON
115.33	.7078087	.5708	20.3	.4982	RHODIUM	CARBON
115.33	.5910508	.3675	15.6	.4402	SILVER	CARBON
115.33	.3608713	.2454	17.1	.4251	GOLD	CARBON
115.33	.2839764	.3264	28.9	.4747	MOLYBDENUM	CARBON
115.33	.2650908	.2015	19.1	.4209	PLATINUM	CARBON
104.71	.9434196	.7319	19.5	.4576	RUTHENIUM	STRONTIUM
104.71	.9338507	.6877	18.5	.4390	SILVER	STRONTIUM
104.71	.8971526	.7265	20.4	.4594	RHODIUM	STRONTIUM
104.71	.8439550	.6004	17.9	.4654	SILVER	CALCIUM
104.71	.8439550	.6004	17.9	.4654	SILVER	CALCIUM
104.71	.7416199	.3943	13.4	.4383	PRASEODYMIUM	RHODIUM
104.71	.4853143	.2591	13.4	.4714	GOLD	SAMARIUM
104.71	.4360256	.3218	18.6	.4703	CERIUM	MOLYBDENUM
104.71	.3467946	.2552	18.5	.4630	CADMIUM	NEODYMIUM
104.71	.8439550	.6004	17.9	.4654	SILVER	CALCIUM
104.71	.8204040	.3630	11.1	.4540	PRASEODYMIUM	SILVER
104.71	.7782769	.4000	12.9	.4398	PRASEODYMIUM	RUTHENIUM
104.71	.7765289	.4812	15.6	.4970	SILVER	NEODYMIUM
104.71	.7416199	.3943	13.4	.4383	PRASEODYMIUM	RHODIUM
104.71	.7185995	.5220	18.3	.4789	SILVER	YTTRIUM
104.71	.7059370	.4606	16.4	.4972	SILVER	EUROPIUM
104.71	.5607162	.4966	22.3	.4707	SILVER	CARBON
104.71	.5234735	.5317	25.5	.4861	RUTHENIUM	CARBON
104.71	.4758541	.5156	27.2	.4872	RHODIUM	CARBON
104.71	.2997579	.2588	21.7	.4247	PRASEODYMIUM	CARBON
104.71	.2914830	.2757	23.8	.4311	GOLD	CARBON
104.71	.2218154	.3265	37.0	.4711	MOLYBDENUM	CARBON

TABLE A-16-1

MINIMUM Z ALLOWED IS 5

WAVE-LENGTH	SOLID ANGLE (STERAD.)	R	N (AT NORMAL INCIDENCE)	GAMMA (DE / (DE + DL))	ELEMENT - E	ELEMENT - L
95.06	.8466226	.4864	14.4	.4456	SAMARIUM	SILVER
95.06	.8456917	.4641	13.8	.4537	SAMARIUM	RUTHENIUM
95.06	.7871425	.4402	14.1	.4570	SAMARIUM	RHODIUM
95.06	.7545046	.7125	23.7	.4692	SILVER	STRONTIUM
95.06	.7307504	.6885	23.7	.4602	RUTHENIUM	STRONTIUM
95.06	.5623446	.4599	20.6	.4866	EUROPIUM	RHODIUM
95.06	.3647199	.4772	32.9	.4699	MOLYBDENUM	CALCIUM
95.06	.3146625	.1504	12.0	.4031	PRASEODYMIUM	ANTIMONY
95.06	.2876247	.2951	25.8	.4473	GOLD	YTTRIUM
95.06	.8456917	.4641	13.8	.4537	SAMARIUM	RUTHENIUM
95.06	.7871425	.4402	14.1	.4570	SAMARIUM	RHODIUM
95.06	.7545046	.7125	23.7	.4692	SILVER	STRONTIUM
95.06	.6375146	.3864	15.2	.4586	SAMARIUM	MOLYBDENUM
95.06	.6349187	.6336	25.1	.4866	SILVER	CALCIUM
95.06	.6252152	.3365	13.5	.4724	SAMARIUM	CADMIUM
95.06	.6237275	.3904	15.7	.4561	SAMARIUM	ANTIMONY
95.06	.4021658	.3779	23.6	.4297	SAMARIUM	CARBON
95.06	.3992016	.5323	33.5	.4856	SILVER	CARBON
95.06	.3906010	.5066	32.6	.4775	RUTHENIUM	CARBON
95.06	.3245550	.4590	35.5	.4737	RHODIUM	CARBON
95.06	.3065492	.1733	14.2	.3970	PRASEODYMIUM	CARBON
95.06	.2015884	.2717	33.9	.4323	GOLD	CARBON
86.31	.5584039	.6025	27.1	.4789	RUTHENIUM	STRONTIUM
86.31	.4913518	.5906	30.2	.4830	SILVER	STRONTIUM
86.31	.4741100	.5478	29.0	.4697	RHODIUM	STRONTIUM
86.31	.4638554	.5720	31.0	.4752	RUTHENIUM	CALCIUM
86.31	.3970463	.5540	35.1	.4792	SILVER	CALCIUM
86.31	.3708609	.3815	25.9	.4951	TERBIUM	RHODIUM
86.31	.3010392	.2240	18.7	.4242	GADOLINIUM	CADMIUM
86.31	.2679853	.1699	15.9	.3979	SAMARIUM	ANTIMONY
86.31	.2262272	.3471	38.6	.4885	MOLYBDENUM	YTTRIUM
86.31	.4638554	.5720	31.0	.4752	RUTHENIUM	CALCIUM
86.31	.4384891	.4366	25.0	.4874	TERBIUM	RUTHENIUM
86.31	.3975163	.6084	38.5	.4476	RUTHENIUM	BORON
86.31	.3960339	.4698	29.8	.4933	RUTHENIUM	YTTRIUM
86.31	.3746507	.4191	28.1	.4817	TERBIUM	SILVER
86.31	.3708609	.3815	25.9	.4951	TERBIUM	RHODIUM
86.31	.3010392	.2240	18.7	.4242	GADOLINIUM	CADMIUM
86.31	.2950095	.4851	41.3	.4695	RUTHENIUM	CARBON
86.31	.2606343	.1768	17.0	.3967	SAMARIUM	CARBON
86.31	.2302056	.4476	48.9	.4722	SILVER	CARBON
86.31	.2299501	.4129	45.1	.4594	RHODIUM	CARBON
86.31	.2047679	.2200	27.0	.4084	GADOLINIUM	CARBON
86.31	.1786223	.1996	28.1	.4052	NICKEL	CARBON

TABLE A-16-1
(CONTINUED)

WAVE-LENGTH	SOLID ANGLE (STERAD.)	R	N (AT NORMAL INCIDENCE)	GAMMA (DE / (DE + DL))	MINIMUM % ALLOWED IS 5 ELEMENT - E	ELEMENT - L
78.36	.3995000	.5007	31.5	.4875	RUTHENIUM	STRONTIUM
78.36	.3494729	.5389	38.8	.4681	RUTHENIUM	CALCIUM
78.36	.3447553	.4533	33.0	.4809	RHODIUM	STRONTIUM
78.36	.3228714	.6048	47.1	.4372	RUTHENIUM	BORON
78.36	.2957230	.4873	41.4	.4613	RHODIUM	CALCIUM
78.36	.2274628	.5234	57.8	.4349	SILVER	BORON
78.36	.1815807	.1710	23.7	.4248	NICKEL	YTTRIUM
78.36	.1791365	.1545	21.7	.4090	DYSPROSIUM	CADMIUM
78.36	.1590237	.2210	34.9	.4624	HOLINIUM	MOLYBDENUM
78.36	.3494729	.5389	38.8	.4681	RUTHENIUM	CALCIUM
78.36	.3228714	.6048	47.1	.4372	RUTHENIUM	BORON
78.36	.2883189	.3940	34.3	.5004	RUTHENIUM	YTTRIUM
78.36	.2561682	.2968	29.1	.4663	HOLINIUM	RUTHENIUM
78.36	.2249688	.4662	52.1	.4595	RUTHENIUM	CARBON
78.36	.2191406	.2561	29.4	.4713	HOLINIUM	RHODIUM
78.36	.2088735	.3526	42.4	.4903	RUTHENIUM	SCANDIUM
78.36	.2249688	.4662	52.1	.4595	RUTHENIUM	CARBON
78.36	.1806071	.4047	56.3	.4530	RHODIUM	CARBON
78.36	.1648495	.2222	33.9	.4065	NICKEL	CARBON
78.36	.1612661	.1817	28.3	.3983	DYSPROSIUM	CARBON
78.36	.1584130	.2300	36.5	.4088	COBALT	CARBON
78.36	.1546668	.2019	32.8	.4029	COPPER	CARBON
71.14	.2887339	.6258	54.5	.4288	RUTHENIUM	BORON
71.14	.2821457	.4147	36.9	.4971	RUTHENIUM	STRONTIUM
71.14	.2678040	.5160	48.4	.4621	RUTHENIUM	CALCIUM
71.14	.2670178	.5791	58.9	.4250	RHODIUM	BORON
71.14	.2420276	.3707	38.5	.4921	RHODIUM	STRONTIUM
71.14	.1919490	.2727	35.7	.4099	NICKEL	CALCIUM
71.14	.1483105	.1602	27.1	.4413	COBALT	YTTRIUM
71.14	.1403053	.2234	40.0	.4034	COPPER	CARBON
71.14	.1230798	.1631	33.3	.4063	THULIUM	LANTHANUM
71.14	.2821457	.4147	36.9	.4971	RUTHENIUM	STRONTIUM
71.14	.2678040	.5160	48.4	.4621	RUTHENIUM	CALCIUM
71.14	.1979651	.4106	52.1	.4769	STRONTIUM	LANTHANUM
71.14	.1964099	.3156	40.4	.4909	YTTRIUM	RUTHENIUM
71.14	.1795601	.3351	46.9	.4984	STRONTIUM	MOLYBDENUM
71.14	.1753296	.4572	65.5	.4500	RUTHENIUM	CARBON
71.14	.1668662	.4241	63.9	.4587	RUTHENIUM	BARIUM
71.14	.1753296	.4572	65.5	.4500	RUTHENIUM	CARBON
71.14	.1516755	.2494	41.3	.4052	NICKEL	CARBON
71.14	.1460848	.2591	44.6	.4074	COBALT	CARBON
71.14	.1403870	.3979	71.2	.4450	RHODIUM	CARBON
71.14	.1403053	.2234	40.0	.4034	COPPER	CARBON
71.14	.1236250	.2565	52.2	.4116	IRON	CARBON

TABLE A-16-1
(CONTINUED)

WAVE-LENGTH	SOLID ANGLE (STERAD.)	R	N (AT NORMAL INCIDENCE)	GAMMA (DH / (DH + DL))	MINIMUM % ALLOWED IS 5 ELEMENT - H	ELEMENT - L
64.59	.2047819	.4929	60.5	.4565	RUTHENIUM	CALCIUM
64.59	.1863534	.3231	43.6	.4909	STRONTIUM	RUTHENIUM
64.59	.1727932	.2942	42.8	.4100	NICKEL	CALCIUM
64.59	.1706688	.3087	45.5	.4129	COBALT	CALCIUM
64.59	.1580743	.1794	28.5	.4420	NICKEL	STRONTIUM
64.59	.1339003	.2891	54.3	.4062	COBALT	CARBON
64.59	.1286219	.2407	47.0	.4045	COPPER	BARIUM
64.59	.1240253	.1727	35.0	.4577	BORON	RHODIUM
64.59	.1077671	.1481	34.5	.4615	IRON	YTTRIUM
64.59	.1863534	.3231	43.6	.4909	STRONTIUM	RUTHENIUM
64.59	.1580743	.1794	28.5	.4420	NICKEL	STRONTIUM
64.59	.1494373	.2650	44.6	.5000	STRONTIUM	RHODIUM
64.59	.1391260	.2779	50.2	.4040	NICKEL	CARBON
64.59	.1388851	.2685	48.6	.4065	NICKEL	BARIUM
64.59	.1373621	.5446	99.6	.4971	CALCIUM	LANTHUNUM
64.59	.1278816	.1471	28.9	.4449	NICKEL	YTTRIUM
64.59	.1391260	.2779	50.2	.4040	NICKEL	CARBON
64.59	.1370018	.4485	82.3	.4415	RUTHENIUM	CARBON
64.59	.1339003	.2891	54.3	.4062	COBALT	CARBON
64.59	.1290764	.2493	48.5	.4022	COPPER	CARBON
64.59	.1135213	.2876	63.7	.4102	IRON	CARBON
64.59	.1038976	.3131	75.7	.4184	CHROMIUM	CARBON
58.64	.1566105	.3209	51.5	.4102	NICKEL	CALCIUM
58.64	.1549364	.4685	76.0	.4503	RUTHENIUM	CALCIUM
58.64	.1539126	.3355	54.8	.4132	COBALT	CALCIUM
58.64	.1471639	.2953	50.4	.4081	COPPER	CALCIUM
58.64	.1242917	.3101	62.7	.4091	COBALT	BARIUM
58.64	.1228815	.2886	59.0	.4014	COPPER	CARBON
58.64	.1188572	.2508	53.0	.4860	STRONTIUM	RUTHENIUM
58.64	.0898366	.2118	59.3	.4322	IRON	SCANDIUM
58.64	.0830368	.1511	45.7	.4921	CHROMIUM	YTTRIUM
58.64	.1291390	.2989	58.2	.4066	NICKEL	BARIUM
58.64	.1290288	.3132	61.0	.4029	NICKEL	CARBON
58.64	.1268476	.1655	32.8	.4518	NICKEL	STRONTIUM
58.64	.1188572	.2508	53.0	.4860	STRONTIUM	RUTHENIUM
58.64	.1139894	.2170	47.8	.4226	NICKEL	SCANDIUM
58.64	.1071287	.1388	32.6	.4562	NICKEL	YTTRIUM
58.64	.1005221	.2097	52.4	.4943	STRONTIUM	RHODIUM
58.64	.1290288	.3132	61.0	.4029	NICKEL	CARBON
58.64	.1240686	.3257	66.0	.4050	COBALT	CARBON
58.64	.1228815	.2886	59.0	.4014	COPPER	CARBON
58.64	.1071790	.4404	103.3	.4330	RUTHENIUM	CARBON
58.64	.1055943	.3255	77.5	.4088	IRON	CARBON
58.64	.0967142	.3530	91.7	.4164	CHROMIUM	CARBON

TABLE A-16-1
(CONTINUED)

MINIMUM Z ALLOWED IS 5

WAVE-LENGTH	SOLID ANGLE (STERAD.)	R	N (AT NORMAL) (INCIDENCE)	GAMMA (DH) (------) (DH + DL)	ELEMENT - H	ELEMENT - L
53.23	.1409989	.3492	62.3	.4103	NICKEL	CALCIUM
53.23	.1380450	.3639	66.2	.4133	COBALT	CALCIUM
53.23	.1332371	.3279	61.9	.4088	COPPER	CALCIUM
53.23	.1226418	.3684	75.5	.4188	IRON	CALCIUM
53.23	.1153214	.3656	79.7	.4039	COBALT	CARBON
53.23	.1117290	.3040	68.4	.4064	COPPER	BARIUM
53.23	.0866387	.1620	47.0	.4759	IRON	STRONTIUM
53.23	.0784517	.1589	50.9	.4062	OSMIUM	SCANDIUM
53.23	.0675862	.1457	54.2	.4023	RHENIUM	LANTHANUM
53.23	.1197478	.3514	73.8	.4020	NICKEL	CARBON
53.23	.1176248	.3241	69.2	.4078	NICKEL	BARIUM
53.23	.1044460	.1622	39.0	.4585	NICKEL	STRONTIUM
53.23	.1036115	.2409	58.4	.4238	NICKEL	SCANDIUM
53.23	.0871383	.1290	37.2	.4675	NICKEL	YTTRIUM
53.23	.0825304	.1534	46.7	.4458	NICKEL	BISMUTH
53.23	.0819250	.1811	55.5	.4308	NICKEL	TELLURIUM
53.23	.1197478	.3514	73.8	.4020	NICKEL	CARBON
53.23	.1153214	.3656	79.7	.4039	COBALT	CARBON
53.23	.1139208	.3298	72.7	.4010	COPPER	CARBON
53.23	.0987587	.3671	93.4	.4076	IRON	CARBON
53.23	.0914583	.2267	62.3	.3965	OSMIUM	CARBON
53.23	.0911634	.3849	106.1	.4124	MANGANESE	CARBON
48.33	.1273051	.3806	75.1	.4105	NICKEL	CALCIUM
48.33	.1242407	.3951	79.9	.4135	COBALT	CALCIUM
48.33	.1200425	.3619	75.8	.4094	COPPER	CALCIUM
48.33	.1152597	.4003	87.3	.4011	NICKEL	CARBON
48.33	.1113426	.4163	94.0	.4030	COBALT	CARBON
48.33	.1001142	.3207	80.5	.4111	COPPER	BARIUM
48.33	.0744190	.1715	57.9	.4049	OSMIUM	SCANDIUM
48.33	.0687448	.1552	56.7	.4845	IRON	STRONTIUM
48.33	.0621529	.1394	56.4	.4059	RHENIUM	LANTHANUM
48.33	.1152597	.4003	87.3	.4011	NICKEL	CARBON
48.33	.1063237	.3386	80.0	.4122	NICKEL	BARIUM
48.33	.0946960	.2675	71.0	.4269	NICKEL	SCANDIUM
48.33	.0856785	.1590	46.7	.4666	NICKEL	STRONTIUM
48.33	.0728979	.1905	65.7	.4364	NICKEL	TELLURIUM
48.33	.0727610	.1801	62.2	.4409	NICKEL	MAGNESIUM
48.33	.0719588	.1406	49.1	.4654	NICKEL	BISMUTH
48.33	.1152597	.4003	87.3	.4011	NICKEL	CARBON
48.33	.1113426	.4163	94.0	.4030	COBALT	CARBON
48.33	.1088997	.3804	87.8	.4005	COPPER	CARBON
48.33	.0967508	.4215	109.5	.4064	IRON	CARBON
48.33	.0902940	.4421	123.1	.4109	MANGANESE	CARBON
48.33	.0901246	.4562	127.2	.4131	CHROMIUM	CARBON

TABLE A-16-1
(CONTINUED)

WAVE-LENGTH	SOLID ANGLE (STERAD.)	R	N (AT NORMAL) (INCIDENCE)	GAMMA (DH / (DH + DL))	ELEMENT - H	ELEMENT - L
			MINIMUM Z ALLOWED IS 5			
43.88	.1546158	.5227	85.0	.4004	NICKEL	CARBON
43.88	.1532514	.5453	89.4	.4022	COBALT	CARBON
43.88	.1461565	.5047	86.8	.4000	COPPER	CARBON
43.88	.1428371	.5659	99.6	.4054	IRON	CARBON
43.88	.1120585	.4282	96.0	.4139	COBALT	CALCIUM
43.88	.0867746	.3184	92.2	.4198	COPPER	BARIUM
43.88	.0728119	.1872	64.6	.4049	RHENIUM	SCANDIUM
43.88	.0595973	.1369	57.7	.4111	OSMIUM	MAGNESIUM
43.88	.0525507	.1461	69.9	.4923	IRON	STRONTIUM
43.88	.1151511	.4139	90.3	.4107	NICKEL	CALCIUM
43.88	.0936271	.3366	90.3	.4207	NICKEL	BARIUM
43.88	.0866149	.2971	86.2	.4291	NICKEL	SCANDIUM
43.88	.0682795	.1544	56.9	.4727	NICKEL	STRONTIUM
43.88	.0666384	.2067	78.0	.4412	NICKEL	MAGNESIUM
43.88	.0642230	.1998	78.2	.4420	NICKEL	TELLURIUM
43.88	.0576654	.1896	82.6	.4394	NICKEL	LANTHANUM
43.88	.1532514	.5453	89.4	.4022	COBALT	CARBON
43.88	.1461565	.5047	86.8	.4000	COPPER	CARBON
43.88	.1428371	.5659	99.6	.4054	IRON	CARBON
43.88	.1417442	.6136	108.8	.4116	CHROMIUM	CARBON
43.88	.1404203	.5968	106.8	.4095	MANGANESE	CARBON
43.88	.1169952	.6162	132.4	.4193	VANADIUM	CARBON
39.84	.1057866	.4523	107.5	.4111	NICKEL	CALCIUM
39.84	.1026874	.4663	114.1	.4143	COBALT	CALCIUM
39.84	.0978577	.4306	110.6	.4104	COPPER	CALCIUM
39.84	.0911169	.4702	129.7	.4199	IRON	CALCIUM
39.84	.0767983	.3378	110.5	.4353	COBALT	BARIUM
39.84	.0730672	.3121	107.4	.4280	COPPER	SCANDIUM
39.84	.0578910	.1583	68.7	.4086	RHENIUM	MAGNESIUM
39.84	.0543789	.1430	66.1	.4111	OSMIUM	TELLURIUM
39.84	.0509411	.1424	70.3	.4045	IRIDIUM	TITANIUM
39.84	.0811220	.3330	103.2	.4302	NICKEL	BARIUM
39.84	.0801323	.3335	104.6	.4292	NICKEL	SCANDIUM
39.84	.0607383	.2359	97.6	.4413	NICKEL	MAGNESIUM
39.84	.0573591	.2151	94.3	.4466	NICKEL	TELLURIUM
39.84	.0570527	.1620	71.3	.4758	NICKEL	STRONTIUM
39.84	.0545055	.1552	71.6	.4082	RHENIUM	TITANIUM
39.84	.0519730	.1360	65.8	.4129	RHENIUM	ANTIMONY
39.84	.0436350	.1190	68.5	.4882	NICKEL	CARBON
39.84	.0399549	.1178	74.1	.4960	COBALT	CARBON
39.84	.0390927	.0729	46.9	.4405	RHENIUM	CARBON
39.84	.0387609	.1063	68.9	.4861	COPPER	CARBON
39.84	.0380343	.0709	46.8	.4400	OSMIUM	CARBON
39.84	.0343292	.0628	46.0	.4369	IRIDIUM	CARBON

TABLE A-16-1
(CONTINUED)

MINIMUM % ALLOWED IS 5

WAVE-LENGTH	SOLID ANGLE (STERAD.)	R	N (AT NORMAL) (INCIDENCE)	GAMMA (DH) (DH + DL)	ELEMENT - H	ELEMENT - L
36.17	.1079293	.5142	119.7	.4117	NICKEL	CALCIUM
36.17	.1052996	.5291	126.3	.4149	COBALT	CALCIUM
36.17	.0992654	.4894	123.9	.4107	COPPER	CALCIUM
36.17	.0954722	.5373	141.4	.4205	IRON	CALCIUM
36.17	.0711410	.3796	134.1	.4346	COBALT	SCANDIUM
36.17	.0622236	.3083	124.5	.4352	COPPER	BARIUM
36.17	.0540300	.1780	82.8	.4082	RHENIUM	MAGNESIUM
36.17	.0508651	.1696	83.8	.4065	OSMIUM	TITANIUM
36.17	.0478648	.1425	74.8	.4101	IRIDIUM	TELLURIUM
36.17	.0752697	.3749	125.2	.4296	NICKEL	SCANDIUM
36.17	.0695033	.3331	120.4	.4388	NICKEL	BARIUM
36.17	.0551092	.2684	122.4	.4426	NICKEL	MAGNESIUM
36.17	.0513606	.1736	85.0	.4073	RHENIUM	TITANIUM
36.17	.0512625	.2316	113.5	.4514	NICKEL	TELLURIUM
36.17	.0479842	.1708	89.4	.4792	NICKEL	STRONTIUM
36.17	.0478914	.1461	76.7	.4129	RHENIUM	ANTIMONY
36.17	.0357930	.0844	59.3	.4354	RHENIUM	CARBON
36.17	.0353166	.0823	58.5	.4339	OSMIUM	CARBON
36.17	.0337626	.1239	92.2	.4855	NICKEL	CARBON
36.17	.0334559	.0767	57.6	.4316	IRIDIUM	CARBON
36.17	.0299301	.1195	100.3	.4932	COBALT	CARBON
36.17	.0291180	.1077	93.0	.4829	COPPER	CARBON
32.84	.0760355	.4343	143.6	.4301	NICKEL	SCANDIUM
32.84	.0723791	.4406	153.0	.4351	COBALT	SCANDIUM
32.84	.0683620	.4050	148.9	.4280	COPPER	SCANDIUM
32.84	.0635668	.2577	101.9	.4035	RHENIUM	SCANDIUM
32.84	.0550472	.3391	154.8	.4495	COBALT	BARIUM
32.84	.0502503	.2113	105.7	.4777	COPPER	CALCIUM
32.84	.0501497	.1923	96.4	.4075	OSMIUM	MAGNESIUM
32.84	.0490919	.1950	99.8	.4071	RHENIUM	TITANIUM
32.84	.0447508	.1538	86.4	.4100	IRIDIUM	TELLURIUM
32.84	.0593562	.3390	143.6	.4445	NICKEL	BARIUM
32.84	.0566587	.2343	103.9	.4810	NICKEL	CALCIUM
32.84	.0501497	.1923	96.4	.4075	OSMIUM	MAGNESIUM
32.84	.0492293	.1901	97.0	.4059	OSMIUM	TITANIUM
32.84	.0469274	.1623	86.9	.4111	OSMIUM	TELLURIUM
32.84	.0451732	.1512	84.1	.4143	OSMIUM	CADMIUM
32.84	.0446234	.1538	86.6	.4123	OSMIUM	ANTIMONY
32.84	.0343240	.0989	72.4	.4276	OSMIUM	CARBON
32.84	.0339402	.1005	74.5	.4291	RHENIUM	CARBON
32.84	.0327516	.0936	71.9	.4252	IRIDIUM	CARBON
32.84	.0282222	.1377	122.6	.4829	NICKEL	CARBON
32.84	.0267596	.0800	75.2	.4266	PLATINUM	CARBON
32.84	.0263887	.0846	80.6	.4329	TUNGSTEN	CARBON

TABLE A-16-1
(CONTINUED)

WAVE-LENGTH	SOLID ANGLE (STERAD.)	R	N (AT NORMAL INCIDENCE)	GAMMA (DH / (DH + DL))	MINIMUM Z ALLOWED IS 5 ELEMENT - H	ELEMENT - L
29.81	.0559120	.3150	141.6	.4664	NICKEL	CADMIUM
29.81	.0517950	.3143	152.5	.4723	COBALT	CADMIUM
29.81	.0508925	.1887	93.2	.4165	OSMIUM	CADMIUM
29.81	.0506611	.3495	173.4	.4495	NICKEL	BARIUM
29.81	.0497994	.2158	108.9	.4086	OSMIUM	BARIUM
29.81	.0488977	.2241	115.2	.4101	RHENIUM	TITANIUM
29.81	.0448404	.2053	115.1	.4051	IRIDIUM	MAGNESIUM
29.81	.0404998	.2344	145.5	.4898	COBALT	CALCIUM
29.81	.0371765	.1546	104.5	.4100	PLATINUM	TELLURIUM
29.81	.0506611	.3495	173.4	.4495	NICKEL	BARIUM
29.81	.0501451	.3564	178.6	.4469	NICKEL	TITANIUM
29.81	.0472553	.2156	114.7	.4075	OSMIUM	MAGNESIUM
29.81	.0446543	.1785	100.5	.4125	OSMIUM	TELLURIUM
29.81	.0444710	.2375	134.2	.4836	NICKEL	CALCIUM
29.81	.0429494	.1712	100.2	.4135	OSMIUM	ANTIMONY
29.81	.0389680	.1702	109.8	.4844	SCANDIUM	NICKEL
29.81	.0335623	.1198	89.7	.4226	OSMIUM	CARBON
29.81	.0323004	.1196	93.1	.4252	RHENIUM	CARBON
29.81	.0317616	.1129	89.3	.4213	IRIDIUM	CARBON
29.81	.0276681	.1013	92.1	.4211	PLATINUM	CARBON
29.81	.0248609	.0993	100.4	.4271	TUNGSTEN	CARBON
29.81	.0243413	.1563	161.4	.4807	NICKEL	CARBON
27.07	.0440227	.1953	111.5	.4631	TITANIUM	NICKEL
27.07	.0436691	.2228	128.3	.4108	OSMIUM	BARIUM
27.07	.0432784	.3640	211.4	.4547	NICKEL	BARIUM
27.07	.0426534	.2264	133.4	.4123	RHENIUM	BARIUM
27.07	.0436691	.2228	128.3	.4108	OSMIUM	BARIUM
27.07	.0411376	.2393	146.2	.4062	RHENIUM	MAGNESIUM
27.07	.0393512	.1851	118.2	.4119	IRIDIUM	TELLURIUM
27.07	.0354477	.1709	121.2	.4120	PLATINUM	ANTIMONY
27.07	.0315363	.2351	187.4	.4938	COBALT	CALCIUM
27.07	.0436691	.2228	128.3	.4108	OSMIUM	BARIUM
27.07	.0422787	.2356	140.1	.4051	OSMIUM	MAGNESIUM
27.07	.0413935	.1949	118.3	.4136	OSMIUM	TELLURIUM
27.07	.0413027	.1975	120.2	.4566	TITANIUM	COBALT
27.07	.0408097	.1912	117.7	.4138	OSMIUM	ANTIMONY
27.07	.0397765	.1733	109.5	.4680	TITANIUM	COPPER
27.07	.0373478	.1510	101.6	.4237	OSMIUM	CALCIUM
27.07	.0308451	.1382	112.6	.4187	OSMIUM	CARBON
27.07	.0295018	.1312	111.8	.4174	IRIDIUM	CARBON
27.07	.0294847	.1373	117.1	.4211	RHENIUM	CARBON
27.07	.0267463	.1220	114.6	.4178	PLATINUM	CARBON
27.07	.0250122	.1218	122.4	.4210	TUNGSTEN	CARBON
27.07	.0217227	.1064	123.1	.4193	GOLD	CARBON

TABLE A-16-1
(CONTINUED)

MINIMUM Z ALLOWED IS 5

WAVE-LENGTH	SOLID ANGLE (STERAD.)	R	N (AT NORMAL INCIDENCE)	GAMMA (DE / (DE + DL))	ELEMENT - E	ELEMENT - L
24.57	.0589870	.4673	199.1	.4647	NICKEL	VANADIUM
24.57	.0550003	.4679	213.8	.4706	COBALT	VANADIUM
24.57	.0534553	.4317	203.0	.4602	COPPER	VANADIUM
24.57	.0495336	.2631	133.5	.4117	OSMIUM	VANADIUM
24.57	.0439456	.2266	129.6	.4153	OSMIUM	ANTIMONY
24.57	.0397926	.2199	138.9	.4164	RHENIUM	TELLURIUM
24.57	.0375870	.2215	148.1	.4092	IRIDIUM	BARIUM
24.57	.0335841	.2346	175.6	.4027	PLATINUM	MAGNESIUM
24.57	.0289295	.1562	135.7	.4251	TUNGSTEN	CALCIUM
24.57	.0478218	.3931	206.6	.4708	NICKEL	ANTIMONY
24.57	.0412286	.3663	223.3	.4694	NICKEL	TELLURIUM
24.57	.0393335	.2317	148.1	.4098	OSMIUM	BARIUM
24.57	.0385689	.2536	165.3	.4024	OSMIUM	MAGNESIUM
24.57	.0339583	.1657	122.6	.4209	OSMIUM	CALCIUM
24.57	.0321228	.1905	149.0	.4102	OSMIUM	SILICON
24.57	.0318004	.1930	152.5	.4087	OSMIUM	BORON
24.57	.0292276	.1583	136.1	.4153	OSMIUM	CARBON
24.57	.0280091	.1512	135.7	.4144	IRIDIUM	CARBON
24.57	.0277751	.1569	142.0	.4175	RHENIUM	CARBON
24.57	.0248382	.1416	143.3	.4151	PLATINUM	CARBON
24.57	.0240935	.1458	152.1	.4191	TUNGSTEN	CARBON
24.57	.0207348	.1268	153.6	.4157	GOLD	CARBON
22.31	.0587077	.4944	211.7	.4764	NICKEL	TELLURIUM
22.31	.0547751	.4643	213.0	.4704	COPPER	TELLURIUM
22.31	.0543757	.4932	228.0	.4817	COBALT	TELLURIUM
22.31	.0506030	.2839	141.0	.4164	OSMIUM	TELLURIUM
22.31	.0370208	.2523	171.3	.4096	OSMIUM	BARIUM
22.31	.0351164	.2868	205.2	.4014	RHENIUM	MAGNESIUM
22.31	.0307373	.1808	147.9	.4179	IRIDIUM	CALCIUM
22.31	.0254956	.1901	187.4	.4065	PLATINUM	SILICON
22.31	.0248302	.2095	212.1	.4110	TUNGSTEN	BORON
22.31	.0370208	.2523	171.3	.4096	OSMIUM	BARIUM
22.31	.0364557	.2826	194.8	.4005	OSMIUM	MAGNESIUM
22.31	.0325643	.1913	147.6	.4190	OSMIUM	CALCIUM
22.31	.0310585	.2193	177.5	.4099	OSMIUM	SILICON
22.31	.0307443	.2218	181.3	.4100	OSMIUM	BORON
22.31	.0301941	.4525	376.6	.4899	TELLURIUM	ALUMINUM
22.31	.0301082	.1776	148.3	.4190	OSMIUM	STRONTIUM
22.31	.0285935	.1869	164.3	.4140	OSMIUM	CARBON
22.31	.0271448	.1777	164.5	.4120	IRIDIUM	CARBON
22.31	.0270823	.1861	172.7	.4151	RHENIUM	CARBON
22.31	.0249870	.3686	370.8	.4934	CARBON	TELLURIUM
22.31	.0232579	.1598	172.7	.4105	PLATINUM	CARBON
22.31	.0227181	.1716	189.9	.4165	TUNGSTEN	CARBON

TABLE A-16-1
(CONTINUED)

MINIMUM Z ALLOWED IS 5

WAVE-LENGTH	SOLID ANGLE (STERAD.)	R	N (AT NORMAL INCIDENCE)	GAMMA (DH / (DH + DL))	ELEMENT - H	ELEMENT - L
20.25	.0339823	.2765	204.5	.4094	OSMIUM	BARIUM
20.25	.0332007	.3121	236.2	.3992	OSMIUM	MAGNESIUM
20.25	.0325598	.2639	203.7	.4086	IRIDIUM	BARIUM
20.25	.0323915	.2740	212.6	.4104	RHENIUM	BARIUM
20.25	.0319222	.2981	234.7	.3987	IRIDIUM	MAGNESIUM
20.25	.0284748	.2136	188.5	.4197	RHENIUM	CALCIUM
20.25	.0247290	.2198	223.3	.4087	PLATINUM	SILICON
20.25	.0226086	.2336	259.7	.4108	TUNGSTEN	BORON
20.25	.0189470	.1953	259.0	.4065	GOLD	ALUMINUM
20.25	.0332007	.3121	236.2	.3992	OSMIUM	MAGNESIUM
20.25	.0300769	.2171	181.4	.4193	OSMIUM	CALCIUM
20.25	.0287069	.2479	217.1	.4095	OSMIUM	SILICON
20.25	.0283770	.2521	223.3	.4077	OSMIUM	BORON
20.25	.0278996	.2012	181.3	.4199	OSMIUM	STRONTIUM
20.25	.0278450	.2465	222.5	.4084	OSMIUM	ALUMINUM
20.25	.0274745	.2199	201.2	.4144	OSMIUM	MANGANESE
20.25	.0266681	.2152	202.8	.4145	OSMIUM	CARBON
20.25	.0256515	.2063	202.1	.4116	IRIDIUM	CARBON
20.25	.0250631	.2113	211.8	.4140	RHENIUM	CARBON
20.25	.0228531	.1905	209.6	.4105	PLATINUM	CARBON
20.25	.0209186	.1958	235.3	.4153	TUNGSTEN	CARBON
20.25	.0177950	.1661	234.6	.4111	GOLD	CARBON
18.39	.0309529	.3076	249.8	.4102	RHENIUM	BARIUM
18.39	.0308980	.2965	241.1	.4085	OSMIUM	BARIUM
18.39	.0296619	.3336	282.6	.3976	OSMIUM	MAGNESIUM
18.39	.0296399	.2890	245.1	.4085	IRIDIUM	BARIUM
18.39	.0296619	.3336	282.6	.3976	OSMIUM	MAGNESIUM
18.39	.0260553	.2326	224.3	.4175	IRIDIUM	CALCIUM
18.39	.0229614	.2507	274.4	.4069	PLATINUM	SILICON
18.39	.0212646	.2696	318.7	.4082	TUNGSTEN	BORON
18.39	.0184273	.2265	309.0	.4065	GOLD	ALUMINUM
18.39	.0296619	.3336	282.6	.3976	OSMIUM	MAGNESIUM
18.39	.0272578	.2391	220.5	.4186	OSMIUM	CALCIUM
18.39	.0260220	.2719	262.6	.4069	OSMIUM	SILICON
18.39	.0257311	.2775	271.1	.4048	OSMIUM	BORON
18.39	.0253883	.2220	219.8	.4185	OSMIUM	STRONTIUM
18.39	.0253062	.2718	269.9	.4056	OSMIUM	ALUMINUM
18.39	.0247455	.2220	225.5	.4170	OSMIUM	LANTHUNUM
18.39	.0244106	.2396	246.7	.4137	OSMIUM	CARBON
18.39	.0241044	.2465	257.0	.4157	RHENIUM	CARBON
18.39	.0233138	.2324	250.5	.4137	IRIDIUM	CARBON
18.39	.0214251	.2201	258.2	.4118	PLATINUM	CARBON
18.39	.0199102	.2289	289.0	.4157	TUNGSTEN	CARBON
18.39	.0175305	.1976	283.2	.4103	GOLD	CARBON

TABLE A-16-1
(CONTINUED)

MINIMUM % ALLOWED IS 5

WAVE-LENGTH	SOLID ANGLE (STERAD.)	R	N (AT NORMAL) (INCIDENCE)	GAMMA (DH) (------) (DH + DL)	ELEMENT - H	ELEMENT - L
16.69	.0302132	.3386	281.7	.4084	OSMIUM	BARIUM
16.69	.0297302	.3478	294.0	.4102	RHENIUM	BARIUM
16.69	.0287199	.3221	281.8	.4075	IRIDIUM	BARIUM
16.69	.0273713	.3702	339.9	.3968	OSMIUM	MAGNESIUM
16.69	.0267169	.3813	358.7	.3976	RHENIUM	MAGNESIUM
16.69	.0243132	.2596	268.3	.4173	IRIDIUM	CALCIUM
16.69	.0206375	.2757	335.7	.4049	PLATINUM	SILICON
16.69	.0196983	.2424	309.2	.4251	TUNGSTEN	LANTHUNUM
16.69	.0171050	.2583	379.6	.4036	GOLD	BORON
16.69	.0273713	.3702	339.9	.3968	OSMIUM	MAGNESIUM
16.69	.0256000	.2738	268.8	.4187	OSMIUM	CALCIUM
16.69	.0243656	.2565	264.6	.4218	OSMIUM	LANTHUNUM
16.69	.0243319	.3095	319.7	.4055	OSMIUM	SILICON
16.69	.0240029	.3154	330.3	.4033	OSMIUM	BORON
16.69	.0239109	.2538	266.8	.4202	OSMIUM	STRONTIUM
16.69	.0236605	.3093	328.6	.4042	OSMIUM	ALUMINUM
16.69	.0229770	.2769	302.8	.4117	OSMIUM	CARBON
16.69	.0221826	.2813	318.7	.4137	RHENIUM	CARBON
16.69	.0218954	.2627	301.5	.4106	IRIDIUM	CARBON
16.69	.0193696	.2445	317.2	.4110	PLATINUM	CARBON
16.69	.0183018	.2606	357.9	.4164	TUNGSTEN	CARBON
16.69	.0161076	.2223	346.8	.4104	GOLD	CARBON
15.16	.0292044	.3349	288.2	.4220	OSMIUM	LANTHUNUM
15.16	.0287399	.3428	299.7	.4248	RHENIUM	LANTHUNUM
15.16	.0279035	.3204	288.6	.4205	IRIDIUM	LANTHUNUM
15.16	.0255027	.3032	298.8	.4203	PLATINUM	LANTHUNUM
15.16	.0239363	.4169	437.8	.3968	RHENIUM	MAGNESIUM
15.16	.0224158	.2959	331.7	.4156	IRIDIUM	CALCIUM
15.16	.0192690	.3115	406.3	.4034	PLATINUM	SILICON
15.16	.0178079	.2569	362.5	.4287	TUNGSTEN	CERIUM
15.16	.0160911	.2949	460.7	.4019	GOLD	BORON
15.16	.0246393	.4054	413.5	.3961	OSMIUM	MAGNESIUM
15.16	.0234231	.3098	332.4	.4169	OSMIUM	CALCIUM
15.16	.0221929	.2723	308.4	.4263	OSMIUM	CERIUM
15.16	.0221246	.3458	392.9	.4042	OSMIUM	SILICON
15.16	.0219311	.2863	328.1	.4206	OSMIUM	STRONTIUM
15.16	.0217801	.3524	406.7	.4019	OSMIUM	BORON
15.16	.0215220	.3461	404.2	.4029	OSMIUM	ALUMINUM
15.16	.0210282	.3144	375.7	.4098	OSMIUM	CARBON
15.16	.0202206	.3192	396.8	.4118	RHENIUM	CARBON
15.16	.0201752	.3002	374.0	.4088	IRIDIUM	CARBON
15.16	.0182316	.2815	388.0	.4087	PLATINUM	CARBON
15.16	.0166678	.2975	448.5	.4143	TUNGSTEN	CARBON
15.16	.0153281	.2581	423.2	.4097	GOLD	CARBON

TABLE A-16-1
(CONTINUED)

MINIMUM Z ALLOWED IS 5

WAVE-LENGTH	SOLID ANGLE (STERAD.)	R	N (AT NORMAL) (INCIDENCE)	GAMMA (DE) (------) (DE + DL)	ELEMENT - E	ELEMENT - L
13.76	.0219118	.4399	504.6	.3954	OSMIUM	MAGNESIUM
13.76	.0211930	.4515	535.5	.3961	RHENIUM	MAGNESIUM
13.76	.0211527	.4224	501.9	.3951	IRIDIUM	MAGNESIUM
13.76	.0211250	.3460	411.7	.4153	OSMIUM	CALCIUM
13.76	.0204095	.3515	432.8	.4178	RHENIUM	CALCIUM
13.76	.0191161	.3661	481.4	.4024	IRIDIUM	SILICON
13.76	.0173747	.2657	384.4	.4249	PLATINUM	PRASEODYMIUM
13.76	.0157685	.3014	480.5	.4258	TUNGSTEN	STRONTIUM
13.76	.0146315	.3318	569.9	.4006	GOLD	BORON
13.76	.0211250	.3460	411.7	.4153	OSMIUM	CALCIUM
13.76	.0199059	.2942	371.4	.4284	OSMIUM	PRASEODYMIUM
13.76	.0198436	.3201	405.5	.4195	OSMIUM	STRONTIUM
13.76	.0198362	.3818	483.7	.4031	OSMIUM	SILICON
13.76	.0194821	.3890	501.9	.4007	OSMIUM	BORON
13.76	.0193073	.3826	498.1	.4017	OSMIUM	ALUMINUM
13.76	.0189510	.3517	466.5	.4081	OSMIUM	CARBON
13.76	.0189510	.3517	466.5	.4081	OSMIUM	CARBON
13.76	.0182505	.3371	464.2	.4072	IRIDIUM	CARBON
13.76	.0181562	.3568	493.9	.4100	RHENIUM	CARBON
13.76	.0166332	.3192	482.3	.4071	PLATINUM	CARBON
13.76	.0149249	.3341	562.6	.4124	TUNGSTEN	CARBON
13.76	.0140595	.2950	527.4	.4080	GOLD	CARBON
12.49	.0193475	.4748	616.7	.3949	OSMIUM	MAGNESIUM
12.49	.0188728	.3829	509.9	.4141	OSMIUM	CALCIUM
12.49	.0187512	.4574	613.1	.3946	IRIDIUM	MAGNESIUM
12.49	.0186313	.4856	655.1	.3956	RHENIUM	MAGNESIUM
12.49	.0182078	.3685	508.7	.4128	IRIDIUM	CALCIUM
12.49	.0170538	.3587	528.7	.4212	RHENIUM	STRONTIUM
12.49	.0156572	.3848	617.6	.4014	PLATINUM	SILICON
12.49	.0135991	.4122	761.9	.4023	TUNGSTEN	BORON
12.49	.0130211	.3618	698.3	.4006	GOLD	ALUMINUM
12.49	.0188728	.3829	509.9	.4141	OSMIUM	CALCIUM
12.49	.0178007	.3554	501.8	.4185	OSMIUM	STRONTIUM
12.49	.0176234	.4182	596.4	.4022	OSMIUM	SILICON
12.49	.0172605	.4257	619.9	.3997	OSMIUM	BORON
12.49	.0171684	.4196	614.3	.4007	OSMIUM	ALUMINUM
12.49	.0169050	.3898	579.5	.4067	OSMIUM	CARBON
12.49	.0165797	.3248	492.4	.4238	OSMIUM	ZINC
12.49	.0169050	.3898	579.5	.4067	OSMIUM	CARBON
12.49	.0163405	.3749	576.6	.4058	IRIDIUM	CARBON
12.49	.0161360	.3945	614.4	.4084	RHENIUM	CARBON
12.49	.0149561	.3570	599.9	.4057	PLATINUM	CARBON
12.49	.0131850	.3703	705.9	.4108	TUNGSTEN	CARBON
12.49	.0127047	.3320	656.8	.4065	GOLD	CARBON

TABLE A-16-1
(CONTINUED)

MINIMUM Z ALLOWED IS 5

WAVE-LENGTH	SOLID ANGLE (STERAD.)	R	N (AT NORMAL INCIDENCE)	GAMMA (DE / (DE + DL))	ELEMENT - H	ELEMENT - L
11.34	.0170552	.3785	557.8	.4262	OSMIUM	EUROPIUM
11.34	.0169669	.5103	755.9	.3945	OSMIUM	MAGNESIUM
11.34	.0166923	.4208	633.6	.4129	OSMIUM	CALCIUM
11.34	.0165173	.4938	751.3	.3942	IRIDIUM	MAGNESIUM
11.34	.0165173	.4938	751.3	.3942	IRIDIUM	MAGNESIUM
11.34	.0160507	.4259	666.9	.4151	RHENIUM	CALCIUM
11.34	.0140881	.3614	644.6	.4163	PLATINUM	STRONTIUM
11.34	.0121346	.4387	908.7	.4044	TUNGSTEN	SILICON
11.34	.0116782	.4063	874.5	.3987	GOLD	BORON
11.34	.0169669	.5103	755.9	.3945	OSMIUM	MAGNESIUM
11.34	.0166923	.4208	633.6	.4129	OSMIUM	CALCIUM
11.34	.0158163	.3918	622.6	.4177	OSMIUM	STRONTIUM
11.34	.0155041	.4551	737.8	.4014	OSMIUM	SILICON
11.34	.0151326	.4628	768.7	.3988	OSMIUM	BORON
11.34	.0151226	.4570	759.5	.3999	OSMIUM	ALUMINUM
11.34	.0149117	.4283	721.9	.4054	OSMIUM	CARBON
11.34	.0149117	.4283	721.9	.4054	OSMIUM	CARBON
11.34	.0144763	.4137	718.3	.4046	IRIDIUM	CARBON
11.34	.0142254	.4333	765.5	.4071	RHENIUM	CARBON
11.34	.0133126	.3960	747.7	.4045	PLATINUM	CARBON
11.34	.0115034	.4067	888.5	.4093	TUNGSTEN	CARBON
11.34	.0113888	.3713	819.3	.4052	GOLD	CARBON
10.30	.0155575	.4428	715.4	.4192	OSMIUM	GERMANIUM
10.30	.0151181	.4298	714.4	.4178	IRIDIUM	GERMANIUM
10.30	.0150244	.4479	749.2	.4219	RHENIUM	GERMANIUM
10.30	.0147759	.5448	926.6	.3941	OSMIUM	MAGNESIUM
10.30	.0144378	.5289	920.8	.3938	IRIDIUM	MAGNESIUM
10.30	.0139776	.4621	831.0	.4140	RHENIUM	CALCIUM
10.30	.0124402	.3970	802.1	.4155	PLATINUM	STRONTIUM
10.30	.0105349	.4358	1039.6	.4005	GOLD	SILICON
10.30	.0100792	.4732	1179.9	.4017	TUNGSTEN	ALUMINUM
10.30	.0147759	.5448	926.6	.3941	OSMIUM	MAGNESIUM
10.30	.0145311	.4568	790.0	.4118	OSMIUM	CALCIUM
10.30	.0138409	.4267	774.8	.4169	OSMIUM	STRONTIUM
10.30	.0134360	.4897	916.0	.4007	OSMIUM	SILICON
10.30	.0131381	.4923	941.8	.3992	OSMIUM	ALUMINUM
10.30	.0130606	.4973	957.0	.3980	OSMIUM	BORON
10.30	.0129370	.4645	902.5	.4043	OSMIUM	CARBON
10.30	.0129370	.4645	902.5	.4043	OSMIUM	CARBON
10.30	.0126053	.4503	897.8	.4035	IRIDIUM	CARBON
10.30	.0123470	.4699	956.6	.4058	RHENIUM	CARBON
10.30	.0116523	.4332	934.3	.4034	PLATINUM	CARBON
10.30	.0100346	.4091	1024.7	.4041	GOLD	CARBON
10.30	.0098322	.4400	1124.7	.4078	TUNGSTEN	CARBON

TABLE A-16-1
(CONTINUED)

MINIMUM Z ALLOWED IS 5

WAVE-LENGTH	SOLID ANGLE (STERAD.)	R	N (AT NORMAL INCIDENCE)	GAMMA (DE / (DE + DL))	ELEMENT - H	ELEMENT - L
9.35	.0128618	.4041	789.7	.4377	OSMIUM	MAGNESIUM
9.35	.0125407	.3930	787.5	.4357	IRIDIUM	MAGNESIUM
9.35	.0124796	.4906	988.0	.4108	OSMIUM	CALCIUM
9.35	.0123989	.4076	826.2	.4416	RHENIUM	MAGNESIUM
9.35	.0121904	.4777	984.8	.4097	IRIDIUM	CALCIUM
9.35	.0114960	.4651	1016.8	.4187	RHENIUM	STRONTIUM
9.35	.0105109	.4926	1177.9	.3994	PLATINUM	SILICON
9.35	.0090101	.4747	1324.0	.3984	GOLD	ALUMINUM
9.35	.0084470	.5226	1554.9	.4001	RHODIUM	BORON
9.35	.0124796	.4906	988.0	.4108	OSMIUM	CALCIUM
9.35	.0119599	.4603	967.3	.4161	OSMIUM	STRONTIUM
9.35	.0115026	.5222	1140.9	.4000	OSMIUM	SILICON
9.35	.0113097	.5260	1168.8	.3985	OSMIUM	ALUMINUM
9.35	.0111230	.5293	1195.9	.3972	OSMIUM	BORON
9.35	.0110657	.4985	1132.3	.4032	OSMIUM	CARBON
9.35	.0102848	.3264	797.5	.4464	OSMIUM	BOLINIUM
9.35	.0110657	.4985	1132.3	.4032	OSMIUM	CARBON
9.35	.0108284	.4850	1125.6	.4024	IRIDIUM	CARBON
9.35	.0105865	.5052	1199.3	.4046	RHENIUM	CARBON
9.35	.0100744	.4689	1169.7	.4024	PLATINUM	CARBON
9.35	.0087317	.4457	1282.8	.4030	GOLD	CARBON
9.35	.0083461	.4841	1457.7	.4078	RHODIUM	CARBON
8.49	.0115547	.3882	844.4	.4555	OSMIUM	THULIUM
8.49	.0113271	.3787	840.2	.4530	IRIDIUM	THULIUM
8.49	.0111940	.3930	882.3	.4586	RHENIUM	THULIUM
8.49	.0106539	.3659	863.3	.4528	PLATINUM	THULIUM
8.49	.0103209	.5086	1238.6	.4088	IRIDIUM	CALCIUM
8.49	.0098701	.4259	1084.6	.4402	RHENIUM	MAGNESIUM
8.49	.0093521	.4654	1250.7	.4140	PLATINUM	STRONTIUM
8.49	.0078947	.5117	1629.1	.3978	GOLD	ALUMINUM
8.49	.0077362	.5565	1807.9	.4032	RHODIUM	SILICON
8.49	.0105097	.5205	1244.6	.4099	OSMIUM	CALCIUM
8.49	.0102465	.4221	1035.3	.4363	OSMIUM	MAGNESIUM
8.49	.0101469	.4908	1215.7	.4154	OSMIUM	STRONTIUM
8.49	.0096752	.5511	1431.5	.3994	OSMIUM	SILICON
8.49	.0096711	.5581	1450.4	.3980	OSMIUM	ALUMINUM
8.49	.0092893	.5570	1507.1	.3966	OSMIUM	BORON
8.49	.0092718	.5284	1432.2	.4021	OSMIUM	CARBON
8.49	.0092718	.5284	1432.2	.4021	OSMIUM	CARBON
8.49	.0091235	.5159	1421.1	.4014	IRIDIUM	CARBON
8.49	.0088938	.5365	1516.2	.4036	RHENIUM	CARBON
8.49	.0085617	.5014	1472.0	.4014	PLATINUM	CARBON
8.49	.0074784	.4796	1611.7	.4019	GOLD	CARBON
8.49	.0073021	.5275	1815.6	.4069	RHODIUM	CARBON

TABLE A-16-1
(CONTINUED)

MINIMUM % ALLOWED IS 5

WAVE-LENGTH	SOLID ANGLE (STERAD.)	R	N (AT NORMAL) (INCIDENCE)	GAMMA (DH) (------) (DH + DL)	ELEMENT - H	ELEMENT - L
7.71	.0085990	.5456	1594.5	.4088	OSMIUM	CALCIUM
7.71	.0085197	.5356	1580.1	.4078	IRIDIUM	CALCIUM
7.71	.0083859	.5163	1547.4	.4146	OSMIUM	STRONTIUM
7.71	.0083525	.5549	1669.8	.4109	RHENIUM	CALCIUM
7.71	.0083063	.5069	1533.7	.4134	IRIDIUM	STRONTIUM
7.71	.0080549	.4500	1404.1	.4389	RHENIUM	MAGNESIUM
7.71	.0075324	.5540	1848.3	.3982	PLATINUM	SILICON
7.71	.0063541	.5710	2258.3	.4061	RHODIUM	CARBON
7.71	.0063348	.5389	2138.1	.3958	GOLD	BORON
7.71	.0083859	.5163	1547.4	.4146	OSMIUM	STRONTIUM
7.71	.0083264	.4448	1342.7	.4349	OSMIUM	MAGNESIUM
7.71	.0079439	.5755	1820.8	.3987	OSMIUM	SILICON
7.71	.0075345	.5521	1841.5	.4012	OSMIUM	CARBON
7.71	.0075335	.5789	1931.2	.3959	OSMIUM	BORON
7.71	.0074203	.3665	1241.2	.4524	OSMIUM	ALUMINUM
7.71	.0070121	.4362	1563.4	.4263	OSMIUM	SCANDIUM
7.71	.0075345	.5521	1841.5	.4012	OSMIUM	CARBON
7.71	.0074839	.5416	1818.8	.4005	IRIDIUM	CARBON
7.71	.0072576	.5618	1945.6	.4025	RHENIUM	CARBON
7.71	.0071260	.5303	1870.4	.4005	PLATINUM	CARBON
7.71	.0063541	.5710	2258.3	.4061	RHODIUM	CARBON
7.71	.0063302	.5848	2321.9	.4077	RUTHENIUM	CARBON
7.00	.0066911	.5521	2073.7	.4068	IRIDIUM	CALCIUM
7.00	.0066423	.5252	1987.3	.4129	IRIDIUM	STRONTIUM
7.00	.0066146	.5575	2118.4	.4078	OSMIUM	CALCIUM
7.00	.0065676	.5475	2095.0	.4068	PLATINUM	CALCIUM
7.00	.0065656	.5300	2028.9	.4140	OSMIUM	STRONTIUM
7.00	.0063143	.4468	1778.3	.4316	PLATINUM	MAGNESIUM
7.00	.0061648	.6070	2474.4	.3992	RHENIUM	SILICON
7.00	.0054738	.6117	2808.6	.4053	RHODIUM	CARBON
7.00	.0053958	.6584	3066.9	.3994	RUTHENIUM	BORON
7.00	.0066423	.5252	1987.3	.4129	IRIDIUM	STRONTIUM
7.00	.0064464	.4516	1760.8	.4318	IRIDIUM	MAGNESIUM
7.00	.0063424	.5847	2316.8	.3976	IRIDIUM	SILICON
7.00	.0058253	.5806	2504.8	.3950	IRIDIUM	BORON
7.00	.0058210	.5558	2399.7	.3997	IRIDIUM	CARBON
7.00	.0054355	.4436	2051.1	.4233	IRIDIUM	SCANDIUM
7.00	.0054105	.3602	1673.4	.4500	IRIDIUM	ALUMINUM
7.00	.0058210	.5558	2399.7	.3997	IRIDIUM	CARBON
7.00	.0057308	.5615	2462.3	.4003	OSMIUM	CARBON
7.00	.0057072	.5509	2425.8	.3997	PLATINUM	CARBON
7.00	.0056282	.5760	2572.0	.4016	RHENIUM	CARBON
7.00	.0054738	.6117	2808.6	.4053	RHODIUM	CARBON
7.00	.0054633	.6262	2891.3	.4070	RUTHENIUM	CARBON

TABLE A-16-1
(CONTINUED)

MINIMUM S ALLOWED IS 5

WAVE-LENGTH	SOLID ANGLE (STERAD.)	R	N (AT NORMAL INCIDENCE)	GAMMA (DE / (DE + DL))	ELEMENT - E	ELEMENT - L
6.35	.0055529	.6443	2916.0	.4149	RHODIUM	CALCIUM
6.35	.0055303	.6573	2987.2	.4176	RUTHENIUM	CALCIUM
6.35	.0053529	.5329	2501.8	.4475	RHODIUM	MAGNESIUM
6.35	.0053116	.5434	2571.3	.4522	RUTHENIUM	MAGNESIUM
6.35	.0053116	.5434	2571.3	.4522	RUTHENIUM	MAGNESIUM
6.35	.0043115	.3657	2131.7	.4526	PLATINUM	STRONTIUM
6.35	.0041620	.3707	2238.6	.4521	GOLD	SILICON
6.35	.0036517	.6051	4164.5	.4051	SILVER	CARBON
6.35	.0036169	.6026	4187.2	.3965	NICKEL	BORON
6.35	.0053529	.5329	2501.8	.4475	RHODIUM	MAGNESIUM
6.35	.0051526	.4503	2196.5	.4716	RHODIUM	STRONTIUM
6.35	.0051057	.4571	2250.0	.4689	RHODIUM	SILICON
6.35	.0046690	.6501	3499.4	.4046	RHODIUM	CARBON
6.35	.0046169	.6783	3692.5	.3978	RHODIUM	BORON
6.35	.0044289	.4994	2833.7	.4450	RHODIUM	YTTRIUM
6.35	.0044136	.5226	2975.9	.4368	RHODIUM	SCANDIUM
6.35	.0046690	.6501	3499.4	.4046	RHODIUM	CARBON
6.35	.0046173	.6639	3613.6	.4064	RUTHENIUM	CARBON
6.35	.0040042	.5440	3414.4	.3989	PLATINUM	CARBON
6.35	.0039062	.5457	3510.9	.3993	GOLD	CARBON
6.35	.0036517	.6051	4164.5	.4051	SILVER	CARBON
6.35	.0036100	.5730	3989.1	.4024	NICKEL	CARBON

TABLE A-16-1
(CONTINUED)

OPTIMUM X-RAY MULTILAYER PARAMETERS

UR
LLE

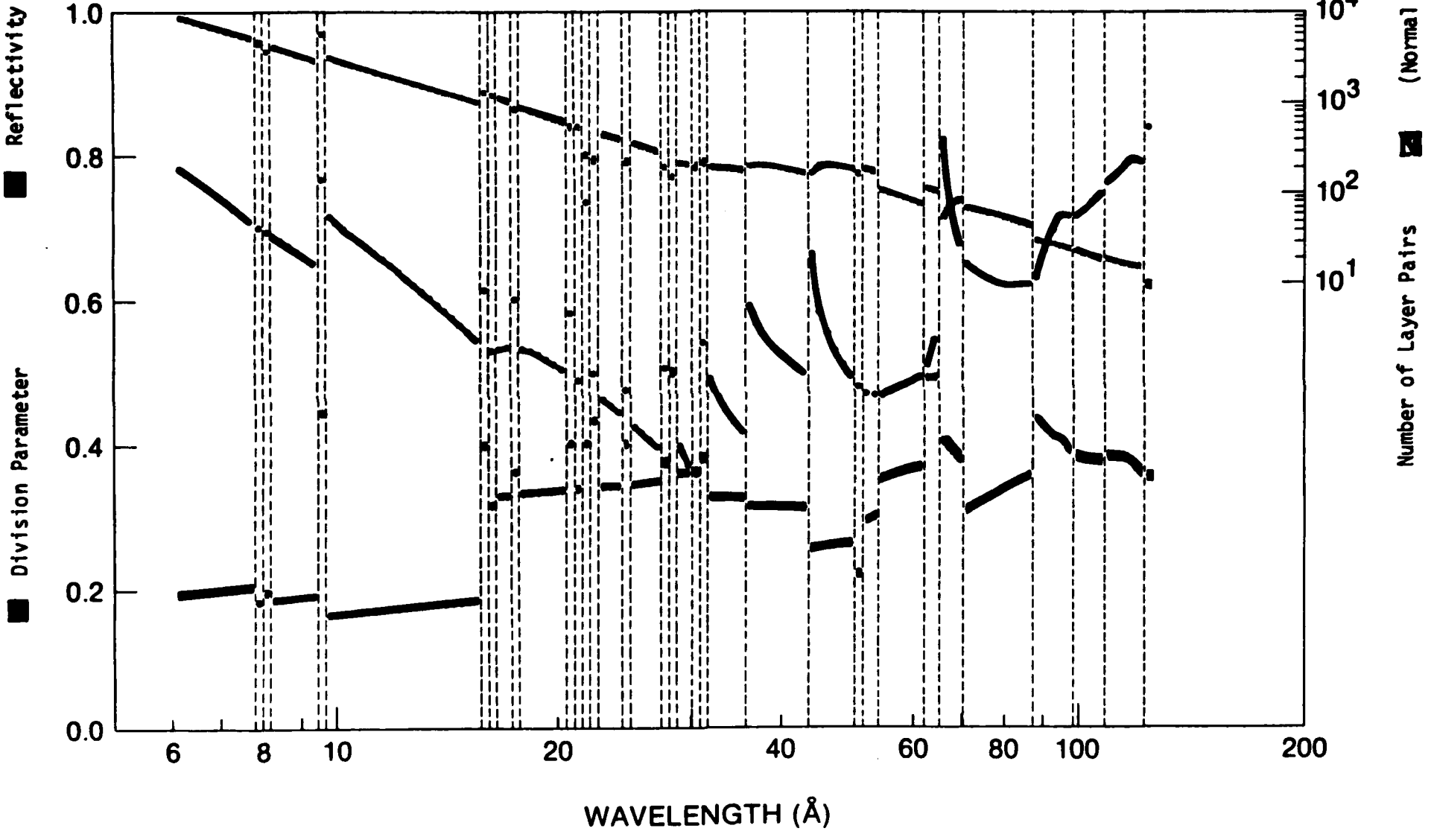

X316

Acknowledgements

This research would not have been possible without the support of a number of sponsors, including the Air Force Office of Scientific Research, grant #AFOSR-82-0059.

This research was also partially supported by: Exxon Research and Engineering Company, General Electric Company, Northeast Utilities, New York State Energy Research and Development Authority, The Standard Oil Company of Ohio, The University of Rochester, and Empire State Electric Energy Research Corporation. Such support does not imply endorsement of the content by any of the above parties.


FILM
2-84